

$K^- p \rightarrow K \Xi$ reaction and Λ^* and Σ^* resonances

Sang-Ho Kim (金相鎬)

Soongsil University, Seoul

Origin of Matter and Evolution of Galaxy (OMEG) Institute



In collaboration with

J.K.Ahn, Sh.H.Kim (Korea Univ.), S.i.Nam (PKNU), M.K.Cheoun (Soongsil Univ.)

APCTP Workshop on Nuclear Physics 2022
11-16, July, 2022, Jeju

Contents

1. introduction
2. theoretical framework
3. numerical results
4. application
5. summary & future work

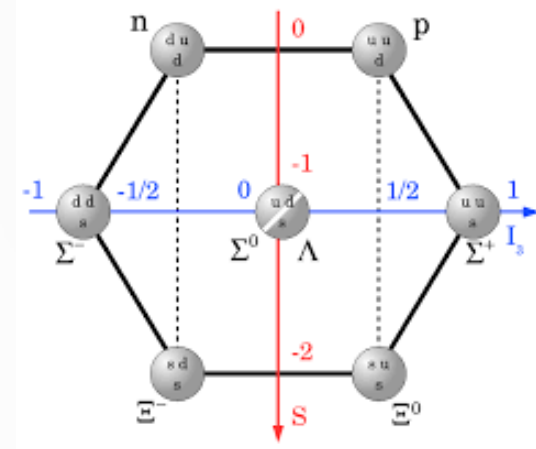
1. introduction

How to produce **multistrangeness baryons** in hadron physics?

1. introduction

How to produce **multistrangeness baryons** in hadron physics?

- ❑ **Multistrangeness baryons** are of importance in our understanding of strong interactions. However, the information of them is very limited currently.
- ❑ SU(3) flavor symmetry allows as many $S = -2$ baryons, i.e. Ξ , but only 11 Ξ baryons are observed, whereas there are ~ 25 Λ^* or Σ^* resonances ($S = -1$).

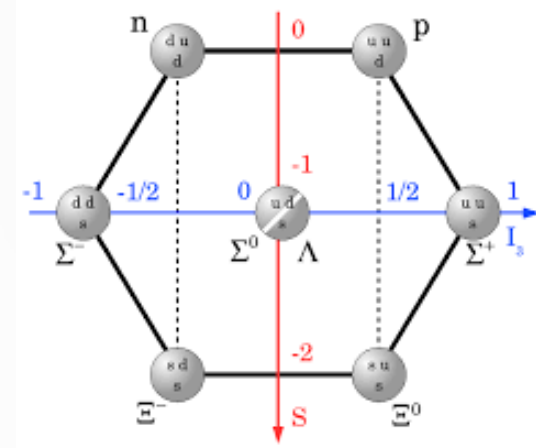


Particle	J^P	Overall status
$\Xi(1318)$	$1/2+$	****
$\Xi(1530)$	$3/2+$	****
$\Xi(1620)$		*
$\Xi(1690)$		***
$\Xi(1820)$	$3/2-$	***
$\Xi(1950)$		***
$\Xi(2030)$		***
$\Xi(2120)$		*
$\Xi(2250)$		**
$\Xi(2370)$		**
$\Xi(2500)$		*

1. introduction

How to produce **multistrangeness baryons** in hadron physics?

- ❑ **Multistrangeness baryons** are of importance in our understanding of strong interactions. However, the information of them is very limited currently.
- ❑ SU(3) flavor symmetry allows as many $S = -2$ baryons, i.e. Ξ , but only 11 Ξ baryons are observed, whereas there are ~ 25 Λ^* or Σ^* resonances ($S = -1$).
- ❑ This is mainly because multistrangeness hadron production have small cross section rates relatively.
- ❑ Recently, the situation becomes better since more precise and abundant data are expected to be produced in the future experiments via various beams:
 - a. photoproduction ($\gamma p \rightarrow K K \Xi, K K K \Omega$) at JLab
 - b. $p\bar{p}$ interaction ($p\bar{p} \rightarrow \Xi\bar{\Xi}, \Omega\bar{\Omega}$) at GSI-FAIR
 - c. K induced reaction ($K^- p \rightarrow K \Xi$) at J-PARC

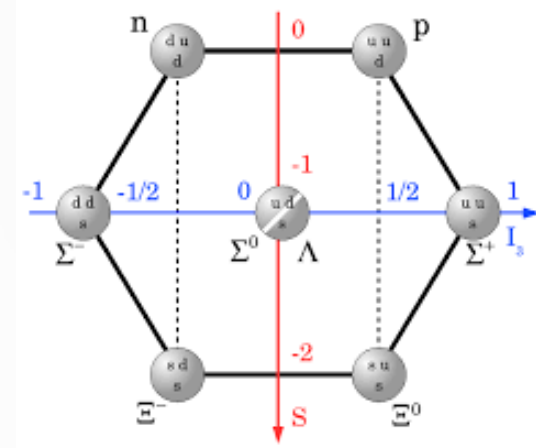


Particle	J^P	Overall status
$\Xi(1318)$	$1/2+$	****
$\Xi(1530)$	$3/2+$	****
$\Xi(1620)$		*
$\Xi(1690)$		***
$\Xi(1820)$	$3/2-$	***
$\Xi(1950)$		***
$\Xi(2030)$		***
$\Xi(2120)$		*
$\Xi(2250)$		**
$\Xi(2370)$		**
$\Xi(2500)$		*

1. introduction

How to produce **multistrangeness baryons** in hadron physics?

- ❑ **Multistrangeness baryons** are of importance in our understanding of strong interactions. However, the information of them is very limited currently.
- ❑ SU(3) flavor symmetry allows as many $S = -2$ baryons, i.e. Ξ , but only 11 Ξ baryons are observed, whereas there are ~ 25 Λ^* or Σ^* resonances ($S = -1$).
- ❑ This is mainly because multistrangeness hadron production have small cross section rates relatively.
- ❑ Recently, the situation becomes better since more precise and abundant data are expected to be produced in the future experiments via various beams:
 - a. photoproduction ($\gamma p \rightarrow K K \Xi, K K K \Omega$) at JLab
 - b. $p\bar{p}$ interaction ($p\bar{p} \rightarrow \Xi\bar{\Xi}, \Omega\bar{\Omega}$) at GSI-FAIR
 - c. K induced reaction ($K^- p \rightarrow K \Xi$) at J-PARC
- > May provide substantial contributions to the spectroscopy of hyperon and cascade baryons.

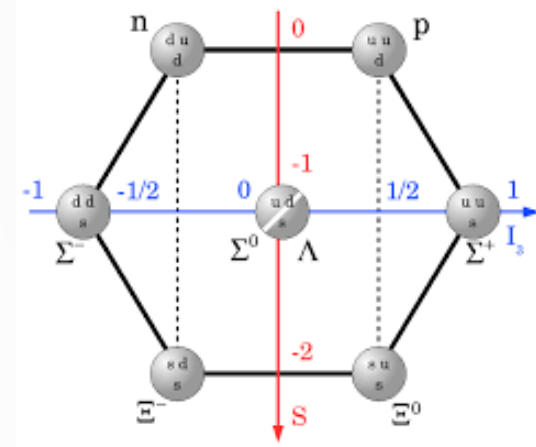


Particle	J^P	Overall status
$\Xi(1318)$	1/2+	****
$\Xi(1530)$	3/2+	****
$\Xi(1620)$		*
$\Xi(1690)$		***
$\Xi(1820)$	3/2-	***
$\Xi(1950)$		***
$\Xi(2030)$		***
$\Xi(2120)$		*
$\Xi(2250)$		**
$\Xi(2370)$		**
$\Xi(2500)$		*

1. introduction

How to produce **multistrangeness baryons** in hadron physics?

- ❑ **Multistrangeness baryons** are of importance in our understanding of strong interactions. However, the information of them is very limited currently.
- ❑ SU(3) flavor symmetry allows as many $S = -2$ baryons, i.e. Ξ , but only 11 Ξ baryons are observed, whereas there are ~ 25 Λ^* or Σ^* resonances ($S = -1$).
- ❑ This is mainly because multistrangeness hadron production have small cross section rates relatively.
- ❑ Recently, the situation becomes better since more precise and abundant data are expected to be produced in the future experiments via various beams:
 - photoproduction ($\gamma p \rightarrow K K \Xi, K K K \Omega$) at JLab
 - $p\bar{p}$ interaction ($p\bar{p} \rightarrow \Xi\bar{\Xi}, \Omega\bar{\Omega}$) at GSI-FAIR
 - K induced reaction ($K^- p \rightarrow K \Xi$) at J-PARC**
- > May provide substantial contributions to the spectroscopy of hyperon and cascade baryons.



Particle	J^P	Overall status
$\Xi(1318)$	$1/2+$	****
$\Xi(1530)$	$3/2+$	****
$\Xi(1620)$		*
$\Xi(1690)$		***
$\Xi(1820)$	$3/2-$	***
$\Xi(1950)$		***
$\Xi(2030)$		***
$\Xi(2120)$		*
$\Xi(2250)$		**
$\Xi(2370)$		**
$\Xi(2500)$		*

1. introduction

□ Multistrangeness production in hadron physics

a. photoproduction ($\gamma p \rightarrow K K \Xi$)

> CLAS & GlueX Collaborations at JLab is producing the data.

> The production mechanism is a two-step process.

> The hadron coupling constants are not well known.

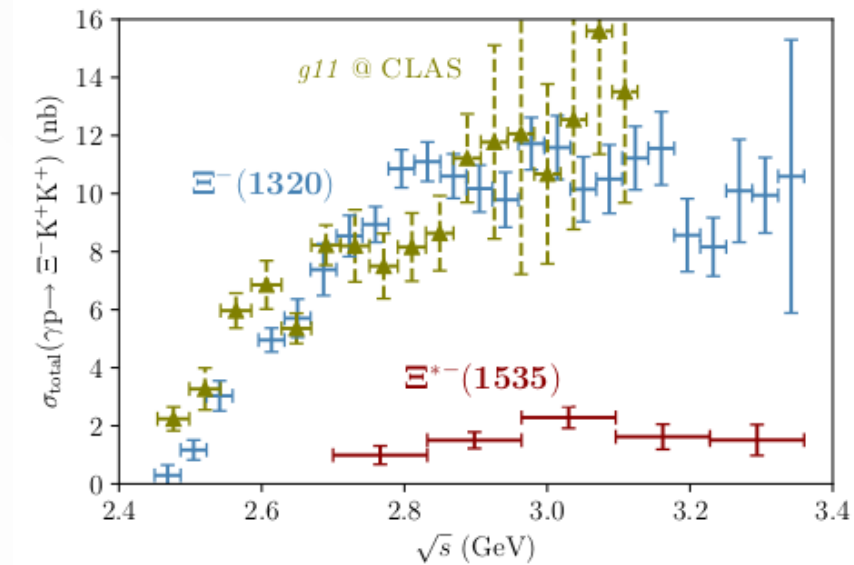
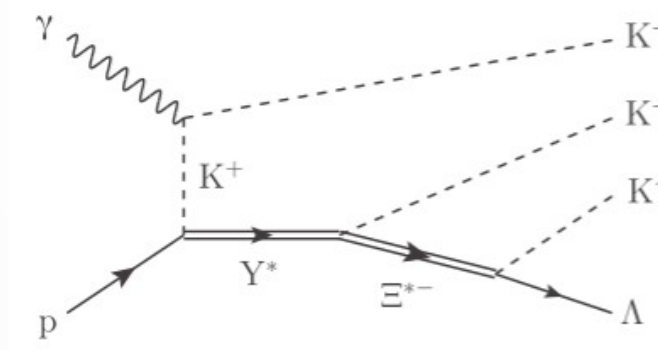
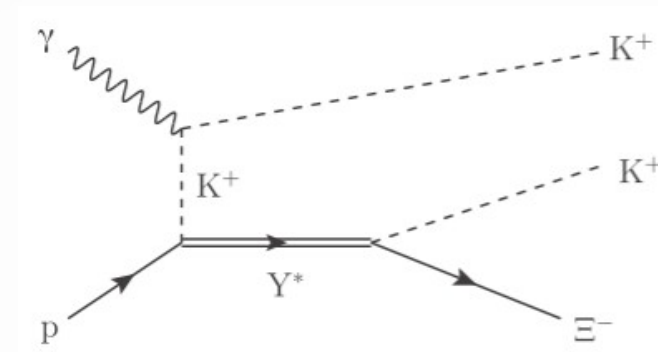
> Theoretical analyses

$\gamma p \rightarrow K K \Xi(1318)$

Nakayama et al. PRC.74.035205 (2006)

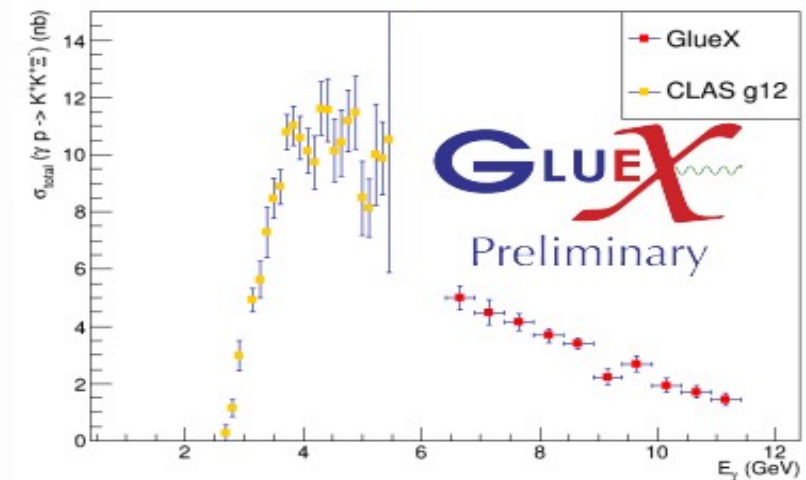
$\gamma p \rightarrow K^+ K^+ \Xi^{*-}(1530)$

No analyses yet



Goetz (CLAS) PRC.98.062201(R) (2018)

$\gamma p \rightarrow K^+ K^+ \Xi(1318)$



Ernst (GlueX) AIP.CP.2249.030041 (2020) 04

1. introduction

☐ Multistrangeness production in hadron physics

a. photoproduction ($\gamma p \rightarrow K K \Xi$)

> CLAS & GlueX Collaborations at JLab is producing the data.

> The production mechanism is a two-step process.

> The hadron coupling constants are not well known.

> Theoretical analyses

$\gamma p \rightarrow K K \Xi(1318)$

Nakayama et al. PRC.74.035205 (2006)

$\gamma p \rightarrow K^+ K^+ \Xi^*(1530)$

No analyses yet

Ξ^0

$$I(J^P) = 1/2(1/2^+)$$

PDG 2022

The parity has not actually been measured, but $^+$ is of course expected.

Goetz (CLAS) PRC.98.062201(R) (2018)

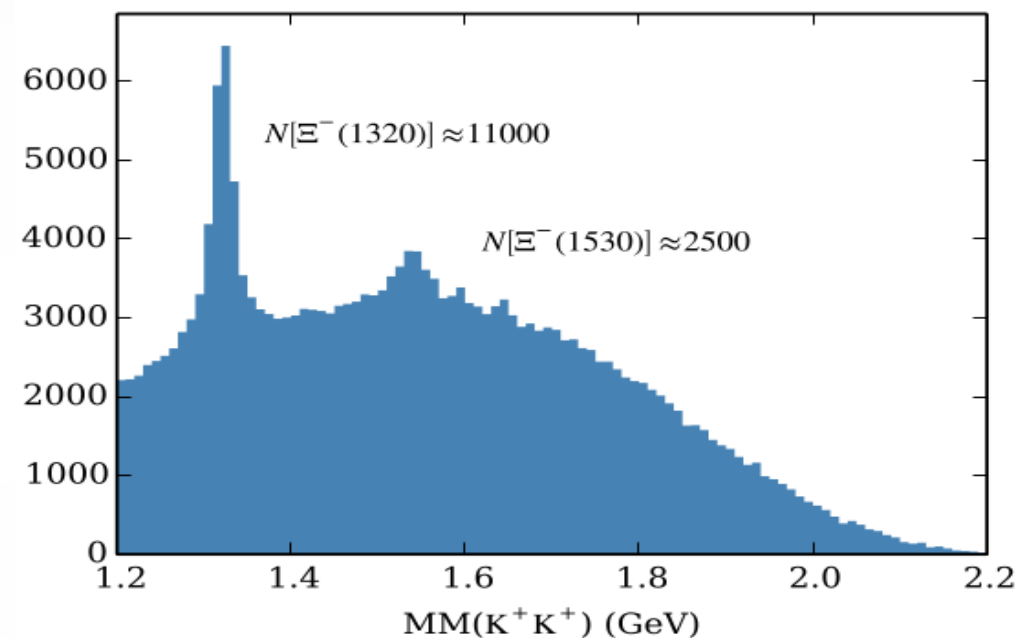


FIG. 2. Missing mass off of (K^+K^+) showing the Ξ spectrum above a smooth background, summed over all angles and all E_γ .

In the missing mass off of K^+K^+ (Fig. 2), the strong peak at 1.32 GeV corresponds to the Ξ ground state ($J^P = \frac{1}{2}^-$), and the smaller peak at 1.53 GeV is the Ξ^* first excited state ($J^P = \frac{3}{2}^-$). No other statistically significant structures are seen in this mass spectrum.

1. introduction

□ Multistrangeness production in hadron physics

a. photoproduction ($\gamma p \rightarrow K K \Xi$)

> CLAS & GlueX Collaborations at JLab is producing the data.

> The production mechanism is a two-step process.

> The hadron coupling constants are not well known.

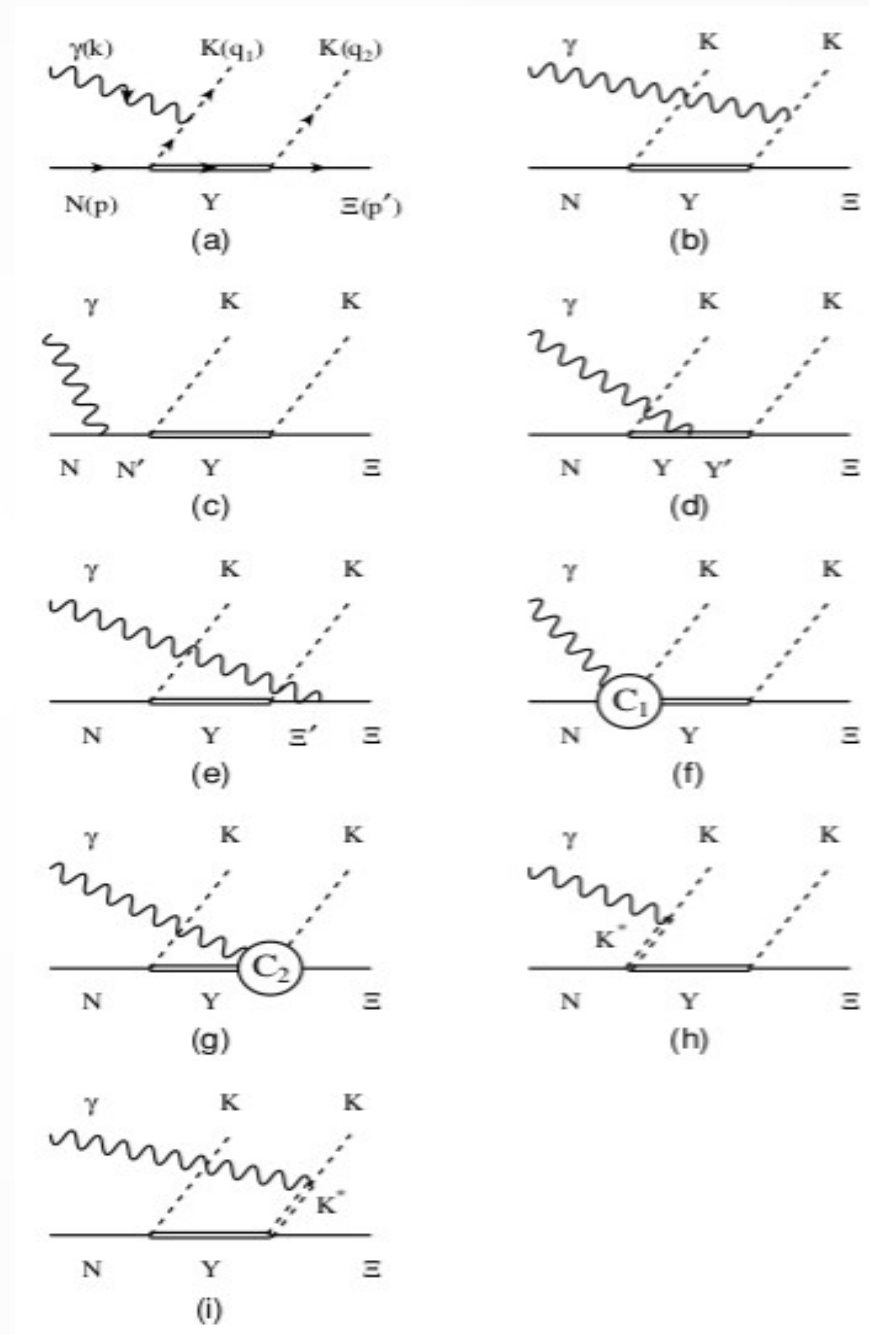
> Theoretical analyses

$\gamma p \rightarrow K K \Xi(1318)$

Nakayama et al. PRC.74.035205 (2006)

$\gamma p \rightarrow K^+ K^+ \Xi^{*-}(1530)$

No analyses yet



1. introduction

□ Multistrangeness production in hadron physics

b. $p\bar{p}$ interaction ($p\bar{p} \rightarrow \Xi\bar{\Xi}$)

> **FANDA** Collaboration at GSI-FAIR will produce the data.

Lutz et al. 0903.3905 [hep-ex] Physics Performance Report

> The production mechanism is a two-step process.

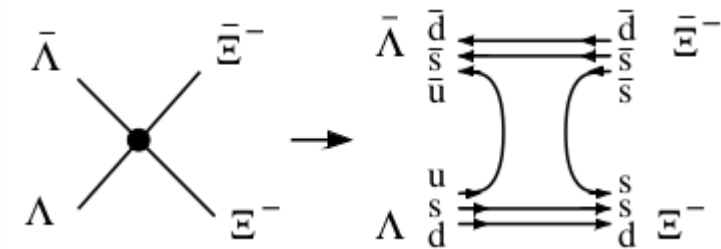
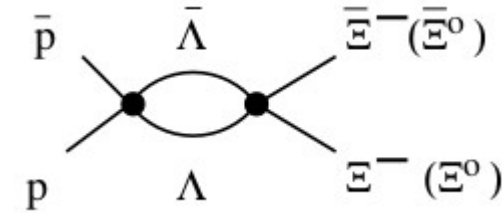
> The amplitudes are described by the loop diagrams within a modified Regge type model.

Titov et al. 1105.3847 [hep-ph]

> More rigorous analyses are called for.

Titov et al. 1105.3847 [hep-ph]

□ Loop diagrams



> K & K* exchanges are possible.

□ Scattering amplitude

$$T^{\bar{p}p \rightarrow \bar{\Xi}\Xi} \simeq T_{\text{cut}}^{\bar{p}p \rightarrow \bar{\Xi}\Xi} \\ = i \frac{Q_\Lambda}{8\pi\sqrt{s}} \int \frac{d\Omega_\Lambda}{4\pi} \sum_{\text{spins } \bar{\Lambda}\Lambda} T^{\bar{p}p \rightarrow \bar{\Lambda}\Lambda} T^{\bar{\Lambda}\Lambda \rightarrow \bar{\Xi}\Xi}$$

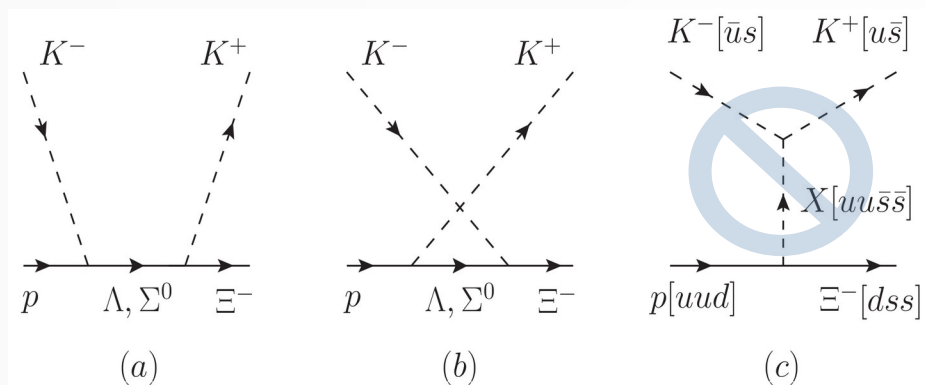
2. $K^- p \rightarrow K \Xi$ theoretical framework

□ Multistrangeness production in hadron physics (c. $K^- p \rightarrow K \Xi$)

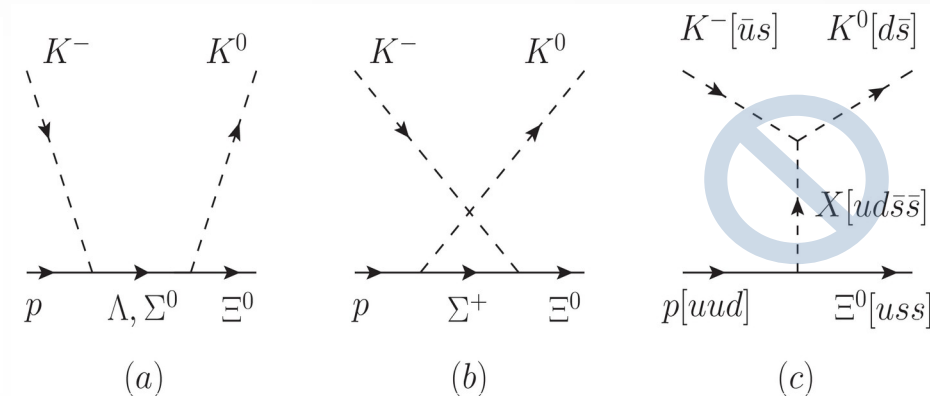
> Only ($\Lambda^{(*)}$ & $\Sigma^{(*)}$) hyperons mediate in the Born diagrams.

> t -channel meson exchanges are not possible because no meson of strangeness two exists.

(A) $K^- p \rightarrow K^+ \Xi^-$



(B) $K^- p \rightarrow K^0 \Xi^0$



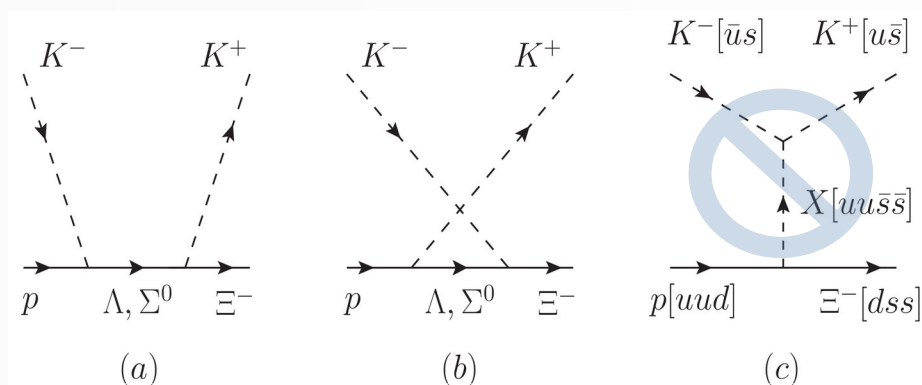
2. $K^- p \rightarrow K \Xi$ theoretical framework

□ **Multistrangeness production** in hadron physics (c. $K^- p \rightarrow K \Xi$)

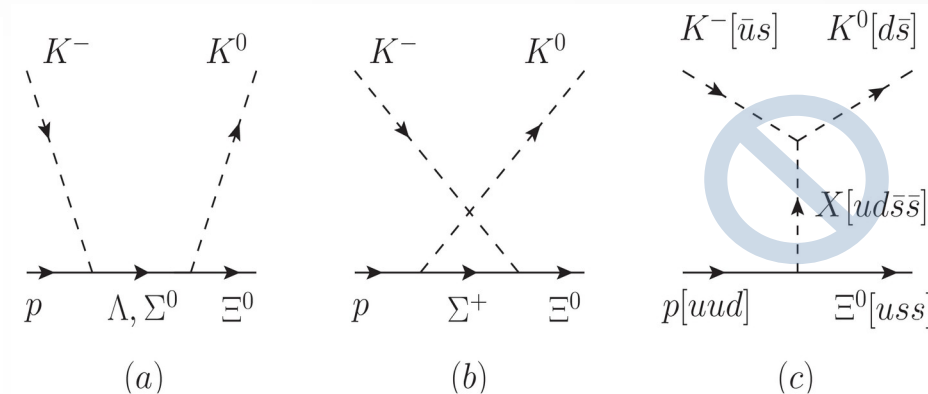
> Only ($\Lambda^{(*)}$ & $\Sigma^{(*)}$) hyperons mediate in the Born diagrams.

> t -channel meson exchanges are not possible because no meson of strangeness two exists.

(A) $K^- p \rightarrow K^+ \Xi^-$



(B) $K^- p \rightarrow K^0 \Xi^0$



□ tetraquark in **charm sector** [LHCb, Nature Physics (2022)]

> First observation with $[cc\bar{u}\bar{d}]$ content, $T_{cc}(3875, 1^+)$, width $\Gamma \sim 410$ keV in the mass spectrum of “ $D^0 D^0 \pi^+$ ”

□ tetraquark in **strange sector**

> No meson of strangeness two is known to exist.

□ The evidence of the pentaquark in **charm sector**, $P_c^+[uudc\bar{c}]$, is clearer than that in **strange sector**, $P_s^+[uud\bar{s}\bar{s}]$ & $\theta^+[uudd\bar{s}]$.

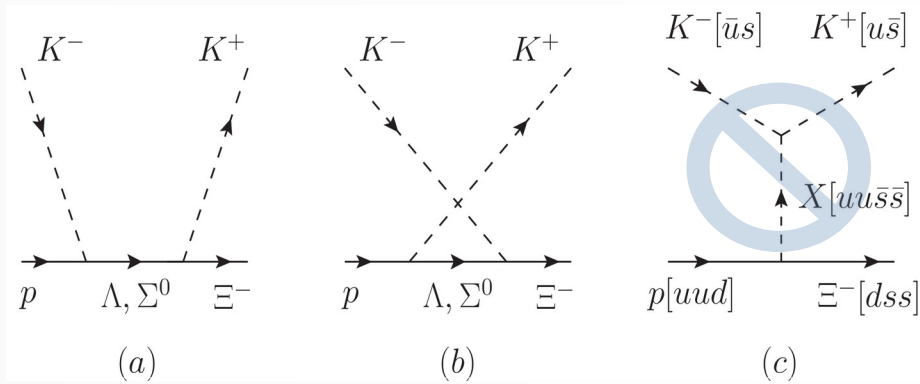
2. $K^- p \rightarrow K \Xi$ theoretical framework

□ Multistrangeness production in hadron physics (c. $K^- p \rightarrow K \Xi$)

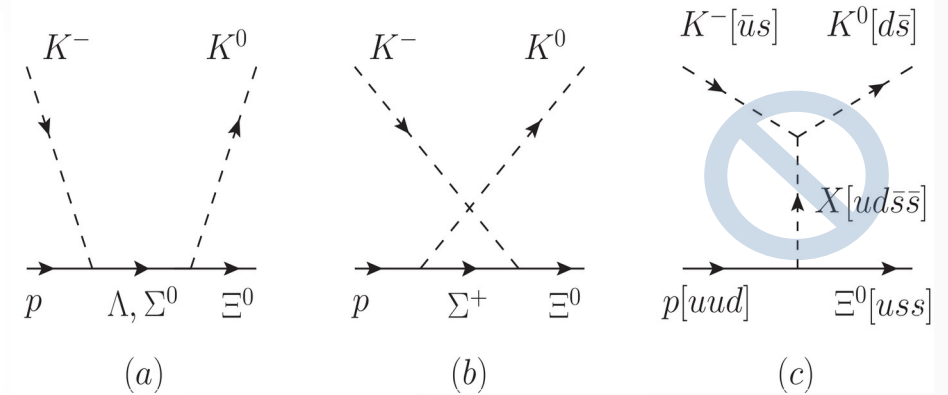
> Only ($\Lambda^{(*)}$ & $\Sigma^{(*)}$) hyperons mediate in the Born diagrams.

> t -channel meson exchanges are not possible because no meson of strangeness two exists.

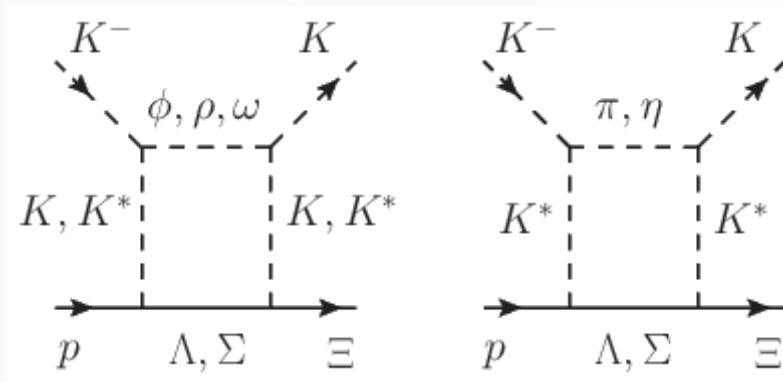
(A) $K^- p \rightarrow K^+ \Xi^-$



(B) $K^- p \rightarrow K^0 \Xi^0$



Rescattering effect



$$g_{K^*K\rho} = g_{K^*K\omega} = \frac{1}{\sqrt{2}}g_{K^*K\phi} = \frac{1}{2}g_{\omega\rho\pi}$$

$$g_{KK\rho} = g_{KK\omega} = \frac{1}{2}g_{\pi\pi\rho}$$

► Use the dominant decay process: $\phi \rightarrow K^+K^-$, $K^* \rightarrow K\pi$, etc

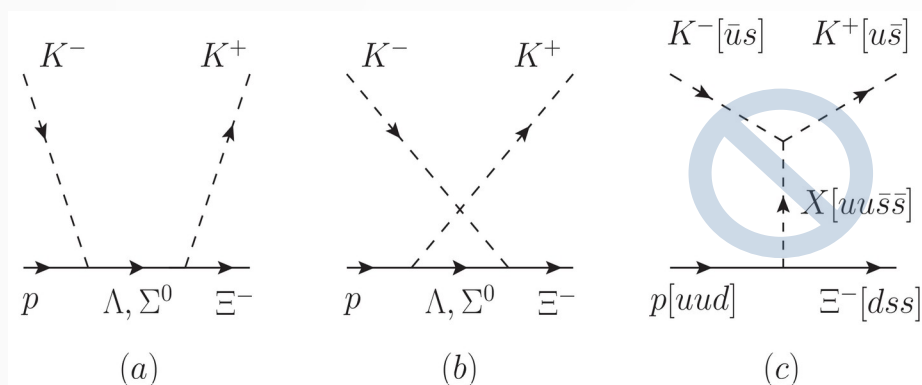
2. $K^- p \rightarrow K \Xi$ theoretical framework

□ Multistrangeness production in hadron physics (c. $K^- p \rightarrow K \Xi$)

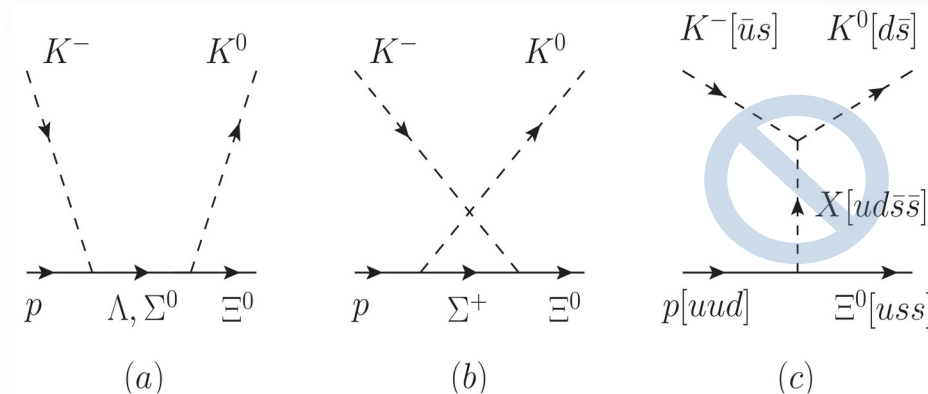
> Only ($\Lambda^{(*)}$ & $\Sigma^{(*)}$) hyperons mediate in the Born diagrams.

> t -channel meson exchanges are not possible because no meson of strangeness two exists.

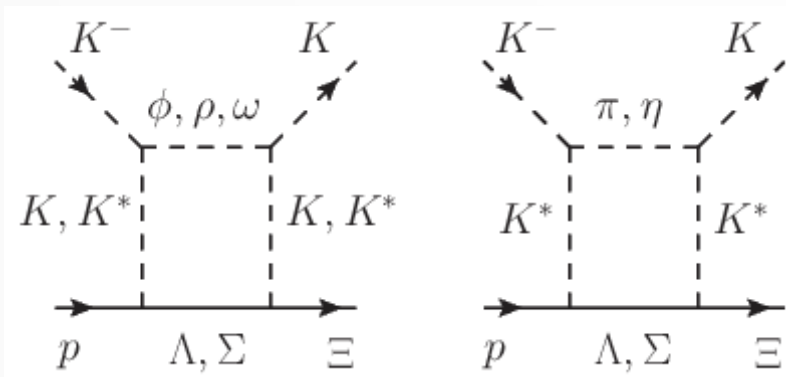
(A) $K^- p \rightarrow K^+ \Xi^-$



(B) $K^- p \rightarrow K^0 \Xi^0$



Rescattering effect



$$g_{K^*K\rho} = g_{K^*K\omega} = \frac{1}{\sqrt{2}}g_{K^*K\phi} = \frac{1}{2}g_{\omega\rho\pi}$$

$$g_{KK\rho} = g_{KK\omega} = \frac{1}{2}g_{\pi\pi\rho}$$

► Use the dominant decay process: $\phi \rightarrow K^+K^-$, $K^* \rightarrow K\pi$, etc

□ We employ a “Regge + Resonance + Rescattering” approach.

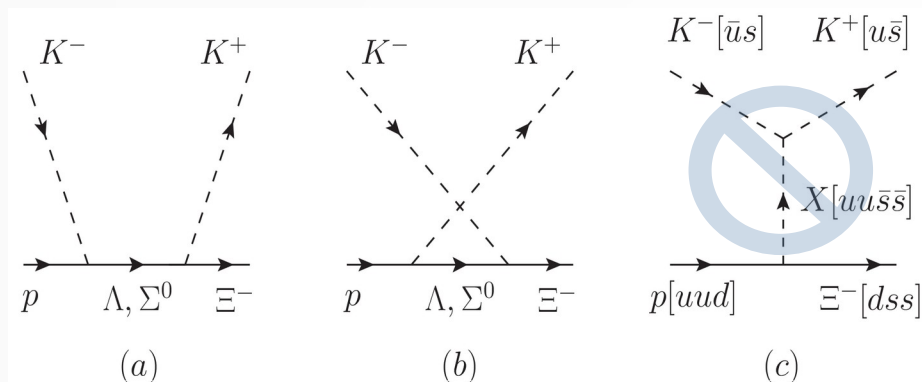
2. $K^- p \rightarrow K \Xi$ theoretical framework

□ Multistrangeness production in hadron physics (c. $K^- p \rightarrow K \Xi$)

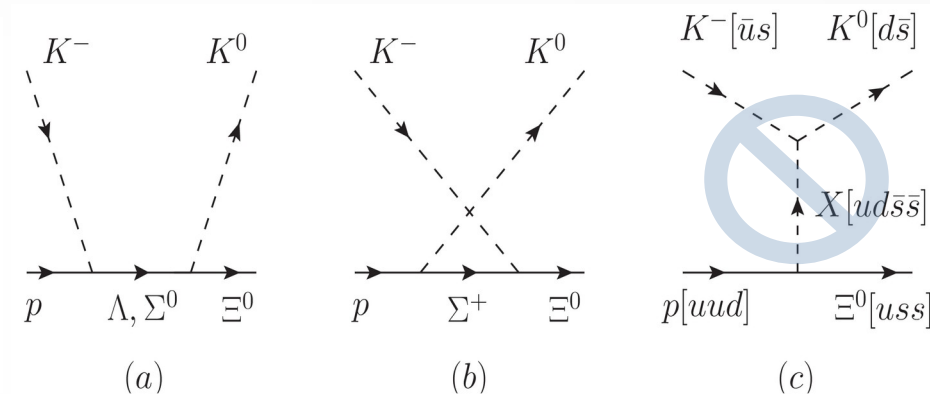
> Only ($\Lambda^{(*)}$ & $\Sigma^{(*)}$) hyperons mediate in the Born diagrams.

> t -channel meson exchanges are not possible because no meson of strangeness two exists.

(A) $K^- p \rightarrow K^+ \Xi^-$



(B) $K^- p \rightarrow K^0 \Xi^0$



□ Effective Lagrangians

$$\mathcal{L}_{\Lambda NK}^{1/2(\pm)} \equiv g_{\Lambda NK} \bar{\Lambda} (D_{\Lambda NK}^{1/2(\pm)} \bar{K}) N + \text{H.c.}$$

$$\mathcal{L}_{\Lambda NK}^{3/2(\pm)} = \frac{g_{\Lambda NK}}{m_K} \bar{\Lambda}^\nu (D_\nu^{3/2(\pm)} \bar{K}) N + \text{H.c.}$$

$$\mathcal{L}_{\Lambda NK}^{5/2(\pm)} = \frac{g_{\Lambda NK}}{m_K^2} \bar{\Lambda}^{\mu\nu} (D_{\mu\nu}^{5/2(\pm)} \bar{K}) N + \text{H.c.}$$

$$\mathcal{L}_{\Lambda NK}^{7/2(\pm)} = \frac{g_{\Lambda NK}}{m_K^3} \bar{\Lambda}^{\mu\nu\rho} (D_{\mu\nu\rho}^{7/2(\pm)} \bar{K}) N + \text{H.c.}$$

$$D_{B'BM}^{1/2(\pm)} \equiv -\Gamma^{(\pm)} \left(\pm i\lambda + \frac{1 - \lambda}{m_{B'} \pm m_B} \not{\partial} \right),$$

$$D_\nu^{3/2(\pm)} \equiv \Gamma^{(\mp)} \partial_\nu,$$

$$D_{\mu\nu}^{5/2(\pm)} \equiv -i\Gamma^{(\pm)} \partial_\mu \partial_\nu,$$

$$D_{\mu\nu\rho}^{7/2(\pm)} \equiv -\Gamma^{(\mp)} \partial_\mu \partial_\nu \partial_\rho,$$

($\lambda = 1$) Pseudoscalar (PS) form
 ($\lambda = 0$) Pseudovector (PV) form

□ Coupling constants

Y	g_{NYK}	$g_{\Xi YK}$
$\Lambda(1116)_{\frac{1}{2}}^{1+}$	-13.24	3.52
$\Sigma(1193)_{\frac{1}{2}}^{1+}$	3.58	-13.26

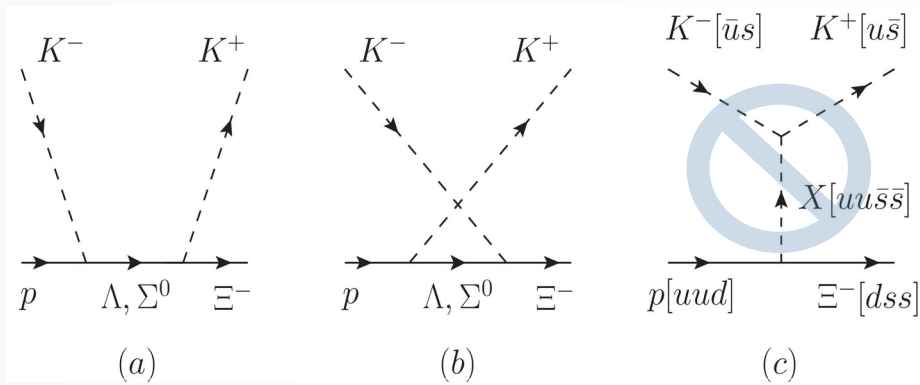
2. $K^- p \rightarrow K \Xi$ theoretical framework

□ Multistrangeness production in hadron physics (c. $K^- p \rightarrow K \Xi$)

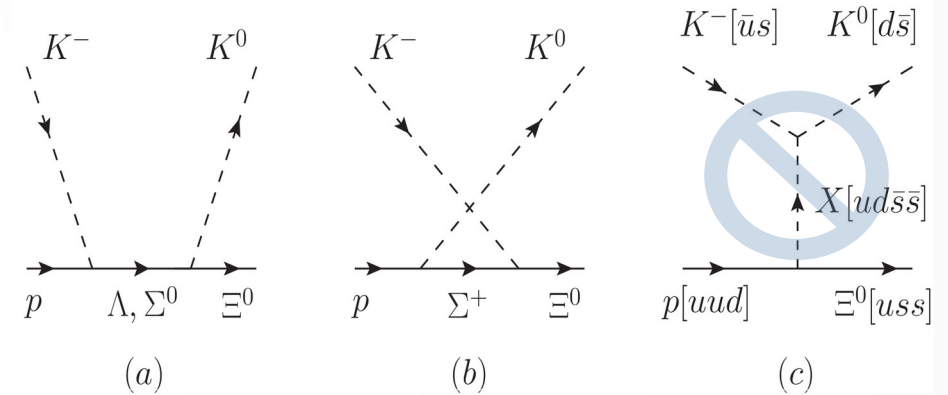
> Only ($\Lambda^{(*)}$ & $\Sigma^{(*)}$) hyperons mediate in the Born diagrams.

> t -channel meson exchanges are not possible because no meson of strangeness two exists.

(A) $K^- p \rightarrow K^+ \Xi^-$



(B) $K^- p \rightarrow K^0 \Xi^0$



□ (Fig. b) We employ a hybridized **Regge model** to describe the backward angles in the u channel.

“Baryon exchange processes” [Storror, Phys.Rept.103.317 \(1984\)](#)

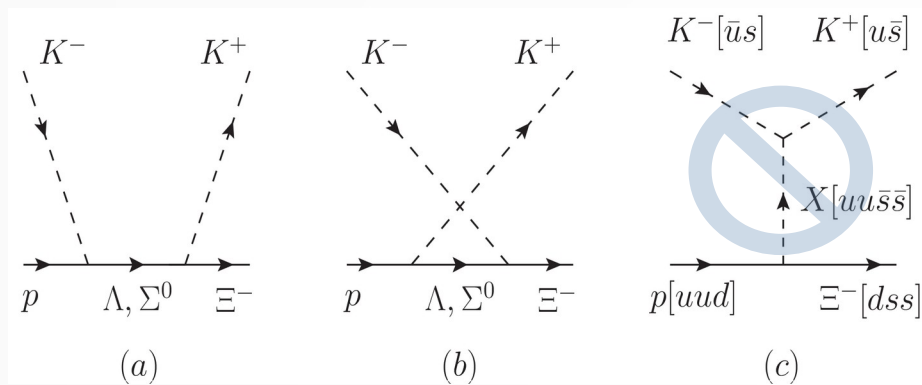
2. $K^- p \rightarrow K \Xi$ theoretical framework

□ Multistrangeness production in hadron physics (c. $K^- p \rightarrow K \Xi$)

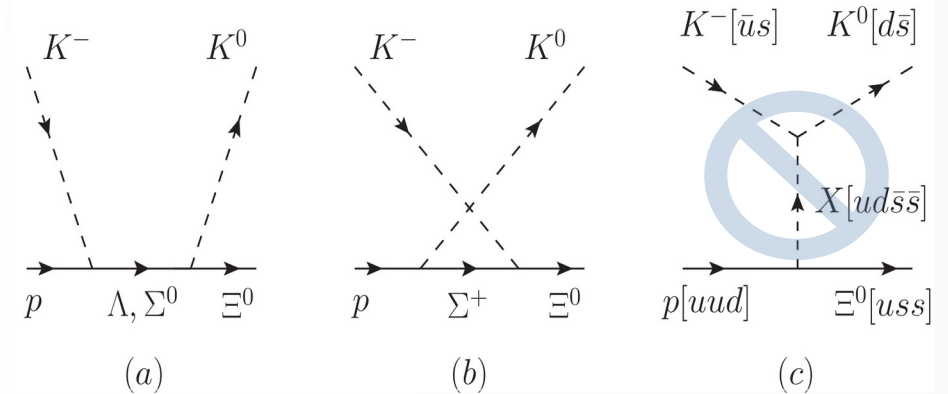
> Only ($\Lambda^{(*)}$ & $\Sigma^{(*)}$) hyperons mediate in the Born diagrams.

> t -channel meson exchanges are not possible because no meson of strangeness two exists.

(A) $K^- p \rightarrow K^+ \Xi^-$



(B) $K^- p \rightarrow K^0 \Xi^0$



□ (Fig. b) We employ a hybridized **Regge model** to describe the backward angles in the u channel.

“Baryon exchange processes” [Storror, Phys.Rept.103.317 \(1984\)](#)

□ (Fig. a) Additionally, in the s channel, we include (Λ^* & Σ^*) resonances which couple strongly to $\bar{K}N$ & $K\Xi$ channels.

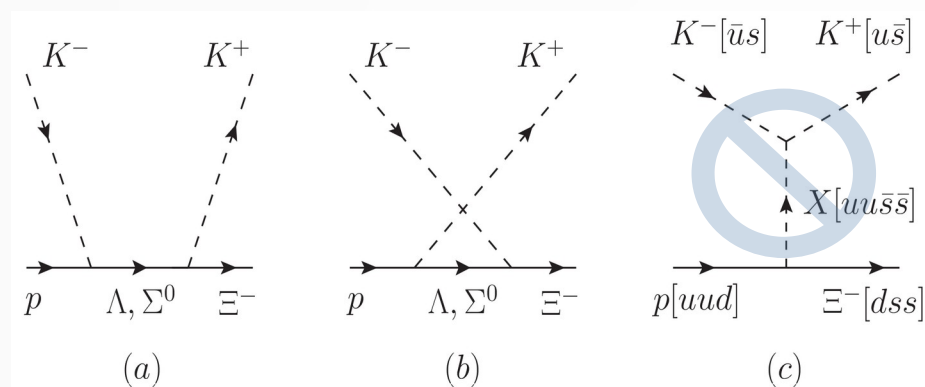
2. $K^- p \rightarrow K \Xi$ theoretical framework

□ **Multistrangeness production** in hadron physics (c. $K^- p \rightarrow K \Xi$)

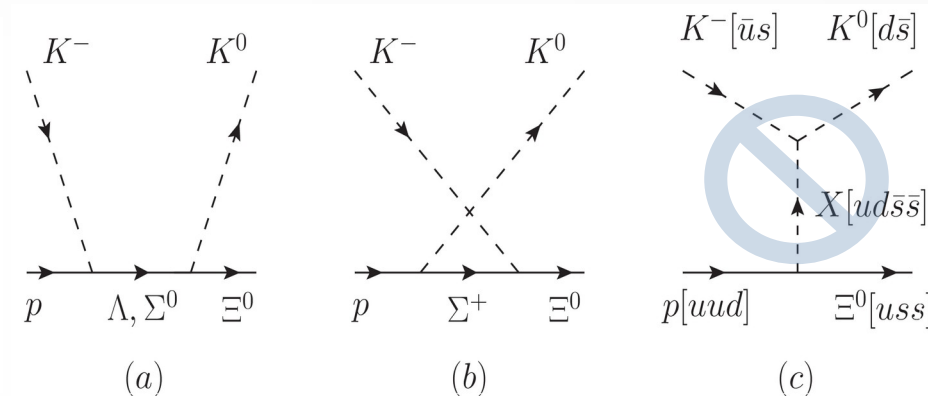
> Only ($\Lambda^{(*)}$ & $\Sigma^{(*)}$) hyperons mediate in the Born diagrams.

> t -channel meson exchanges are not possible because no meson of strangeness two exists.

(A) $K^- p \rightarrow K^+ \Xi^-$



(B) $K^- p \rightarrow K^0 \Xi^0$



□ (Fig. b) We employ a hybridized **Regge model** to describe the backward angles in the u channel.

“Baryon exchange processes” [Storror, Phys.Rept.103.317 \(1984\)](#)

□ (Fig. a) Additionally, in the s channel, we include (Λ^* & Σ^*) resonances which couple strongly to $\bar{K}N$ & $K\Xi$ channels.

□ **Box diagram** is calculated from the 3-dimensional reduction of the Bethe-Salpeter equation.

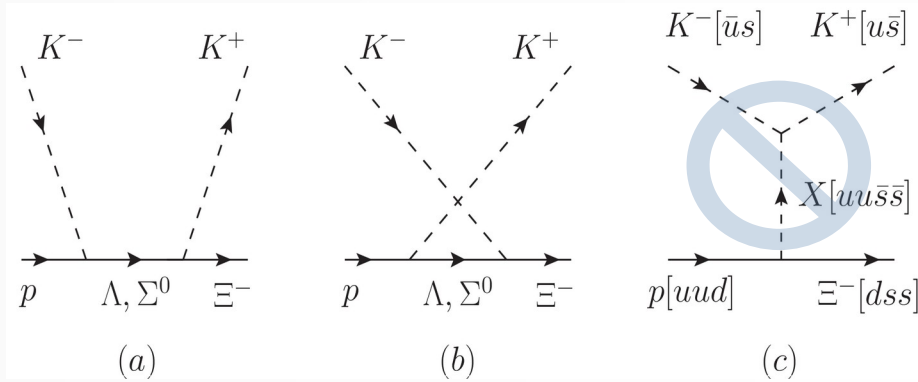
2. $K^- p \rightarrow K \Xi$ theoretical framework

□ Multistrangeness production in hadron physics (c. $K^- p \rightarrow K \Xi$)

> Only ($\Lambda^{(*)}$ & $\Sigma^{(*)}$) hyperons mediate in the Born diagrams.

> t -channel meson exchanges are not possible because no meson of strangeness two exists.

(A) $K^- p \rightarrow K^+ \Xi^-$

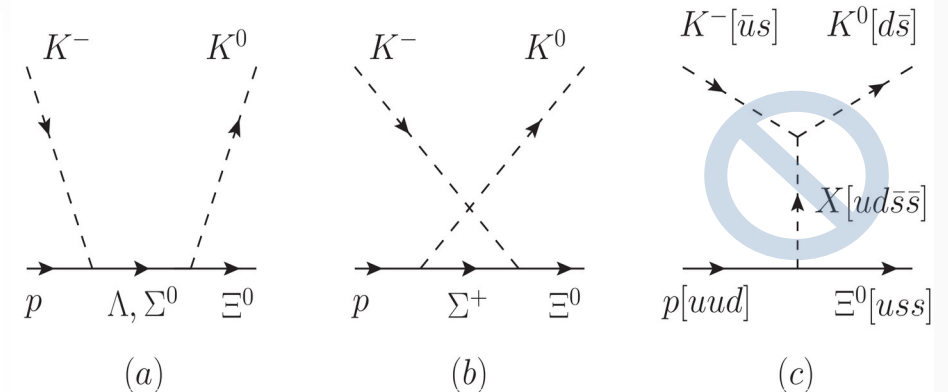


$1(1) \quad -1(1)$

$1(1) \quad -1(1)$

[isospin factors]

(B) $K^- p \rightarrow K^0 \Xi^0$



$1(1) \quad 1(1)$

$\sqrt{2} \quad -\sqrt{2}$

□ Isospin factors

$$\Lambda \text{ exchange: } \begin{pmatrix} \bar{K}^+ & \bar{K}^0 \end{pmatrix} \Lambda \begin{pmatrix} p \\ n \end{pmatrix} = 1\bar{K}^+\Lambda p + 1\bar{K}^0\Lambda n$$

$$\Sigma \text{ exchange: } \begin{pmatrix} \bar{K}^+ & \bar{K}^0 \end{pmatrix} \begin{pmatrix} \Sigma^0 & \sqrt{2}\Sigma^+ \\ \sqrt{2}\Sigma^- & -\Sigma^- \end{pmatrix} \begin{pmatrix} p \\ n \end{pmatrix} = 1\bar{K}^+\Sigma^0 p + \sqrt{2}(\bar{K}^+\Sigma^+ n + \bar{K}^0\Sigma^- p) - 1\bar{K}^0\Sigma^0 n$$

□ u -channel Σ exchange: $\sigma(K^- p \rightarrow K^+ \Xi^-) \times 4 = \sigma(K^- p \rightarrow K^0 \Xi^0)$

□ We consider two different isospin channels simultaneously: useful to constrain model parameters.

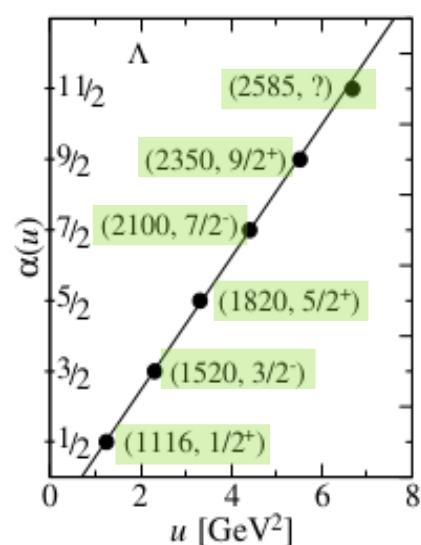
2. $K^- p \rightarrow K \Xi$ theoretical framework

Λ hyperons

	J^P	status
$\Lambda(1116)$	$1/2^+$	****
$\Lambda(1380)$	$1/2^-$	**
$\Lambda(1405)$	$1/2^-$	****
$\Lambda(1520)$	$3/2^-$	****
$\Lambda(1600)$	$1/2^+$	****
$\Lambda(1670)$	$1/2^-$	****
$\Lambda(1690)$	$3/2^-$	****
$\Lambda(1710)$	$1/2^+$	*
$\Lambda(1800)$	$1/2^-$	***
$\Lambda(1810)$	$1/2^+$	***
$\Lambda(1820)$	$5/2^+$	****
$\Lambda(1830)$	$5/2^-$	****
$\Lambda(1890)$	$3/2^+$	****
$\Lambda(2000)$	$1/2^-$	*
$\Lambda(2050)$	$3/2^-$	*
$\Lambda(2070)$	$3/2^+$	*
$\Lambda(2080)$	$5/2^-$	*
$\Lambda(2085)$	$7/2^+$	**
$\Lambda(2100)$	$7/2^-$	****
$\Lambda(2110)$	$5/2^+$	***
$\Lambda(2325)$	$3/2^-$	*
$\Lambda(2350)$	$9/2^+$	***
$\Lambda(2585)$		*

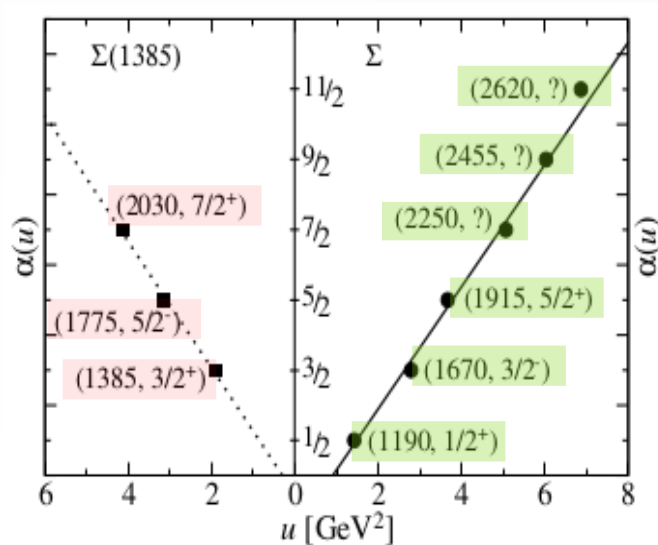
Hyperon Regge trajectories

Storror, Phys.Rept.103.317 (1984)



$$\Lambda : \alpha(u) = -0.65 + 0.94u$$

$$\Lambda(1405) : \text{excluded}$$



$$\Sigma : \alpha(u) = -0.79 + 0.87u$$

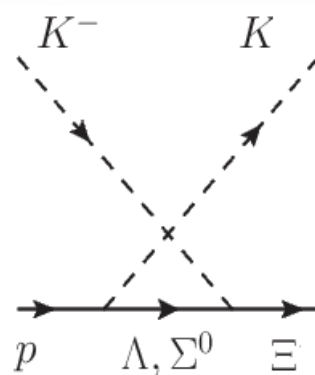
$$\Sigma^* : \alpha(u) = -0.27 + 0.9u$$

Σ hyperons

	J^P	status
$\Sigma(1193)$	$1/2^+$	****
$\Sigma(1385)$	$3/2^+$	****
$\Sigma(1580)$	$3/2^-$	*
$\Sigma(1620)$	$1/2^-$	*
$\Sigma(1660)$	$1/2^+$	***
$\Sigma(1670)$	$3/2^-$	****
$\Sigma(1750)$	$1/2^-$	***
$\Sigma(1775)$	$5/2^-$	****
$\Sigma(1780)$	$3/2^+$	*
$\Sigma(1880)$	$1/2^+$	**
$\Sigma(1900)$	$1/2^-$	**
$\Sigma(1910)$	$3/2^-$	***
$\Sigma(1915)$	$5/2^+$	****
$\Sigma(1940)$	$3/2^+$	*
$\Sigma(2010)$	$3/2^-$	*
$\Sigma(2030)$	$7/2^+$	****
$\Sigma(2070)$	$5/2^+$	*
$\Sigma(2080)$	$3/2^+$	*
$\Sigma(2100)$	$7/2^-$	*
$\Sigma(2110)$	$1/2^-$	*
$\Sigma(2230)$	$3/2^+$	*
$\Sigma(2250)$		**
$\Sigma(2455)$		*
$\Sigma(2620)$		*
$\Sigma(3000)$		*
$\Sigma(3170)$		*

$$s_{\text{th}}(K^- p \rightarrow K \Xi)$$

$$= 1.81 \text{ GeV}$$



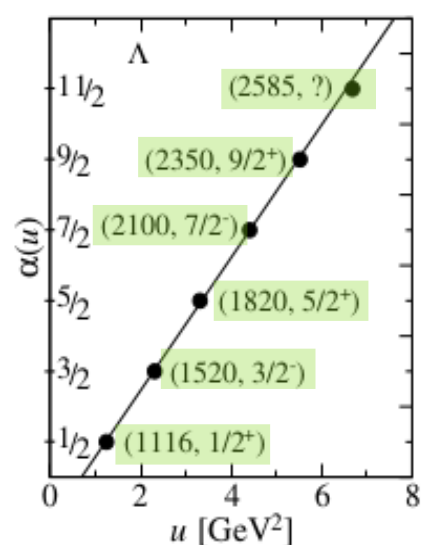
2. $K^- p \rightarrow K \Xi$ theoretical framework

Λ hyperons

	J^P	status
$\Lambda(1116)$	$1/2^+$	****
$\Lambda(1380)$	$1/2^-$	**
$\Lambda(1405)$	$1/2^-$	****
$\Lambda(1520)$	$3/2^-$	****
$\Lambda(1600)$	$1/2^+$	****
$\Lambda(1670)$	$1/2^-$	****
$\Lambda(1690)$	$3/2^-$	****
$\Lambda(1710)$	$1/2^+$	*
$\Lambda(1800)$	$1/2^-$	***
$\Lambda(1810)$	$1/2^+$	***
$\Lambda(1820)$	$5/2^+$	****
$\Lambda(1830)$	$5/2^-$	****
$\Lambda(1890)$	$3/2^+$	****
$\Lambda(2000)$	$1/2^-$	*
$\Lambda(2050)$	$3/2^-$	*
$\Lambda(2070)$	$3/2^+$	*
$\Lambda(2080)$	$5/2^-$	*
$\Lambda(2085)$	$7/2^+$	**
$\Lambda(2100)$	$7/2^-$	****
$\Lambda(2110)$	$5/2^+$	***
$\Lambda(2325)$	$3/2^-$	*
$\Lambda(2350)$	$9/2^+$	***
$\Lambda(2585)$		*

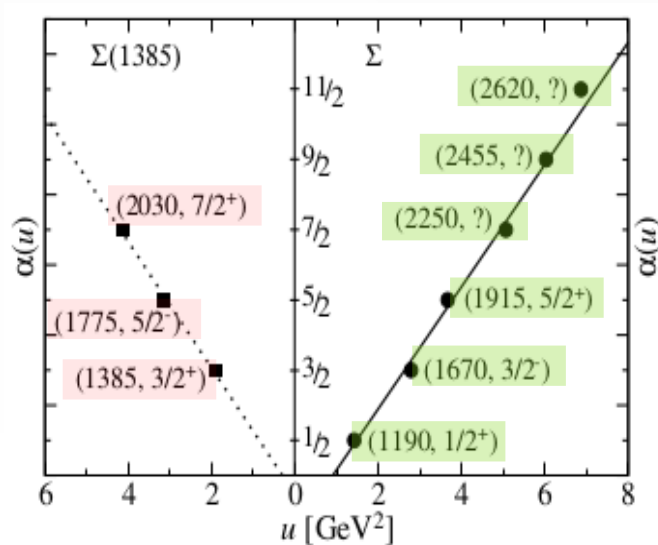
Hyperon Regge trajectories

Storow, Phys.Rept.103.317 (1984)



$$\Lambda : \alpha(u) = -0.65 + 0.94u$$

$$\Lambda(1405) : \text{excluded}$$



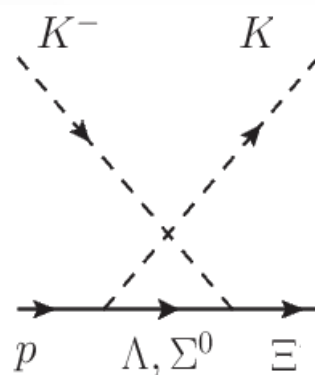
$$\Sigma : \alpha(u) = -0.79 + 0.87u$$

$$\Sigma^* : \alpha(u) = -0.27 + 0.9u$$

Σ hyperons

	J^P	status
$\Sigma(1193)$	$1/2^+$	****
$\Sigma(1385)$	$3/2^+$	****
$\Sigma(1580)$	$3/2^-$	*
$\Sigma(1620)$	$1/2^-$	*
$\Sigma(1660)$	$1/2^+$	***
$\Sigma(1670)$	$3/2^-$	****
$\Sigma(1750)$	$1/2^-$	***
$\Sigma(1775)$	$5/2^-$	****
$\Sigma(1780)$	$3/2^+$	*
$\Sigma(1880)$	$1/2^+$	**
$\Sigma(1900)$	$1/2^-$	**
$\Sigma(1910)$	$3/2^-$	***
$\Sigma(1915)$	$5/2^+$	****
$\Sigma(1940)$	$3/2^+$	*
$\Sigma(2010)$	$3/2^-$	*
$\Sigma(2030)$	$7/2^+$	****
$\Sigma(2070)$	$5/2^+$	*
$\Sigma(2080)$	$3/2^+$	*
$\Sigma(2100)$	$7/2^-$	*
$\Sigma(2110)$	$1/2^-$	*
$\Sigma(2230)$	$3/2^+$	*
$\Sigma(2250)$		**
$\Sigma(2455)$		*
$\Sigma(2620)$		*
$\Sigma(3000)$		*
$\Sigma(3170)$		*

$$s_{\text{th}}(K^- p \rightarrow K \Xi) = 1.81 \text{ GeV}$$



As seen, hyperon Regge trajectories involve many of 3 & 4 star resonances.

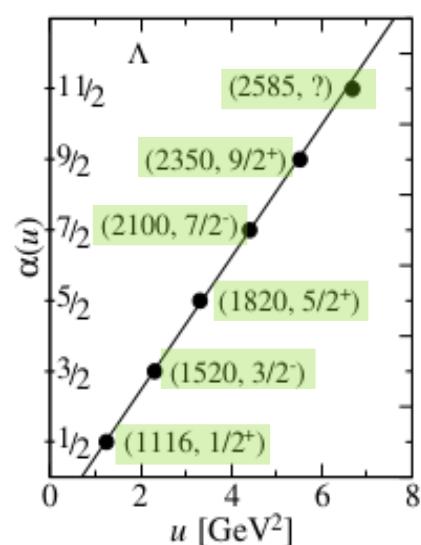
2. $K^- p \rightarrow K \Xi$ theoretical framework

Λ hyperons

	J^P	status
$\Lambda(1116)$	$1/2^+$	****
$\Lambda(1380)$	$1/2^-$	**
$\Lambda(1405)$	$1/2^-$	****
$\Lambda(1520)$	$3/2^-$	****
$\Lambda(1600)$	$1/2^+$	****
$\Lambda(1670)$	$1/2^-$	****
$\Lambda(1690)$	$3/2^-$	****
$\Lambda(1710)$	$1/2^+$	*
$\Lambda(1800)$	$1/2^-$	***
$\Lambda(1810)$	$1/2^+$	***
$\Lambda(1820)$	$5/2^+$	****
$\Lambda(1830)$	$5/2^-$	****
$\Lambda(1890)$	$3/2^+$	****
$\Lambda(2000)$	$1/2^-$	*
$\Lambda(2050)$	$3/2^-$	*
$\Lambda(2070)$	$3/2^+$	*
$\Lambda(2080)$	$5/2^-$	*
$\Lambda(2085)$	$7/2^+$	**
$\Lambda(2100)$	$7/2^-$	****
$\Lambda(2110)$	$5/2^+$	***
$\Lambda(2325)$	$3/2^-$	*
$\Lambda(2350)$	$9/2^+$	***
$\Lambda(2585)$	$11/2^- ?$	*

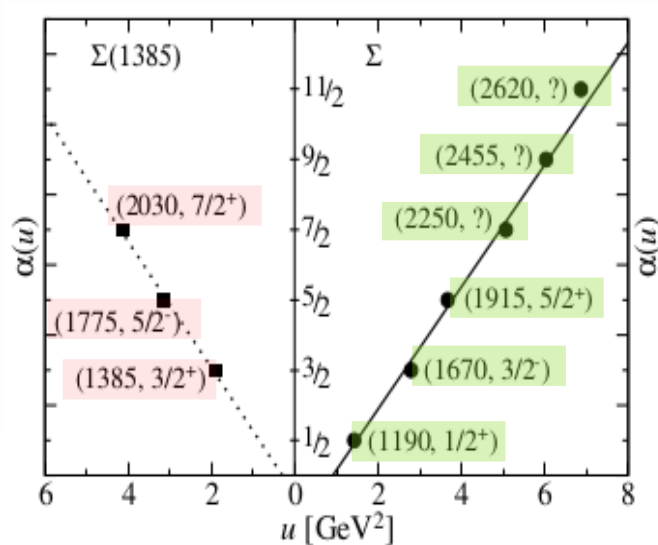
Hyperon Regge trajectories

Storow, Phys.Rept.103.317 (1984)



$$\Lambda : \alpha(u) = -0.65 + 0.94u$$

$$\Lambda(1405) : \text{excluded}$$

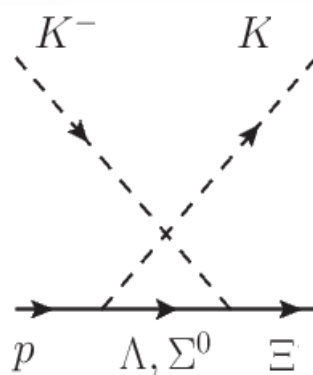


$$\Sigma : \alpha(u) = -0.79 + 0.87u$$

$$\Sigma^* : \alpha(u) = -0.27 + 0.9u$$

$$s_{\text{th}}(K^- p \rightarrow K \Xi)$$

$$= 1.81 \text{ GeV}$$



Σ hyperons

	J^P	status
$\Sigma(1193)$	$1/2^+$	****
$\Sigma(1385)$	$3/2^+$	****
$\Sigma(1580)$	$3/2^-$	*
$\Sigma(1620)$	$1/2^-$	*
$\Sigma(1660)$	$1/2^+$	***
$\Sigma(1670)$	$3/2^-$	****
$\Sigma(1750)$	$1/2^-$	***
$\Sigma(1775)$	$5/2^-$	****
$\Sigma(1780)$	$3/2^+$	*
$\Sigma(1880)$	$1/2^+$	**
$\Sigma(1900)$	$1/2^-$	**
$\Sigma(1910)$	$3/2^-$	***
$\Sigma(1915)$	$5/2^+$	****
$\Sigma(1940)$	$3/2^+$	*
$\Sigma(2010)$	$3/2^-$	*
$\Sigma(2030)$	$7/2^+$	****
$\Sigma(2070)$	$5/2^+$	*
$\Sigma(2080)$	$3/2^+$	*
$\Sigma(2100)$	$7/2^-$	*
$\Sigma(2110)$	$1/2^-$	*
$\Sigma(2230)$	$3/2^+$	*
$\Sigma(2250)$	$7/2^- ?$	**
$\Sigma(2455)$	$9/2^+ ?$	*
$\Sigma(2620)$	$11/2^- ?$	*
$\Sigma(3000)$		*
$\Sigma(3170)$		*

As seen, hyperon Regge trajectories involve many of 3 & 4 star resonances.

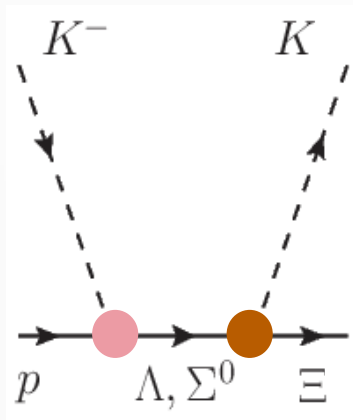
2. $K^- p \rightarrow K \Xi$ theoretical framework

□ PDG 2020

□ We include (Λ^* & Σ^*) resonances which couple strongly to $\bar{K}N$ & $K\Xi$ channels.

□ Partial decay width

$$\Gamma_{Y^* \rightarrow \bar{K}N} = \frac{1}{8\pi} \frac{q_K}{M_{Y^*}^2} \frac{1}{2J_{Y^*} + 1} |\mathcal{M}_{Y^* \rightarrow \bar{K}N}|^2$$



(Λ^*, J^P)	Γ_{Λ^*} [MeV]	status	$\text{Br}_{\Lambda^* \rightarrow N\bar{K}}$ [%]	$ g_{KN\Lambda^*} $	$\text{Br}_{\Lambda^* \rightarrow \Xi K}$ [%]	$ g_{K\Xi\Lambda^*} $
$\Lambda(1820, 5/2^+)$	80	****	55 – 65	8.41	–	–
$\Lambda(1830, 5/2^-)$	90	****	4 – 8	–	–	–
$\Lambda(1890, 3/2^+)$	120	****	24 – 36	1.19	~ 1	0.75
$\Lambda(2000, 1/2^-)$	190	*	27 ± 6	–	–	–
$\Lambda(2050, 3/2^-)$	493	*	19 ± 4	–	–	–
$\Lambda(2070, 3/2^+)$	370	*	12 ± 5	1.01	7 ± 3	1.38
$\Lambda(2080, 5/2^-)$	181	*	11 ± 3	0.71	4 ± 1	1.18
$\Lambda(2085, 7/2^+)$	200	**	–	–	–	–
$\Lambda(2100, 7/2^-)$	200	****	25 – 35	3.40	< 3	< 8.45
$\Lambda(2110, 5/2^+)$	250	***	5 – 25	–	–	–
$\Lambda(2325, 3/2^-)$	168	*	–	–	–	–
$\Lambda(2350, 9/2^+)$	150	***	~ 12	–	–	–
$\Lambda(2585, ?^?)$		**	–	–	–	–

(Σ^*, J^P)	Γ_{Σ^*} [MeV]	status	$\text{Br}_{\Sigma^* \rightarrow N\bar{K}}$ [%]	$ g_{KN\Sigma^*} $	$\text{Br}_{\Sigma^* \rightarrow \Xi K}$ [%]	$ g_{K\Xi\Sigma^*} $
$\Sigma(1880, 1/2^+)$	200	**	10 – 30	–	–	–
$\Sigma(1900, 1/2^-)$	165	**	40 – 70	0.93	3 ± 2	0.1
$\Sigma(1910, 3/2^-)$	220	***	1 – 5	–	–	–
$\Sigma(1915, 5/2^+)$	120	****	5 – 15	1.97	–	–
$\Sigma(1940, 3/2^+)$	250	*	13 ± 2	–	–	–
$\Sigma(2010, 3/2^-)$	178	*	7 ± 3	1.26	3 ± 2	3.71
$\Sigma(2030, 7/2^+)$	180	****	17 – 23	0.82	< 2	< 1.41
$\Sigma(2070, 5/2^+)$	200	*	–	–	–	–
$\Sigma(2080, 3/2^+)$	170	*	–	–	–	–
$\Sigma(2100, 7/2^-)$	260	*	8 ± 2	–	–	–
$\Sigma(2160, 1/2^-)$	313	*	29 ± 7	–	–	–
$\Sigma(2230, 3/2^+)$	345	*	6 ± 2	0.41	2 ± 1	0.34
$\Sigma(2250, ?^?)$	100	***	< 10	< 0.59	–	–
$\Sigma(2455, ?^?)$	120	**	–	–	–	–
$\Sigma(2620, ?^?)$	200	**	–	–	–	–

2. $K^- p \rightarrow K \Xi$ theoretical framework

□ PDG 2020

□ We include (Λ^* & Σ^*) resonances which couple strongly to $\bar{K}N$ & $K\Xi$ channels.

□ Partial decay width

$$\Gamma_{Y^* \rightarrow \bar{K}N} = \frac{1}{8\pi} \frac{q_K}{M_{Y^*}^2} \frac{1}{2J_{Y^*} + 1} |\mathcal{M}_{Y^* \rightarrow \bar{K}N}|^2$$

$$\mathcal{L}_{\Lambda NK}^{1/2(\pm)} \equiv g_{\Lambda NK} \bar{\Lambda} (D_{\Lambda NK}^{1/2(\pm)} \bar{K}) N + \text{H.c.}$$

$$\mathcal{L}_{\Lambda NK}^{3/2(\pm)} = \frac{g_{\Lambda NK}}{m_K} \bar{\Lambda}^\nu (D_\nu^{3/2(\pm)} \bar{K}) N + \text{H.c.}$$

$$\mathcal{L}_{\Lambda NK}^{5/2(\pm)} = \frac{g_{\Lambda NK}}{m_K^2} \bar{\Lambda}^{\mu\nu} (D_{\mu\nu}^{5/2(\pm)} \bar{K}) N + \text{H.c.}$$

$$\mathcal{L}_{\Lambda NK}^{7/2(\pm)} = \frac{g_{\Lambda NK}}{m_K^3} \bar{\Lambda}^{\mu\nu\rho} (D_{\mu\nu\rho}^{7/2(\pm)} \bar{K}) N + \text{H.c.}$$

(Λ^*, J^P)	Γ_{Λ^*} [MeV]	status	$\text{Br}_{\Lambda^* \rightarrow N\bar{K}}$ [%]	$ g_{KN\Lambda^*} $	$\text{Br}_{\Lambda^* \rightarrow \Xi K}$ [%]	$ g_{K\Xi\Lambda^*} $
$\Lambda(1820, 5/2^+)$	80	****	55 – 65	8.41	–	–
$\Lambda(1830, 5/2^-)$	90	****	4 – 8	–	–	–
$\Lambda(1890, 3/2^+)$	120	****	24 – 36	1.19	~ 1	0.75
$\Lambda(2000, 1/2^-)$	190	*	27 ± 6	–	–	–
$\Lambda(2050, 3/2^-)$	493	*	19 ± 4	–	–	–
$\Lambda(2070, 3/2^+)$	370	*	12 ± 5	1.01	7 ± 3	1.38
$\Lambda(2080, 5/2^-)$	181	*	11 ± 3	0.71	4 ± 1	1.18
$\Lambda(2085, 7/2^+)$	200	**	–	–	–	–
$\Lambda(2100, 7/2^-)$	200	****	25 – 35	3.40	< 3	< 8.45
$\Lambda(2110, 5/2^+)$	250	***	5 – 25	–	–	–
$\Lambda(2325, 3/2^-)$	168	*	–	–	–	–
$\Lambda(2350, 9/2^+)$	150	***	~ 12	–	–	–
$\Lambda(2585, ?^?)$		**	–	–	–	–

(Σ^*, J^P)	Γ_{Σ^*} [MeV]	status	$\text{Br}_{\Sigma^* \rightarrow N\bar{K}}$ [%]	$ g_{KN\Sigma^*} $	$\text{Br}_{\Sigma^* \rightarrow \Xi K}$ [%]	$ g_{K\Xi\Sigma^*} $
$\Sigma(1880, 1/2^+)$	200	**	10 – 30	–	–	–
$\Sigma(1900, 1/2^-)$	165	**	40 – 70	0.93	3 ± 2	0.1
$\Sigma(1910, 3/2^-)$	220	***	1 – 5	–	–	–
$\Sigma(1915, 5/2^+)$	120	****	5 – 15	1.97	–	–
$\Sigma(1940, 3/2^+)$	250	*	13 ± 2	–	–	–
$\Sigma(2010, 3/2^-)$	178	*	7 ± 3	1.26	3 ± 2	3.71
$\Sigma(2030, 7/2^+)$	180	****	17 – 23	0.82	< 2	< 1.41
$\Sigma(2070, 5/2^+)$	200	*	–	–	–	–
$\Sigma(2080, 3/2^+)$	170	*	–	–	–	–
$\Sigma(2100, 7/2^-)$	260	*	8 ± 2	–	–	–
$\Sigma(2160, 1/2^-)$	313	*	29 ± 7	–	–	–
$\Sigma(2230, 3/2^+)$	345	*	6 ± 2	0.41	2 ± 1	0.34
$\Sigma(2250, ?^?)$	100	***	< 10	< 0.59	–	–
$\Sigma(2455, ?^?)$	120	**	–	–	–	–
$\Sigma(2620, ?^?)$	200	**	–	–	–	–

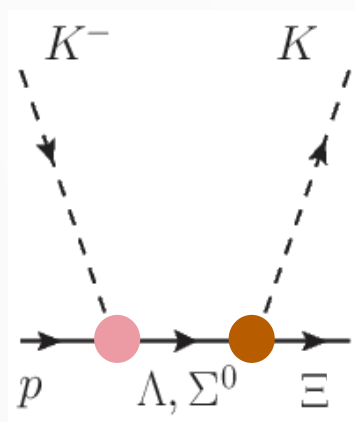
2. $K^- p \rightarrow K \Xi$ theoretical framework

□ PDG 2020

□ We include (Λ^* & Σ^*) resonances which couple strongly to $\bar{K}N$ & $K\Xi$ channels.

□ Partial decay width

$$\Gamma_{Y^* \rightarrow \bar{K}N} = \frac{1}{8\pi} \frac{q_K}{M_{Y^*}^2} \frac{1}{2J_{Y^*} + 1} |\mathcal{M}_{Y^* \rightarrow \bar{K}N}|^2$$



✓ turn out to be important.

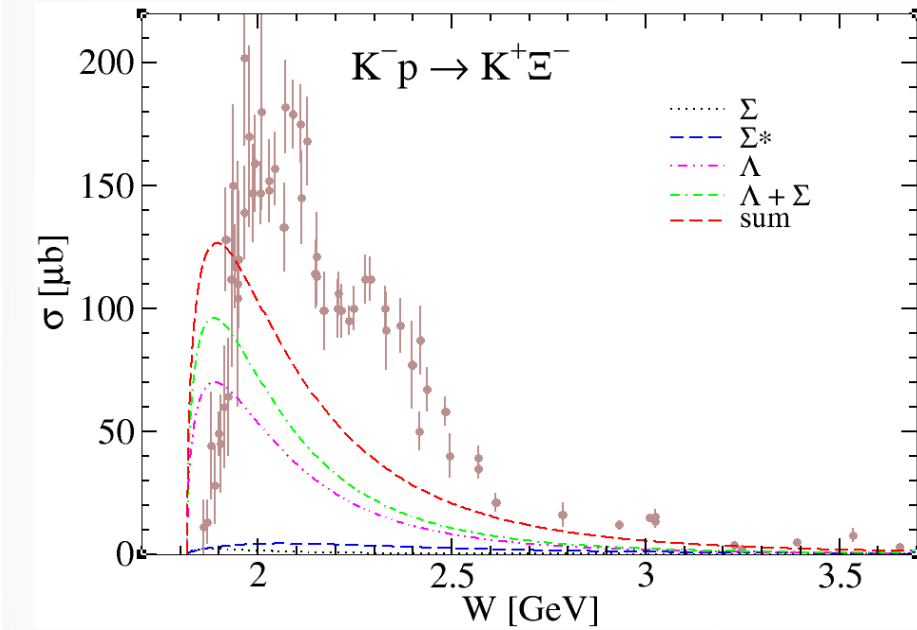
(Λ^*, J^P)	Γ_{Λ^*} [MeV]	status	$\text{Br}_{\Lambda^* \rightarrow N\bar{K}}$ [%]	$ g_{KN\Lambda^*} $	$\text{Br}_{\Lambda^* \rightarrow \Xi K}$ [%]	$ g_{K\Xi\Lambda^*} $
$\Lambda(1820, 5/2^+)$	80	****	55 – 65	8.41	–	–
$\Lambda(1830, 5/2^-)$	90	****	4 – 8	–	–	–
✓ $\Lambda(1890, 3/2^+)$	120	****	24 – 36	1.19	~ 1	0.75
$\Lambda(2000, 1/2^-)$	190	*	27 ± 6	–	–	–
$\Lambda(2050, 3/2^-)$	493	*	19 ± 4	–	–	–
$\Lambda(2070, 3/2^+)$	370	*	12 ± 5	1.01	7 ± 3	1.38
$\Lambda(2080, 5/2^-)$	181	*	11 ± 3	0.71	4 ± 1	1.18
$\Lambda(2085, 7/2^+)$	200	**	–	–	–	–
$\Lambda(2100, 7/2^-)$	200	****	25 – 35	3.40	< 3	< 8.45
$\Lambda(2110, 5/2^+)$	250	***	5 – 25	–	–	–
$\Lambda(2325, 3/2^-)$	168	*	–	–	–	–
$\Lambda(2350, 9/2^+)$	150	***	~ 12	–	–	–
$\Lambda(2585, ?^?)$		**	–	–	–	–

(Σ^*, J^P)	Γ_{Σ^*} [MeV]	status	$\text{Br}_{\Sigma^* \rightarrow N\bar{K}}$ [%]	$ g_{KN\Sigma^*} $	$\text{Br}_{\Sigma^* \rightarrow \Xi K}$ [%]	$ g_{K\Xi\Sigma^*} $
$\Sigma(1880, 1/2^+)$	200	**	10 – 30	–	–	–
$\Sigma(1900, 1/2^-)$	165	**	40 – 70	0.93	3 ± 2	0.1
$\Sigma(1910, 3/2^-)$	220	***	1 – 5	–	–	–
$\Sigma(1915, 5/2^+)$	120	****	5 – 15	1.97	–	–
$\Sigma(1940, 3/2^+)$	250	*	13 ± 2	–	–	–
$\Sigma(2010, 3/2^-)$	178	*	7 ± 3	1.26	3 ± 2	3.71
✓ $\Sigma(2030, 7/2^+)$	180	****	17 – 23	0.82	< 2	< 1.41
$\Sigma(2070, 5/2^+)$	200	*	–	–	–	–
$\Sigma(2080, 3/2^+)$	170	*	–	–	–	–
$\Sigma(2100, 7/2^-)$	260	*	8 ± 2	–	–	–
$\Sigma(2160, 1/2^-)$	313	*	29 ± 7	–	–	–
✓ $\Sigma(2230, 3/2^+)$	345	*	6 ± 2	0.41	2 ± 1	0.34
✓ $\Sigma(2250, ?^?)$	100	***	< 10	< 0.59	–	–
$\Sigma(2455, ?^?)$	120	**	–	–	–	–
$\Sigma(2620, ?^?)$	200	**	–	–	–	–

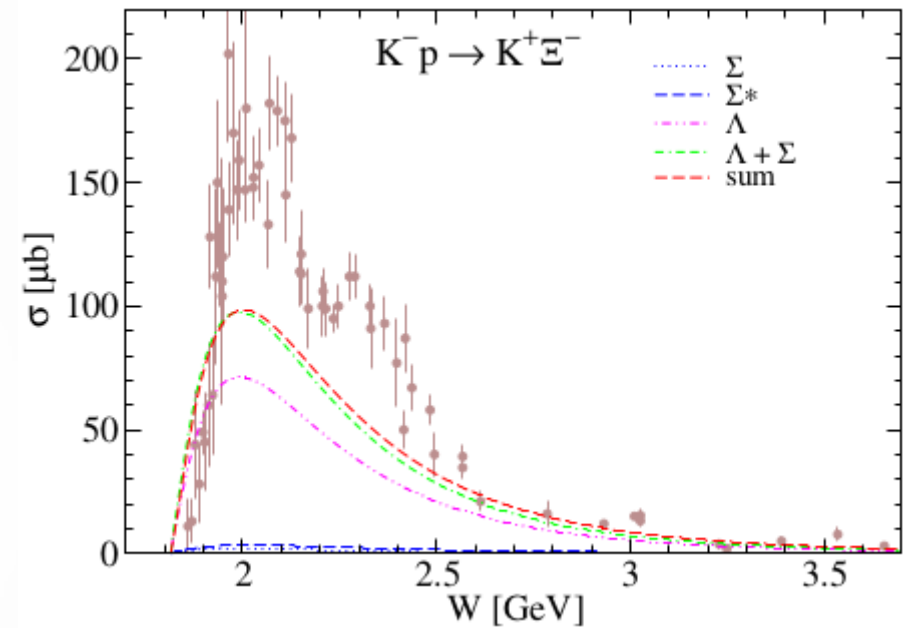
3. $K^- p \rightarrow K^+ \Xi^-$ results

□ Total cross section ($K^- p \rightarrow K^+ \Xi^-$) [u -channel background]

> pseudoscalar (ps) form ($\lambda=1$)

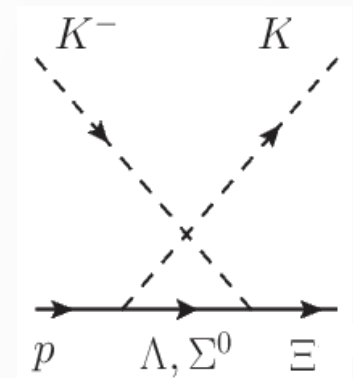


> pseudovector (pv) form ($\lambda=0$)



$$\mathcal{L}_{\Lambda NK}^{1/2(\pm)} \equiv g_{\Lambda NK} \bar{\Lambda} (D_{\Lambda NK}^{1/2(\pm)} \bar{K}) N + \text{H.c.}$$

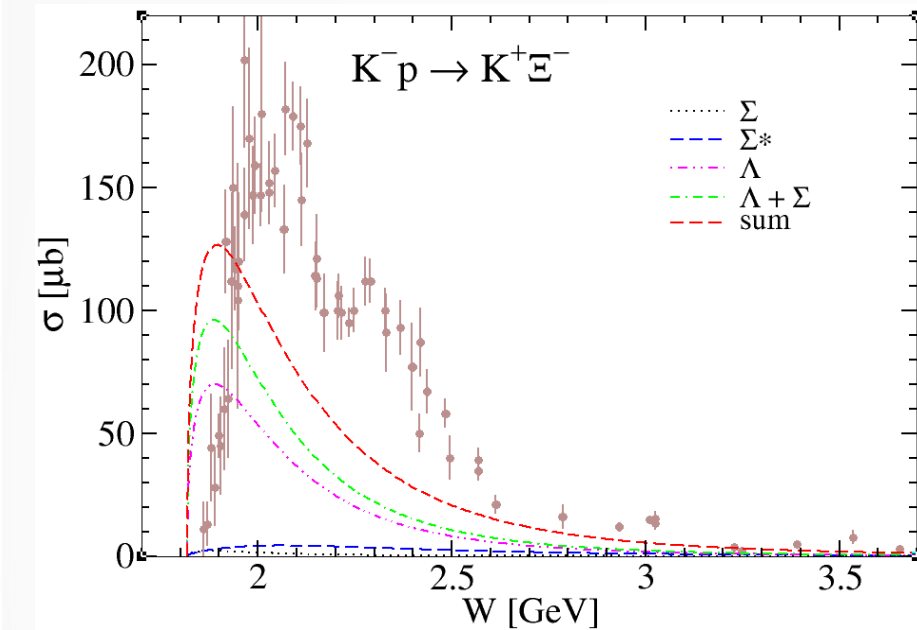
$$D_{B'BM}^{1/2(\pm)} \equiv -\Gamma^{(\pm)} \left(\pm i\lambda + \frac{1 - \lambda}{m_{B'} \pm m_B} \not{\partial} \right)$$



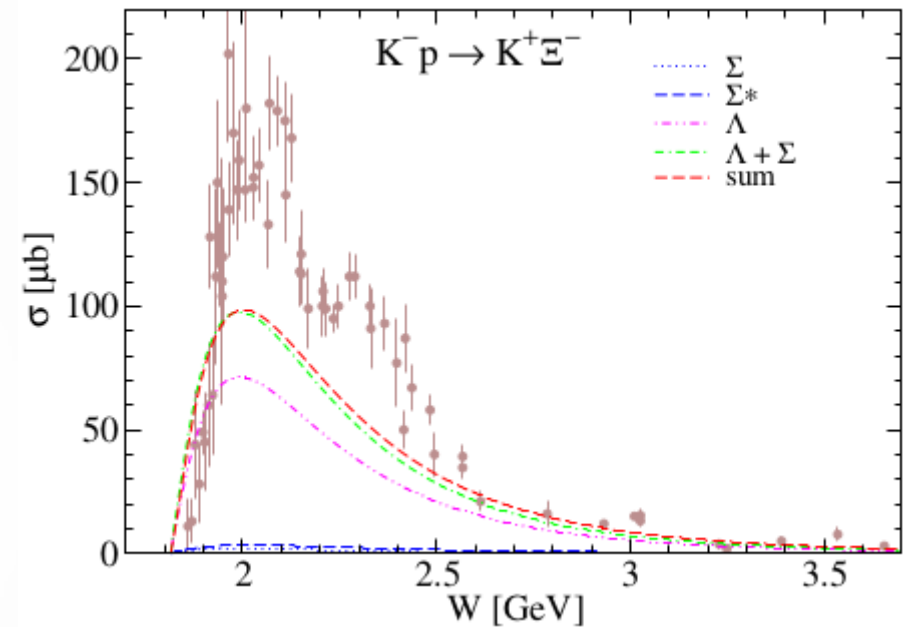
3. $K^- p \rightarrow K^+ \Xi^-$ results

□ Total cross section ($K^- p \rightarrow K^+ \Xi^-$) [u -channel background]

> pseudoscalar (ps) form ($\lambda=1$)



> pseudovector (pv) form ($\lambda=0$)

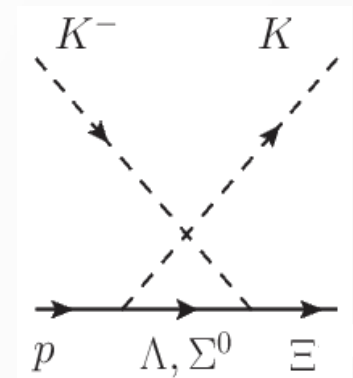


$$\mathcal{L}_{\Lambda NK}^{1/2(\pm)} \equiv g_{\Lambda NK} \bar{\Lambda} (D_{\Lambda NK}^{1/2(\pm)} \bar{K}) N + \text{H.c.}$$

$$D_{B'BM}^{1/2(\pm)} \equiv -\Gamma^{(\pm)} \left(\pm i\lambda + \frac{1 - \lambda}{m_{B'} \pm m_B} \not{\partial} \right)$$

s_{th} : $\sigma(\text{ps}) > \sigma(\text{pv})$

high energy: $\sigma(\text{ps}) < \sigma(\text{pv})$

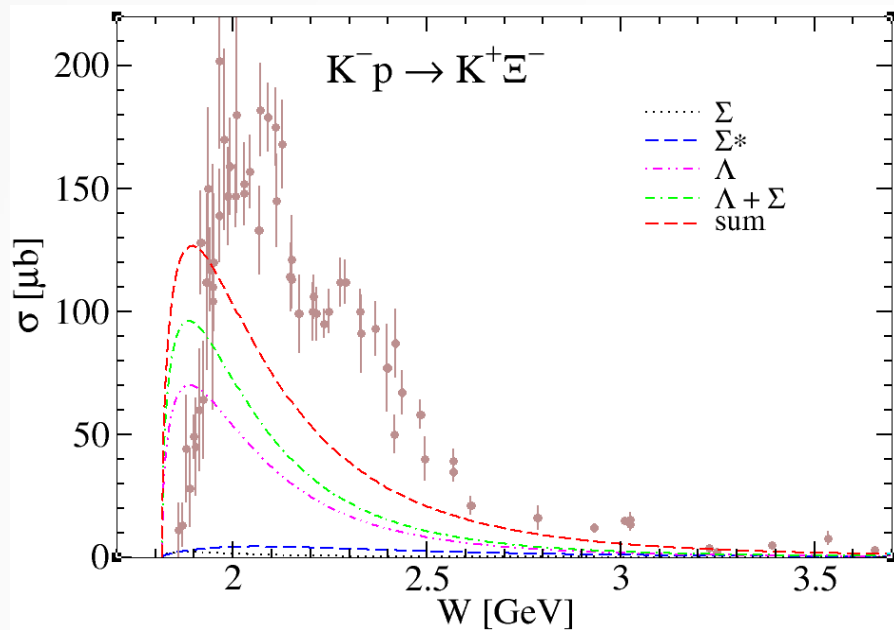


> We adopt the pv scheme rather than the ps scheme.

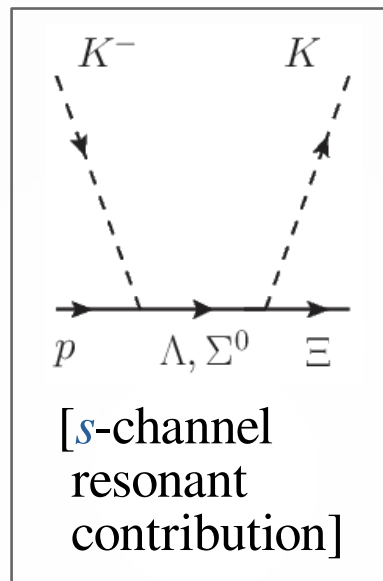
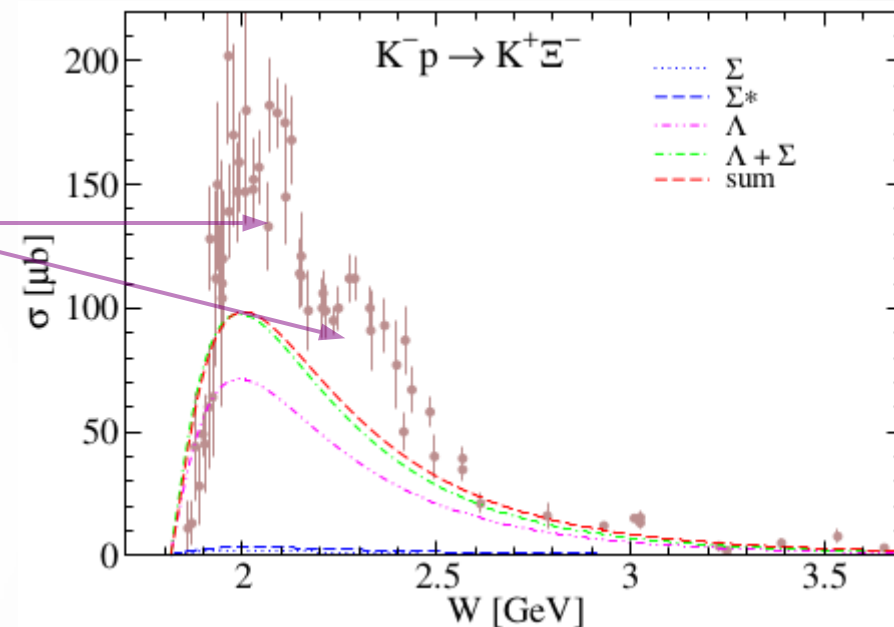
3. $K^- p \rightarrow K^+ \Xi^-$ results

□ Total cross section ($K^- p \rightarrow K^+ \Xi^-$) [u -channel background]

> pseudoscalar (ps) form ($\lambda=1$)



> pseudovector (pv) form ($\lambda=0$)

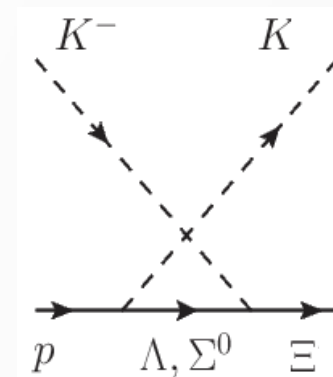


$$\mathcal{L}_{\Lambda NK}^{1/2(\pm)} \equiv g_{\Lambda NK} \bar{\Lambda} (D_{\Lambda NK}^{1/2(\pm)} \bar{K}) N + \text{H.c.}$$

$$D_{B'BM}^{1/2(\pm)} \equiv -\Gamma^{(\pm)} \left(\pm i\lambda + \frac{1 - \lambda}{m_{B'} \pm m_B} \not{\partial} \right)$$

s_{th} : $\sigma(\text{ps}) > \sigma(\text{pv})$

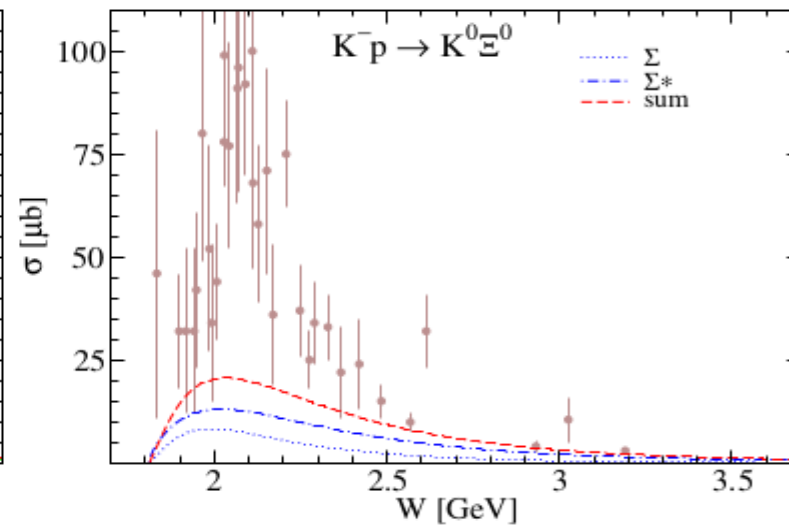
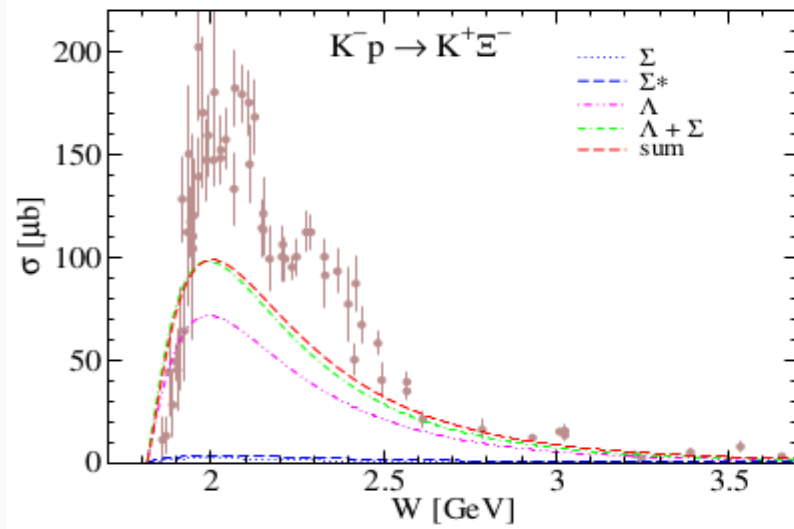
high energy: $\sigma(\text{ps}) < \sigma(\text{pv})$



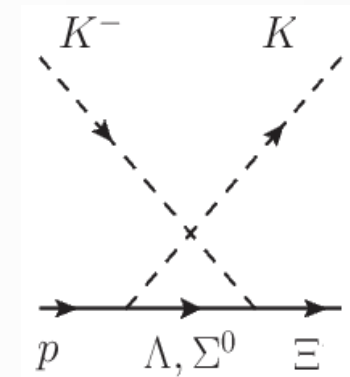
> We adopt the pv scheme rather than the ps scheme.

3. $K^- p \rightarrow K \Xi$ results

□ Total cross section ($K^- p \rightarrow K^+ \Xi^-$ & $K^0 \Xi^0$) [u -channel background, pv form]

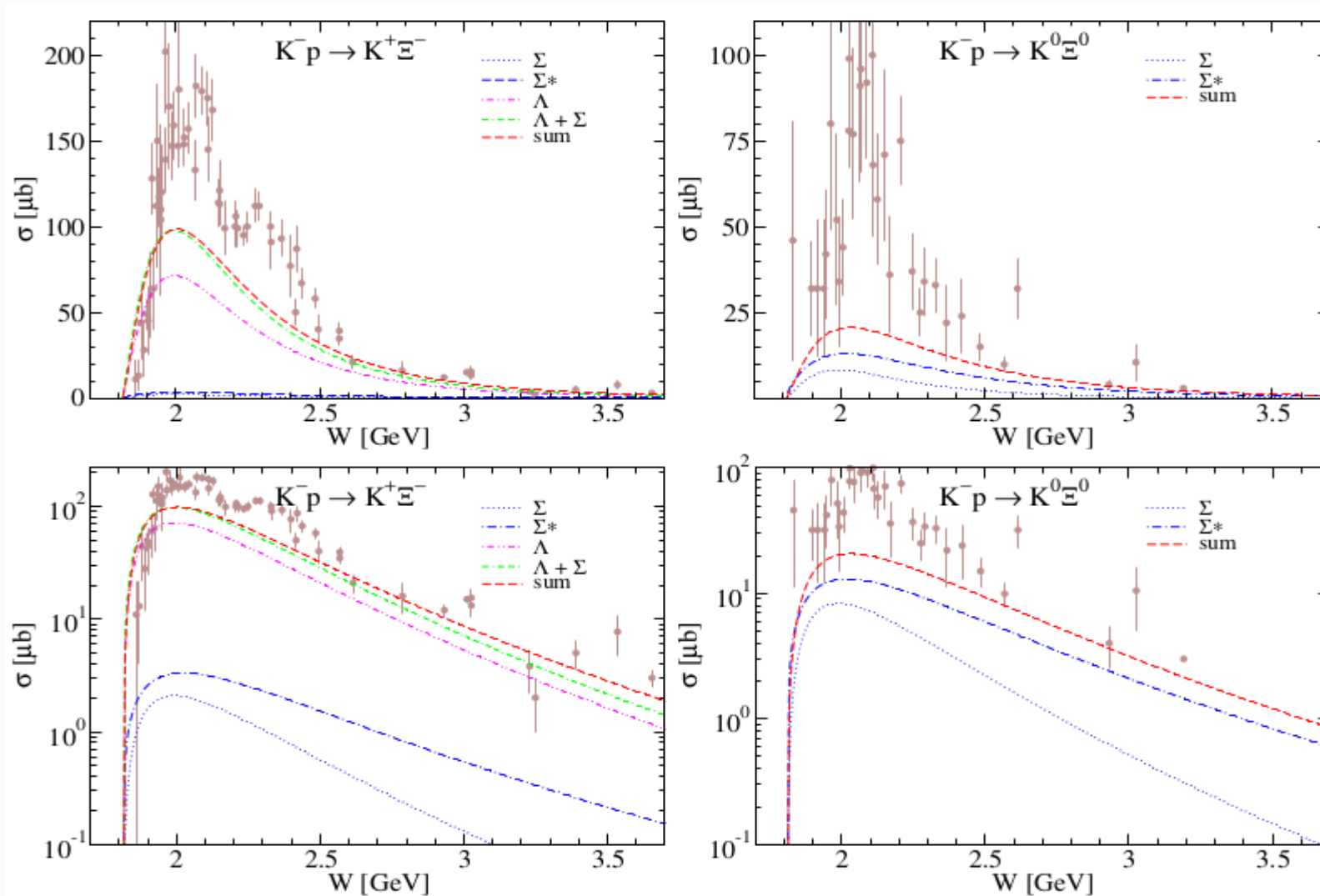


□ Isospin rule
 $> u$ -channel Σ & Σ^* exchange
 $\sigma(K^- p \rightarrow K^+ \Xi^-) \times 4$
 $= \sigma(K^- p \rightarrow K^0 \Xi^0)$



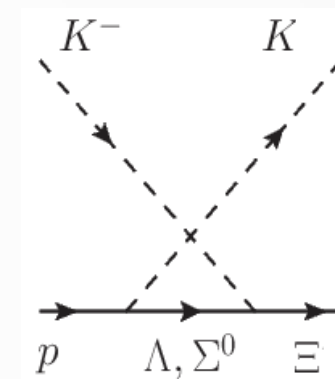
3. $K^- p \rightarrow K \Xi$ results

□ Total cross section ($K^- p \rightarrow K^+ \Xi^-$ & $K^0 \Xi^0$) [u -channel background, pv form]



log scale:

□ Isospin rule
 > u -channel Σ & Σ^* exchange
 $\sigma(K^- p \rightarrow K^+ \Xi^-) \times 4$
 $= \sigma(K^- p \rightarrow K^0 \Xi^0)$



> Analytical behavior:

$$\lim_{s \rightarrow \infty} \sum_{s_i, s_f} |\mathcal{M}_\Sigma(s, u)|^2 \propto s$$

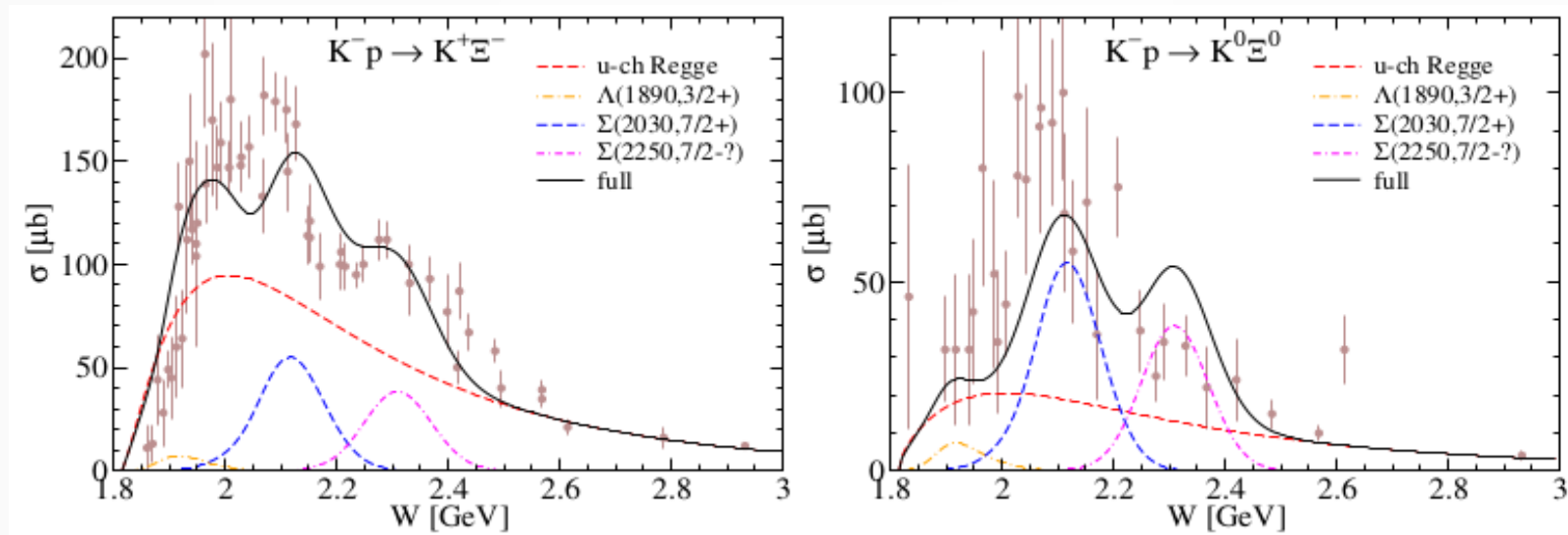
> Asymptotic behavior:

$$\frac{d\sigma}{du}(s \rightarrow \infty, u \rightarrow 0) \propto s^{2\alpha(u)-2}$$

> u -channel Regge amplitudes describe high energies ($W \gtrsim 2.5$ GeV) very well.

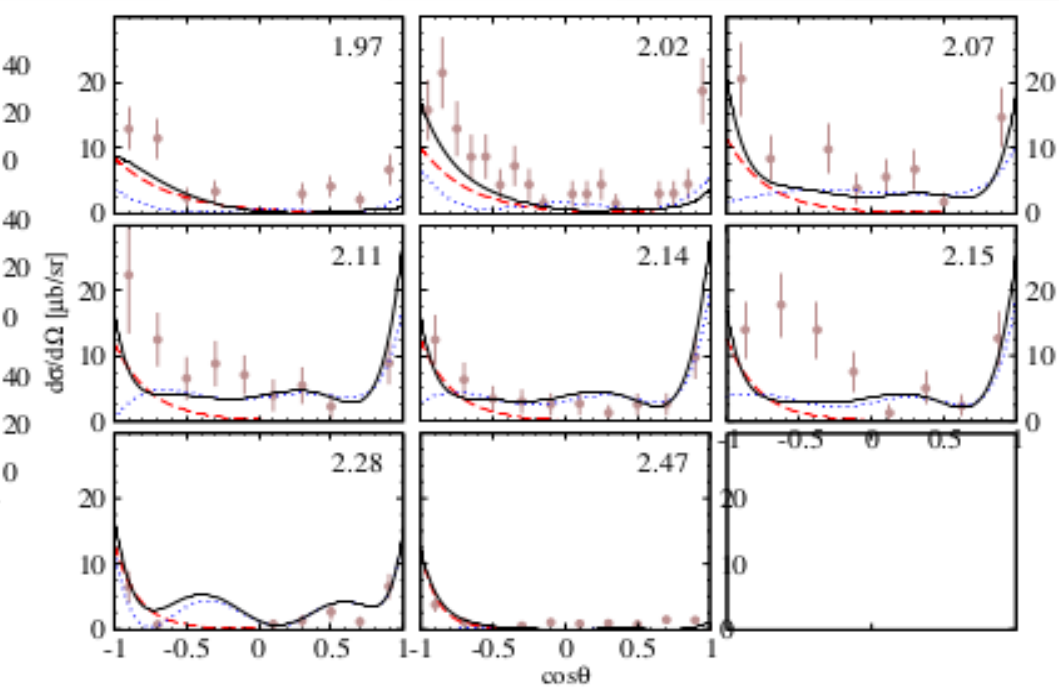
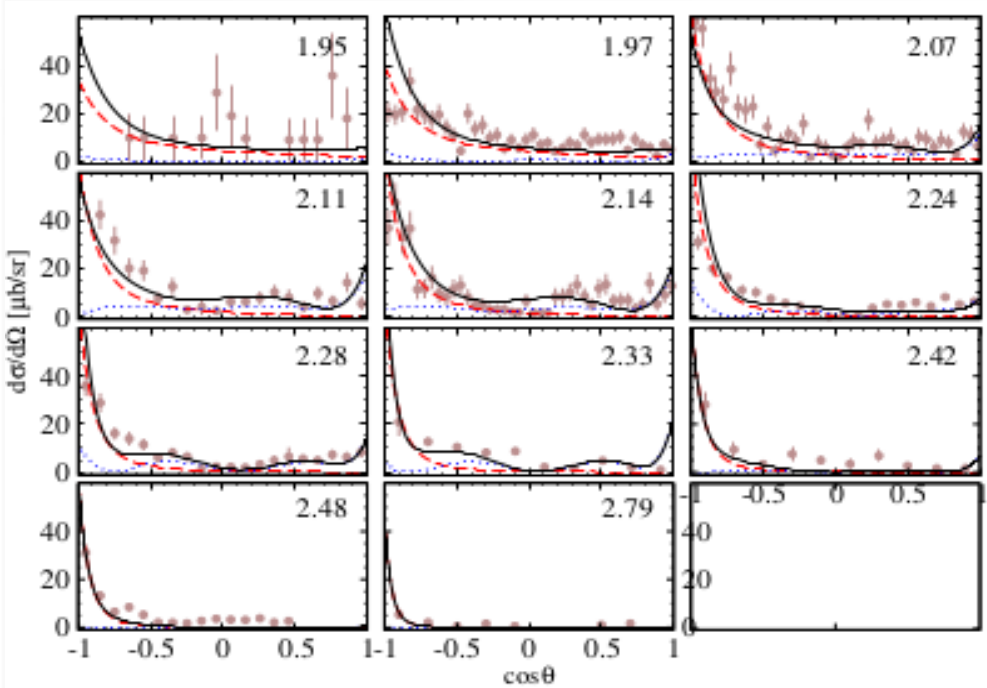
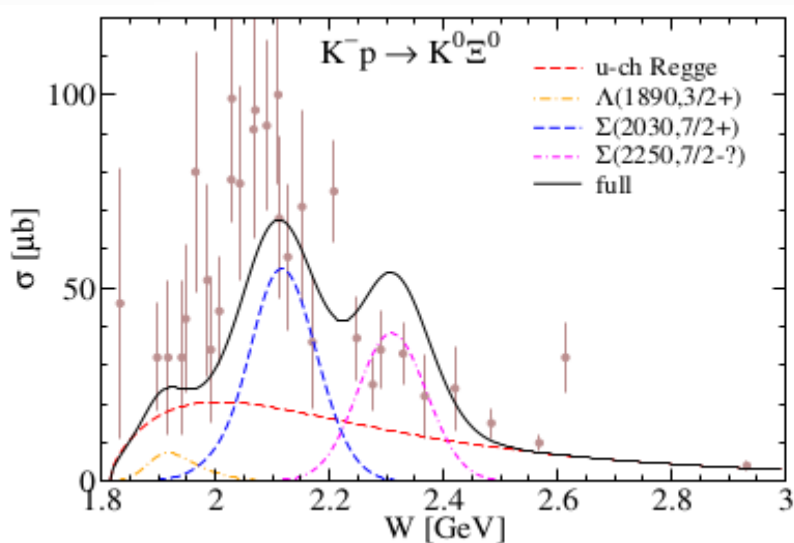
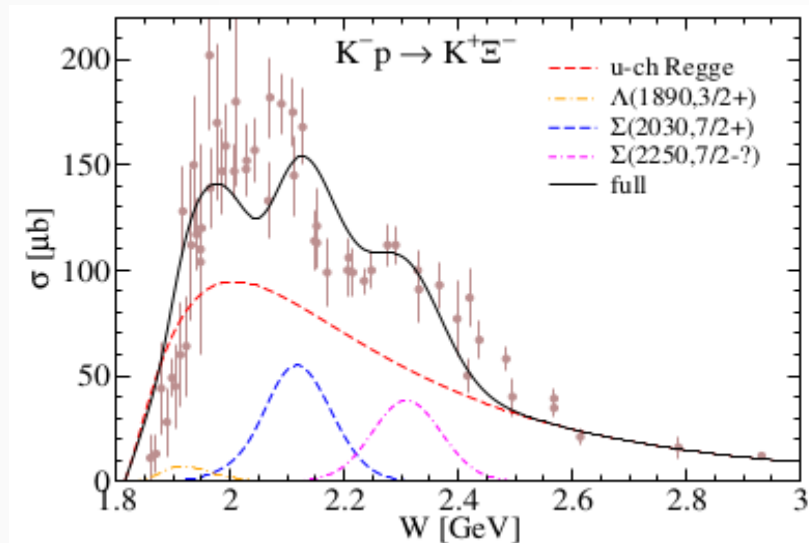
3. $K^- p \rightarrow K \Xi$ results

□ Total & Differential cross sections ($K^- p \rightarrow K^+ \Xi^-$ & $K^0 \Xi^0$) [u -channel background + s -channel Λ^* & Σ^*]



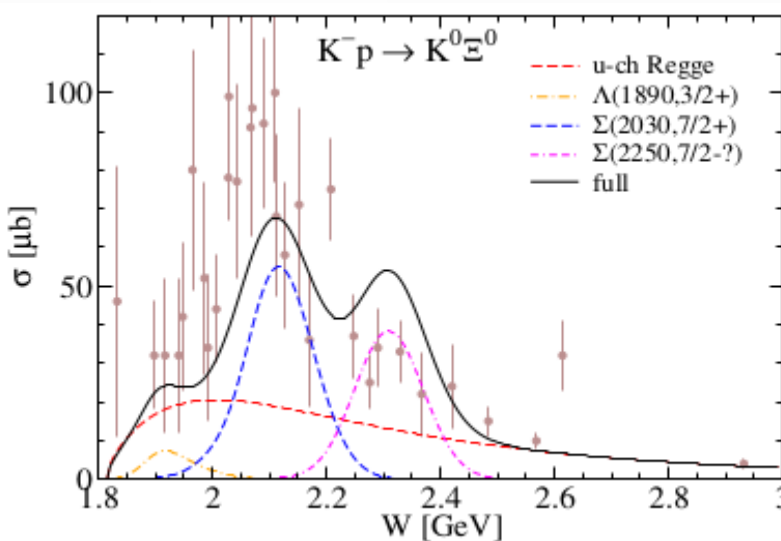
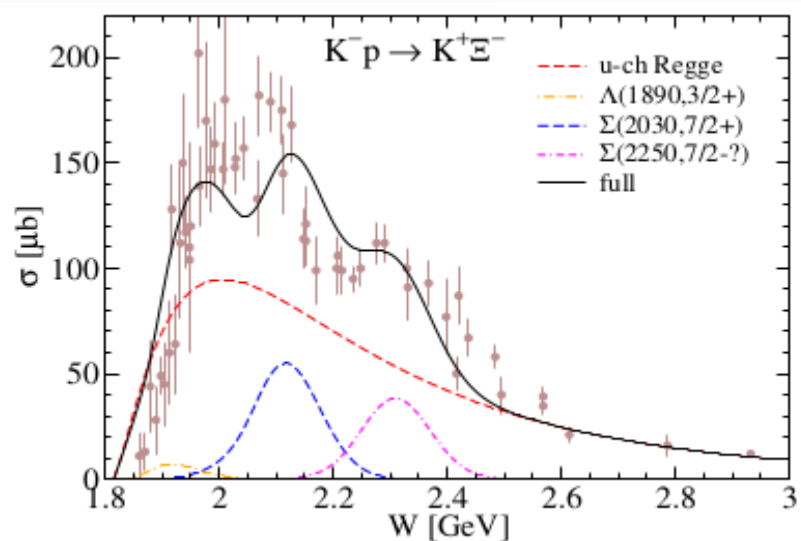
3. $K^- p \rightarrow K \Xi$ results

□ Total & Differential cross sections ($K^- p \rightarrow K^+ \Xi^-$ & $K^0 \Xi^0$) [u -channel background + s -channel Λ^* & Σ^*]

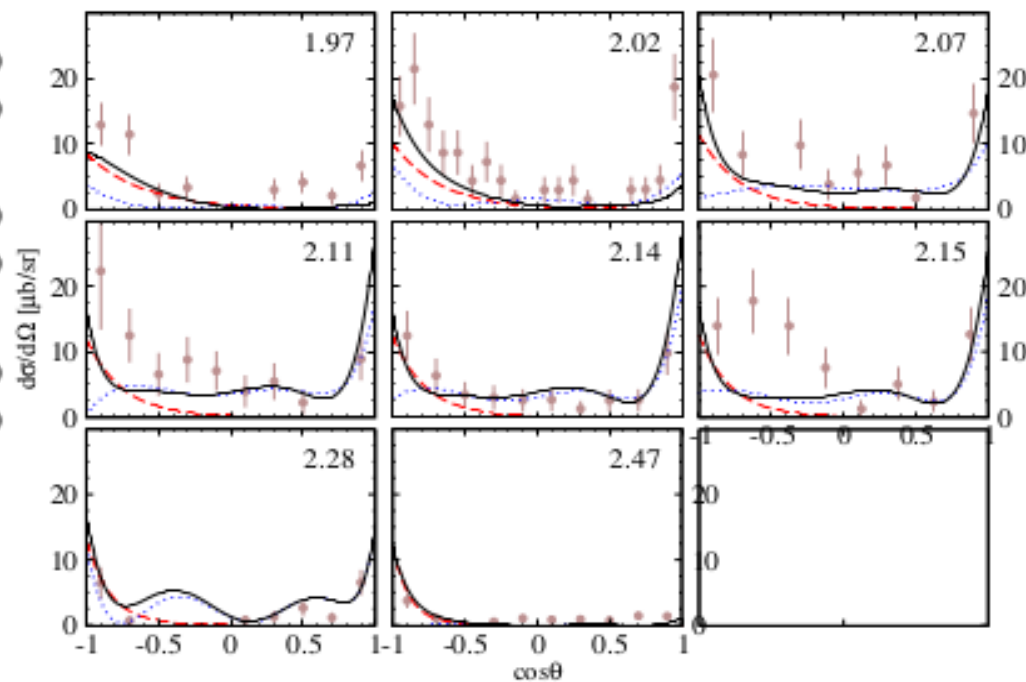
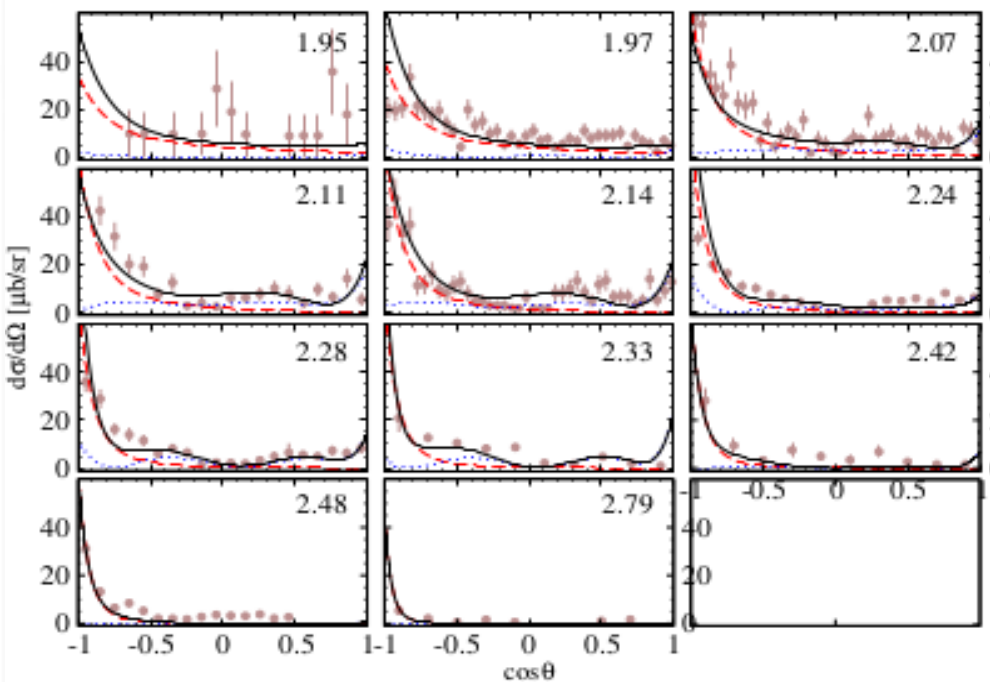


3. $K^- p \rightarrow K \Xi$ results

□ Total & Differential cross sections ($K^- p \rightarrow K^+ \Xi^-$ & $K^0 \Xi^0$) [u -channel background + s -channel Λ^* & Σ^*]



> Backward peaks due to a u -channel background contribution are clearly verified.
 > Inclusion of various s -channel Λ^* & Σ^* resonances provides good agreement with the data.



3. $K^- p \rightarrow K \Xi$ results

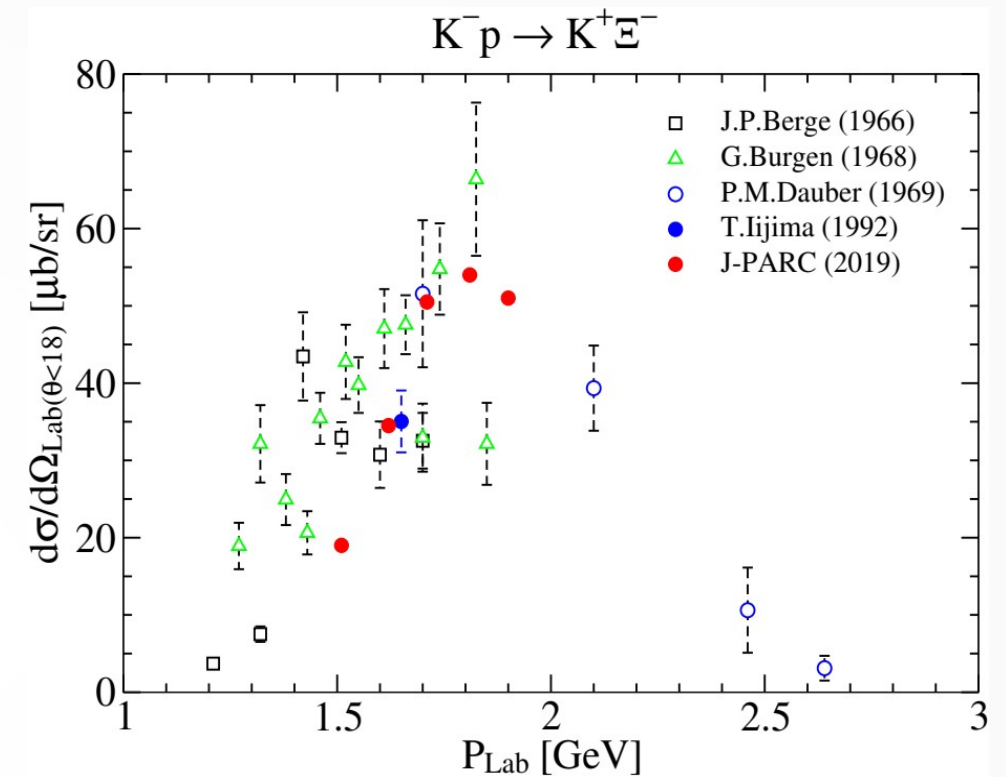
- We used old experimental data taken in 1960s and 1970s.

3. $K^- p \rightarrow K^+ \Xi^-$ results

- We used old experimental data taken in 1960s and 1970s.
- Recently, the J-PARC E05 experiment measured the cross section at forward angles ($\theta_{\text{Lab}} < 18^\circ$).

Nagae et al. AIP Conf. Proc. 2130, 020015 (2019)

Observation of a Ξ^- bound state in the $^{12}\text{C}(K^-, K^+)$ reaction at 1.8 GeV/c



3. $K^- p \rightarrow K^+ \Xi^-$ results

- We used old experimental data taken in 1960s and 1970s.
- Recently, the J-PARC E05 experiment measured the cross section at forward angles ($\theta_{\text{Lab}} < 18^\circ$).

Nagae et al. AIP Conf. Proc. 2130, 020015 (2019)

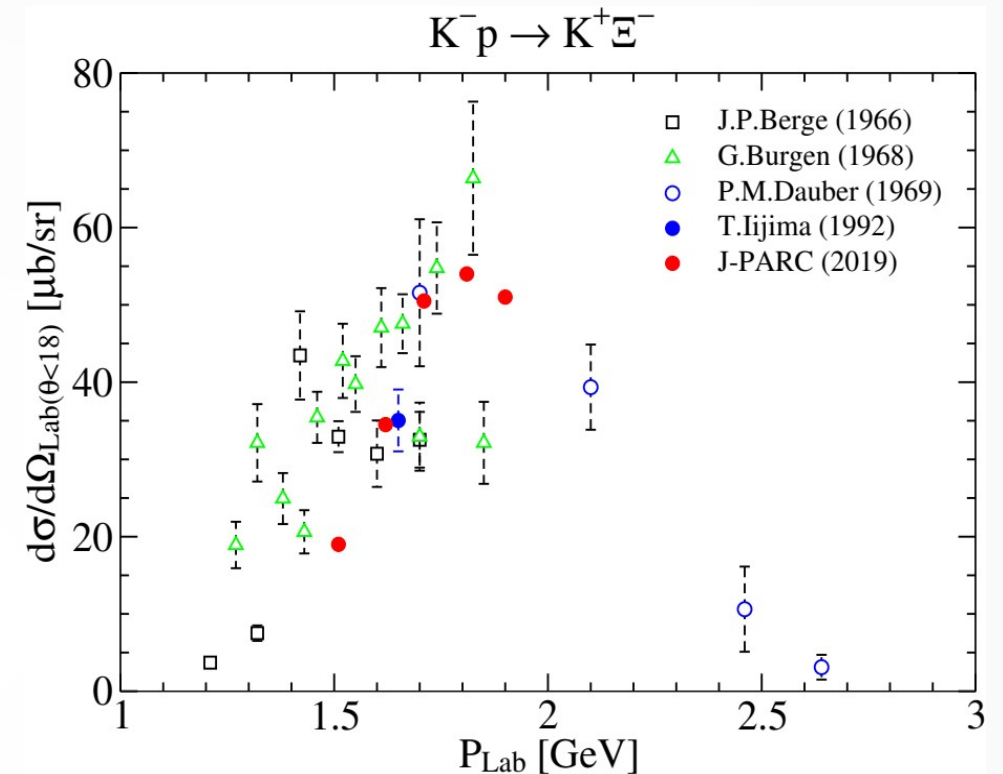
Observation of a Ξ bound state in the $^{12}\text{C}(K^-, K^+)$ reaction at 1.8 GeV/c

- Relations between c.m. and Lab frames:

$$\cos \theta_{\text{lab}} = (\varepsilon_{K^-L} \varepsilon_{K^+L} - \varepsilon_{K^-} \varepsilon_{K^+} + p p_{K^+} \cos \theta_{\text{c.m.}}) / p_{\text{lab}} p_{K^+L}$$

$$\frac{(d\sigma/d\Omega)_L}{(d\sigma/d\Omega)_{\text{c.m.}}} = \frac{m_N p_{\text{lab}} p_{K^+L}}{p p_{K^+}} (\varepsilon_{K^-L} + m_N - p_{\text{lab}} \varepsilon_{K^+L} \cos \theta_{\text{lab}} / p_{K^+L})^{-1}$$

$$\left\langle \frac{d\sigma}{d\Omega_L} \right\rangle_{AV} = \int_0^{\theta_{\text{max}}} d(\cos \theta_L) d\sigma / d\Omega_L \Big/ \int_0^{\theta_{\text{max}}} d(\cos \theta_L)$$



3. $K^- p \rightarrow K^+ \Xi^-$ results

- We used old experimental data taken in 1960s and 1970s.
- Recently, the J-PARC E05 experiment measured the cross section at forward angles ($\theta_{\text{Lab}} < 18^\circ$).

Nagae et al. AIP Conf. Proc. 2130, 020015 (2019)

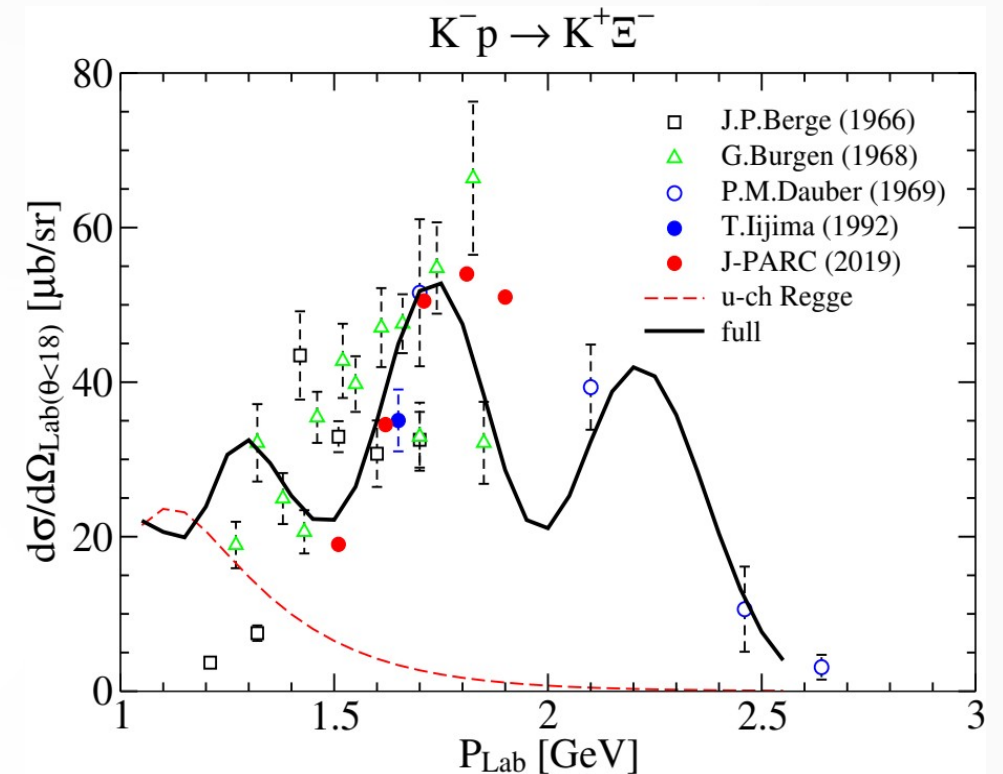
Observation of a Ξ bound state in the $^{12}\text{C}(K^-, K^+)$ reaction at 1.8 GeV/c

- Relations between c.m. and Lab frames:

$$\cos \theta_{\text{lab}} = (\epsilon_{K^-L} \epsilon_{K^+L} - \epsilon_{K^-} \epsilon_{K^+} + p p_{K^+} \cos \theta_{\text{c.m.}}) / p_{\text{lab}} p_{K^+L}$$

$$\frac{(d\sigma/d\Omega)_L}{(d\sigma/d\Omega)_{\text{c.m.}}} = \frac{m_N p_{\text{lab}} p_{K^+L}}{p p_{K^+}} (\epsilon_{K^-L} + m_N - p_{\text{lab}} \epsilon_{K^+L} \cos \theta_{\text{lab}} / p_{K^+L})^{-1}$$

$$\left\langle \frac{d\sigma}{d\Omega_L} \right\rangle_{AV} = \int_0^{\theta_{\text{max}}} d(\cos \theta_L) d\sigma / d\Omega_L \bigg/ \int_0^{\theta_{\text{max}}} d(\cos \theta_L)$$



3. $K^- p \rightarrow K^+ \Xi^-$ results

- We used old experimental data taken in 1960s and 1970s.
- Recently, the J-PARC E05 experiment measured the cross section at forward angles ($\theta_{\text{Lab}} < 18^\circ$).

Nagae et al. AIP Conf. Proc. 2130, 020015 (2019)

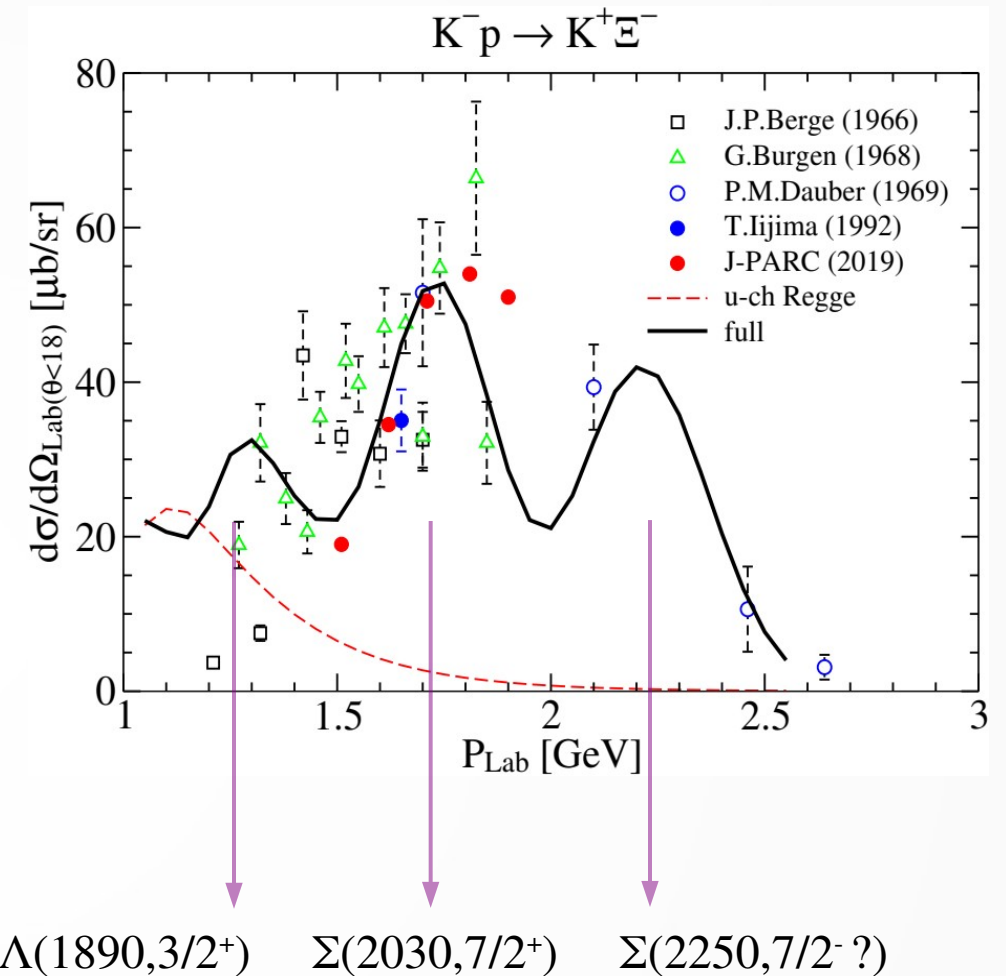
Observation of a Ξ bound state in the $^{12}\text{C}(K^-, K^+)$ reaction at 1.8 GeV/c

- Relations between c.m. and Lab frames:

$$\cos \theta_{\text{lab}} = (\epsilon_{K-L} \epsilon_{K+L} - \epsilon_{K^-} \epsilon_{K^+} + p p_{K^+} \cos \theta_{\text{c.m.}}) / p_{\text{lab}} p_{K+L}$$

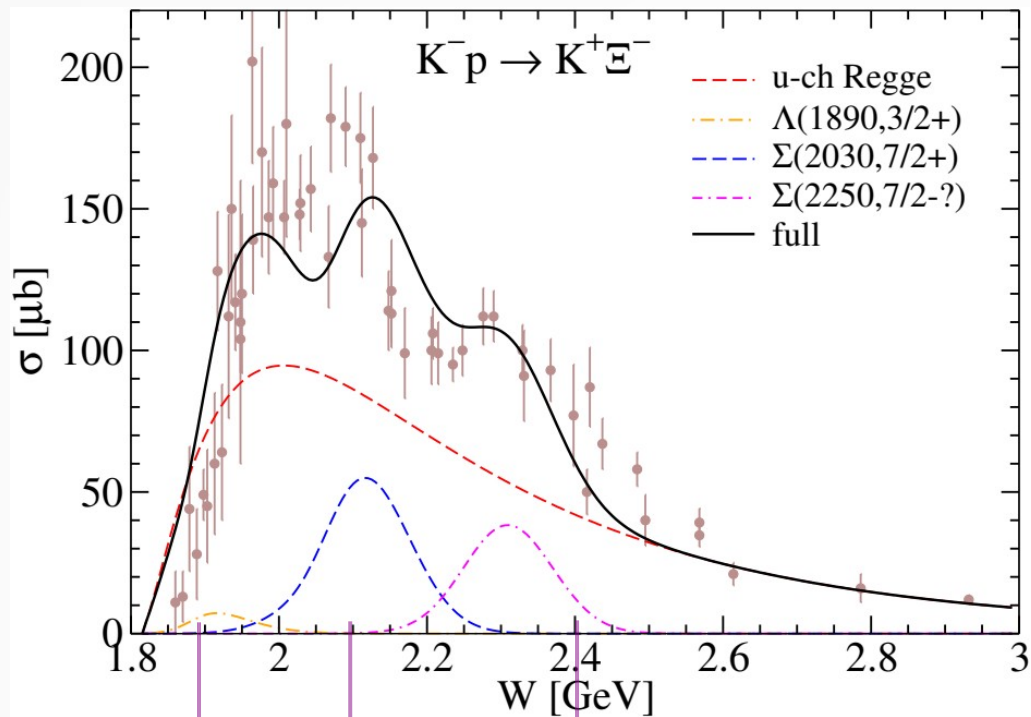
$$\frac{(d\sigma/d\Omega)_L}{(d\sigma/d\Omega)_{\text{c.m.}}} = \frac{m_N p_{\text{lab}} p_{K+L}}{p p_{K^+}} (\epsilon_{K-L} + m_N - p_{\text{lab}} \epsilon_{K+L} \cos \theta_{\text{lab}} / p_{K+L})^{-1}$$

$$\left\langle \frac{d\sigma}{d\Omega_L} \right\rangle_{AV} = \int_0^{\theta_{\text{max}}} d(\cos \theta_L) d\sigma / d\Omega_L \Big/ \int_0^{\theta_{\text{max}}} d(\cos \theta_L)$$

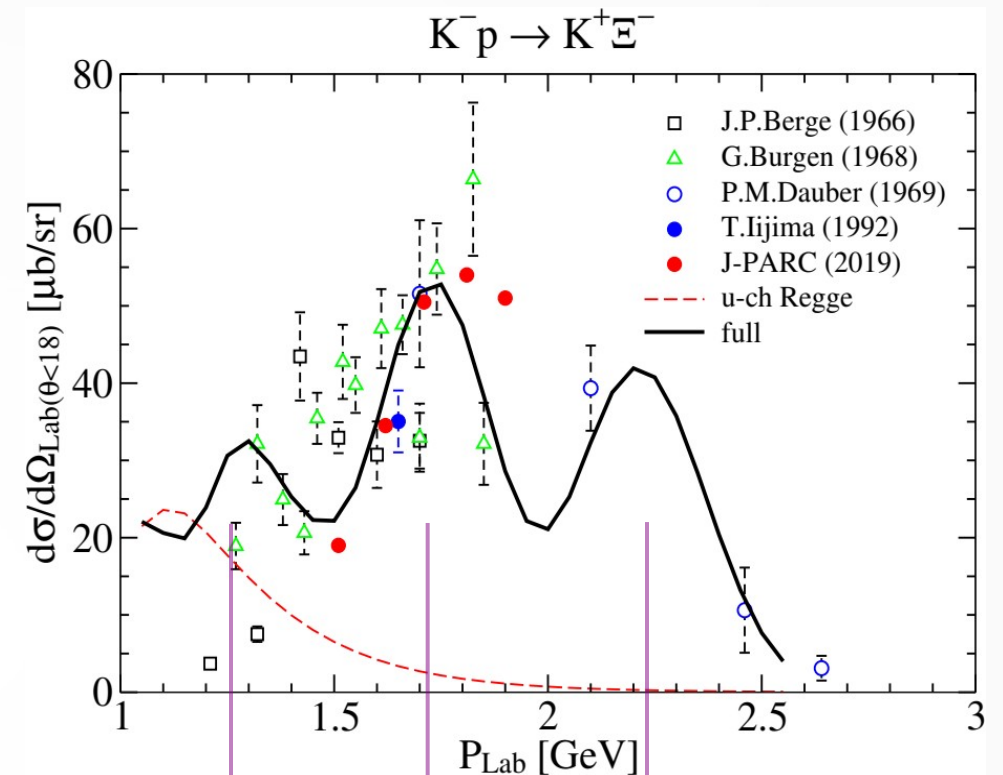


- The evidence of these three Y^* resonances looks very convincing.
- More data from the J-PARC E05 experiment are strongly called for.

3. $K^- p \rightarrow K^+ \Xi^-$ results



$\Lambda(1890, 3/2^+)$ $\Sigma(2030, 7/2^+)$ $\Sigma(2250, 7/2^- ?)$



$\Lambda(1890, 3/2^+)$ $\Sigma(2030, 7/2^+)$ $\Sigma(2250, 7/2^- ?)$

- The evidence of these three Y^* resonances looks very convincing.
- More data from the J-PARC E05 experiment are strongly called for.

Previous works

Sharov et al. EPJA.47.109 (2011)

Shyam et al. PRC.84.042201 (2011)

> Effective Lagrangian approach

Kamano et al. PRC.90.065204 (2014)

> Dynamical coupled-channel approach to \bar{K} induced reactions

Feijoo et al. PRC.92.015206 (2015)

> Coupled-channel unitarized chiral perturbation approach

Nakayama et al. PRC.85.042201 (2012)

Jackson et al. PRC.89.025206 (2014)

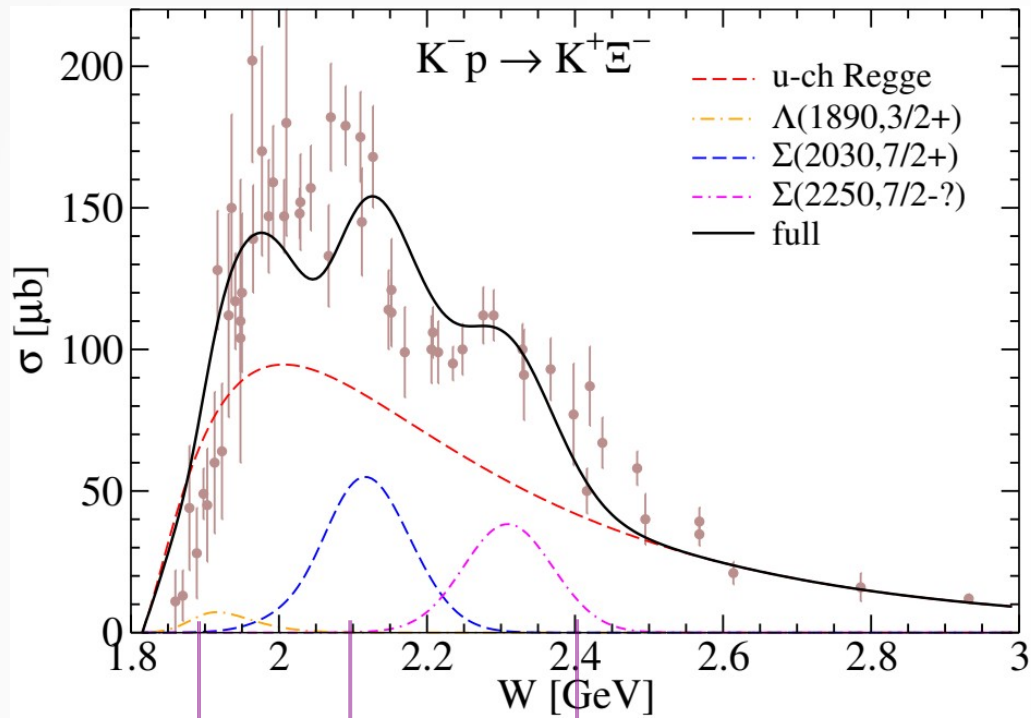
> Model independent aspects

Jackson et al. PRC.91.065208 (2015)

> Effective Lagrangian approach in which “the rescattering contribution” is accounted for by “a phenomenological contact amplitude”

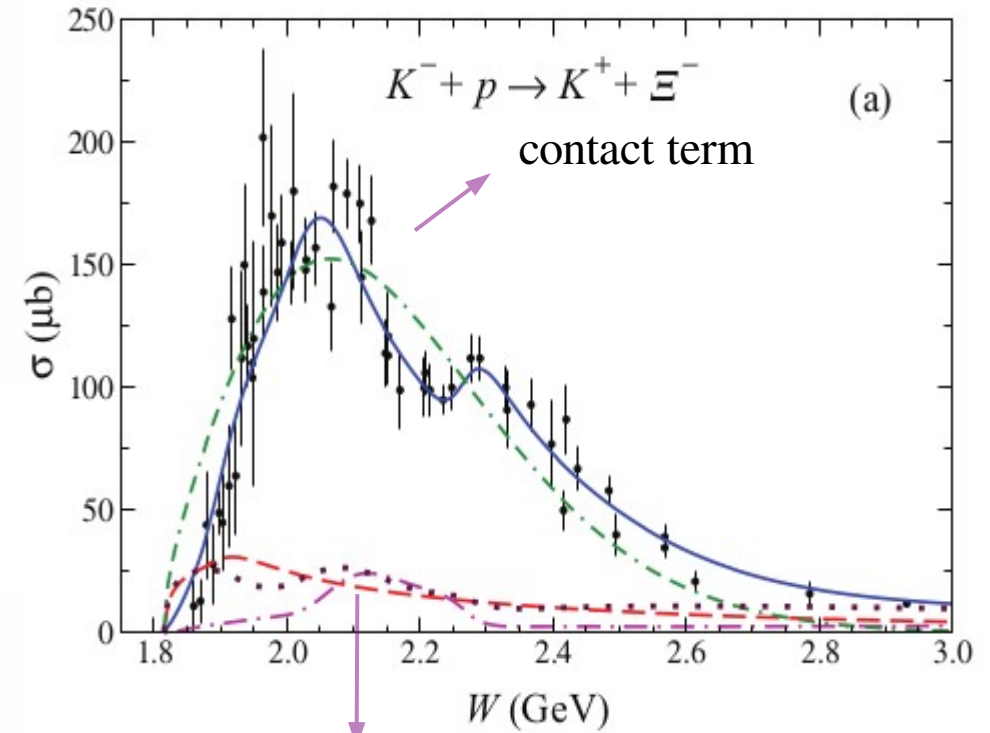
3. $K^- p \rightarrow K^+ \Xi^-$ results

Comparison with other works



$\Lambda(1890, 3/2^+)$ $\Sigma(2030, 7/2^+)$ $\Sigma(2250, 7/2^-?)$

Jackson et al. PRC.91.065208 (2015)

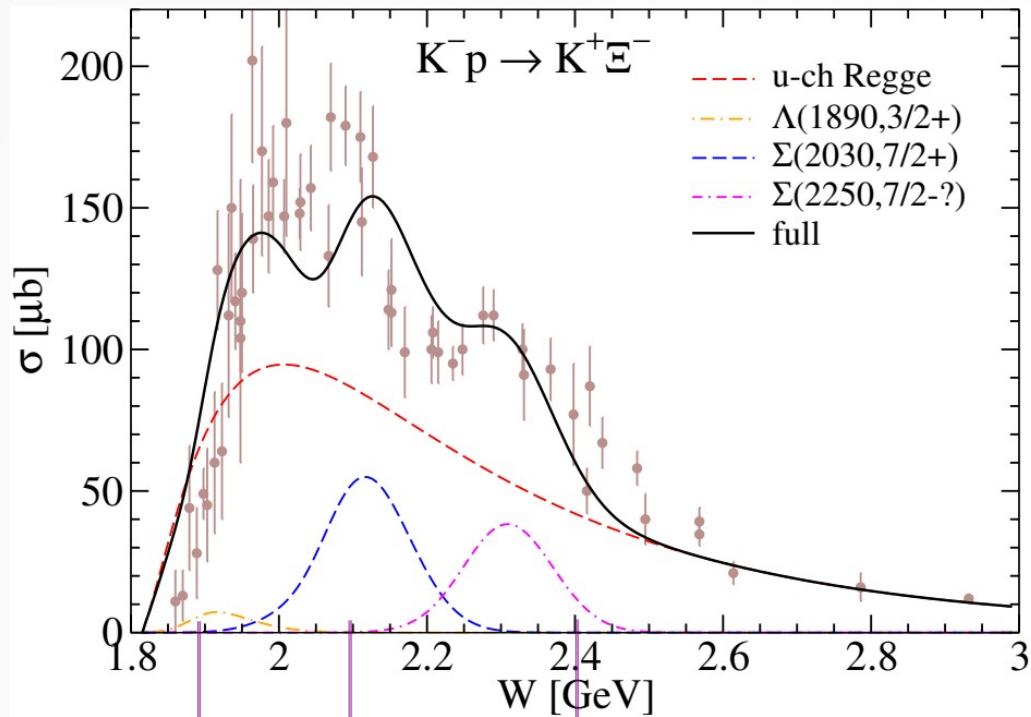


$\Lambda(1890, 3/2^+)$
 $\Sigma(2030, 7/2^+)$
 $\Sigma(2250, 5/2^-?)$

VALUE (MeV)	DOCUMENT ID	TECN	COMMENT
2210 to 2280 (≈ 2250)	OUR ESTIMATE		
2270 \pm 50	DEBELLEFON	1978	DPWA D_5 wave
2210 \pm 30	DEBELLEFON	1978	DPWA G_9 wave

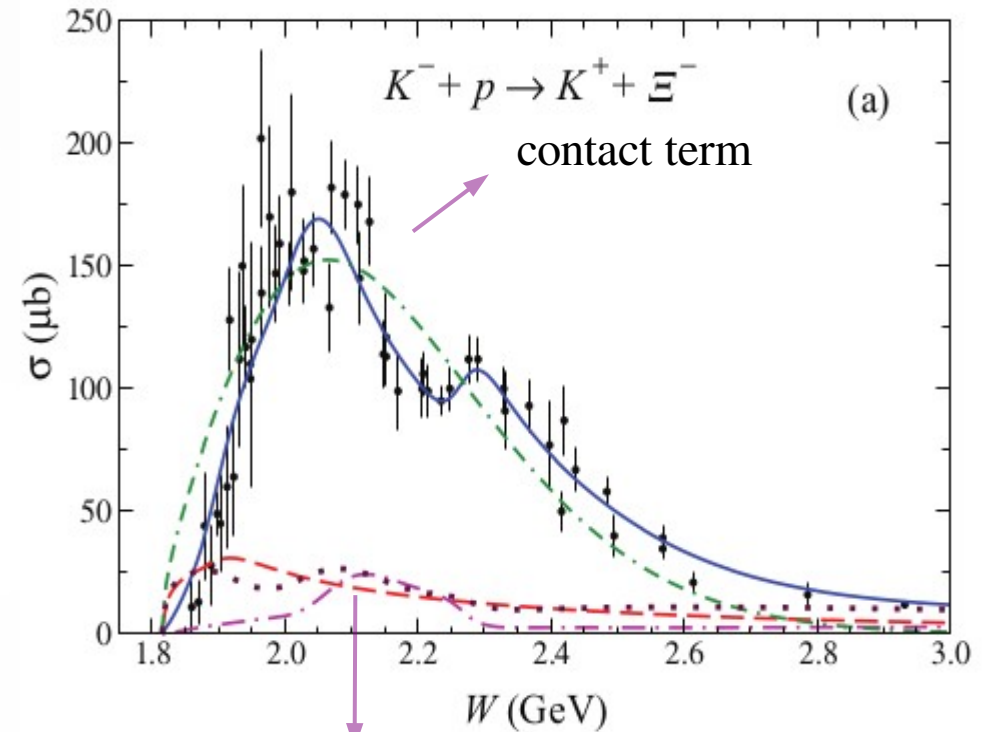
3. $K^- p \rightarrow K \Xi$ results

Comparison with other works



$\Lambda(1890,3/2^+)$ $\Sigma(2030,7/2^+)$ $\Sigma(2250,7/2^-?)$

Jackson et al. PRC.91.065208 (2015)



$\Lambda(1890,3/2^+)$

$\Sigma(2030,7/2^+)$

$\Sigma(2250,5/2^-?)$

- The structure at $W \approx 2.2$ GeV are explained by a destructive effect between “contact term” and “resonant amplitudes”.

3. $K^- p \rightarrow K \Xi$ results

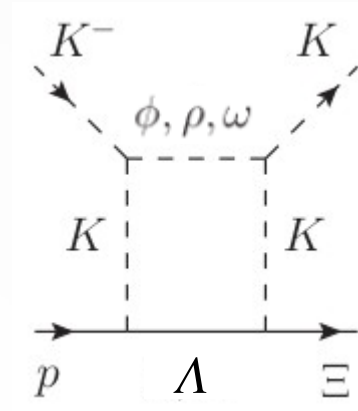
□ Rescattering amplitude

$$T_{V\Lambda} = \int \frac{d^3 \vec{p}}{(2\pi)^3} \frac{M_\Lambda}{E_\Lambda} \frac{1}{p_V^2 - M_V^2 + i\epsilon} T_{K^- p \rightarrow V\Lambda} T_{V\Lambda \rightarrow K\Xi}$$

$$T_{V\Lambda} = -i \frac{p_{c.m.}}{16\pi^2} \frac{M_\Lambda}{\sqrt{s}} \int d\Omega [T_{K^- p \rightarrow V\Lambda}(t_K) T_{V\Lambda \rightarrow K\Xi}(t_K)] + \mathcal{P}$$

$$V = (\varphi, \rho, \omega)$$

$$\int d\Omega = \int d\cos\theta' d\phi'$$



$$K^- p \rightarrow \left\{ \begin{array}{l} \rho \quad \Lambda \\ \omega \quad \Lambda \\ \phi \quad \Lambda \end{array} \right\} \rightarrow \Xi - K^+$$

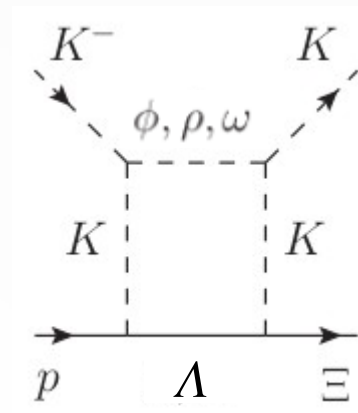
3. $K^- p \rightarrow K \Xi$ results

Rescattering amplitude

$$T_{V\Lambda} = \int \frac{d^3 \vec{p}}{(2\pi)^3} \frac{M_\Lambda}{E_\Lambda} \frac{1}{p_V^2 - M_V^2 + i\epsilon} T_{K^- p \rightarrow V\Lambda} T_{V\Lambda \rightarrow K\Xi}$$

$$T_{V\Lambda} = -i \frac{p_{c.m.}}{16\pi^2} \frac{M_\Lambda}{\sqrt{s}} \int d\Omega [T_{K^- p \rightarrow V\Lambda}(t_K) T_{V\Lambda \rightarrow K\Xi}(t_K)] + \mathcal{P}$$

$$V = (\varphi, \rho, \omega) \quad \int d\Omega = \int d\cos\theta' d\phi'$$

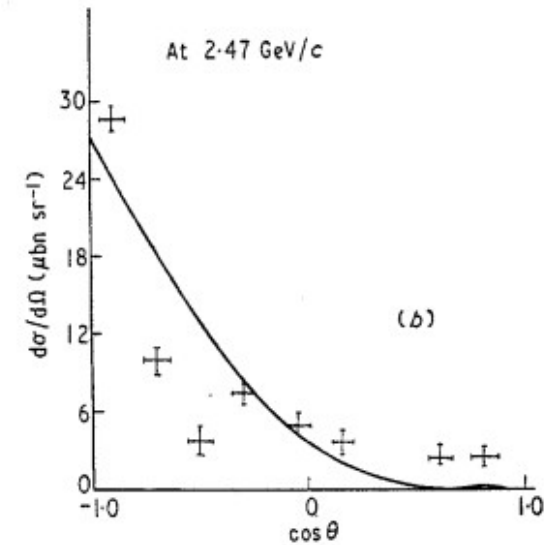
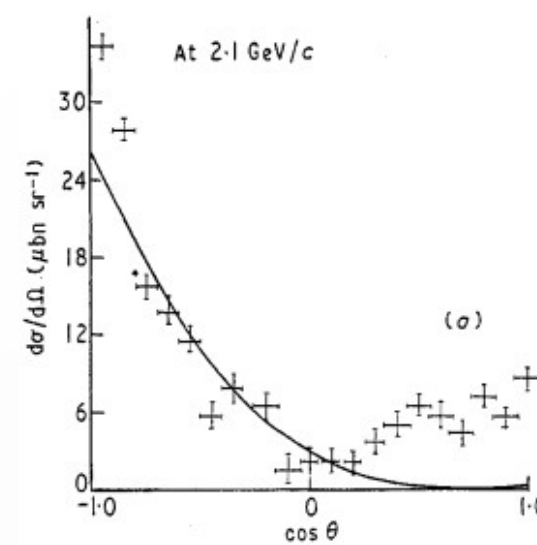


$$K^- p \rightarrow \begin{Bmatrix} \rho & \Lambda \\ \omega & \Lambda \\ \phi & \Lambda \end{Bmatrix} \rightarrow \Xi^- K^+$$

$K^- p \rightarrow K^+ \Xi^-$ process in the two-meson-exchange peripheral model

To cite this article: B K Agarwal *et al* 1971 *J. Phys. A: Gen. Phys.* 4 L52

- Naive calculation by assuming forward production of φ : $\cos\theta' = \hat{q}_{K^-} \cdot \hat{q}_\varphi \rightarrow 1$
- Except for “ $P = 1/(t_1 - M_K^2)(t_2 - M_K^2)$ ”, which is a rapidly varying function of $\cos\theta'$, therefore essentially determines the angular distribution.



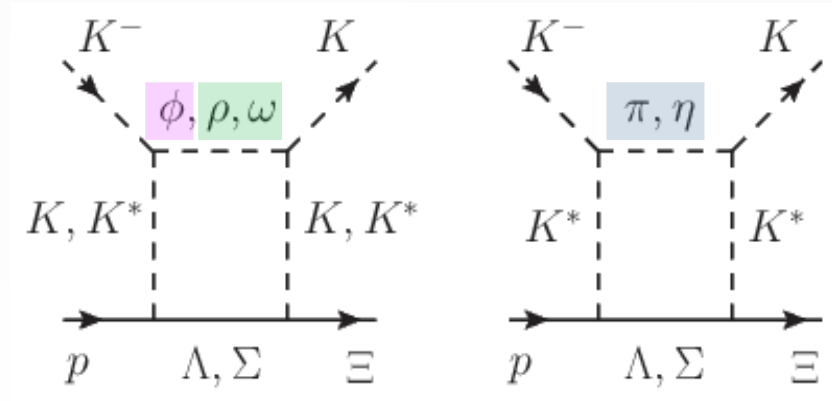
3. $K^- p \rightarrow K \Xi$ results

□ Rescattering amplitude

$$T_{V\Lambda} = \int \frac{d^3 \vec{p}}{(2\pi)^3} \frac{M_\Lambda}{E_\Lambda} \frac{1}{p_V^2 - M_V^2 + i\epsilon} T_{K^- p \rightarrow V\Lambda} T_{V\Lambda \rightarrow K\Xi}$$

$$T_{V\Lambda} = -i \frac{p_{c.m.}}{16\pi^2} \frac{M_\Lambda}{\sqrt{s}} \int d\Omega [T_{K^- p \rightarrow V\Lambda}(t_K) T_{V\Lambda \rightarrow K\Xi}(t_K)] + \mathcal{P}$$

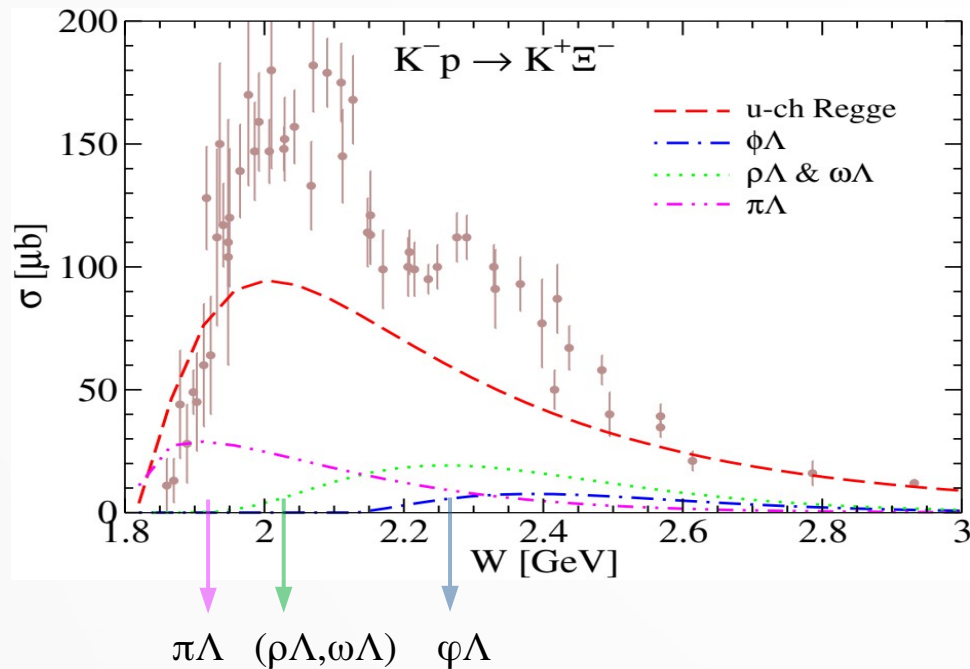
$$V = (\varphi, \rho, \omega)$$



$$g_{K^*K\rho} = g_{K^*K\omega} = \frac{1}{\sqrt{2}} g_{K^*K\phi} = \frac{1}{2} g_{\omega\rho\pi}$$

$$g_{KK\rho} = g_{KK\omega} = \frac{1}{2} g_{\pi\pi\rho}$$

□ We **fully** calculate the singular part.



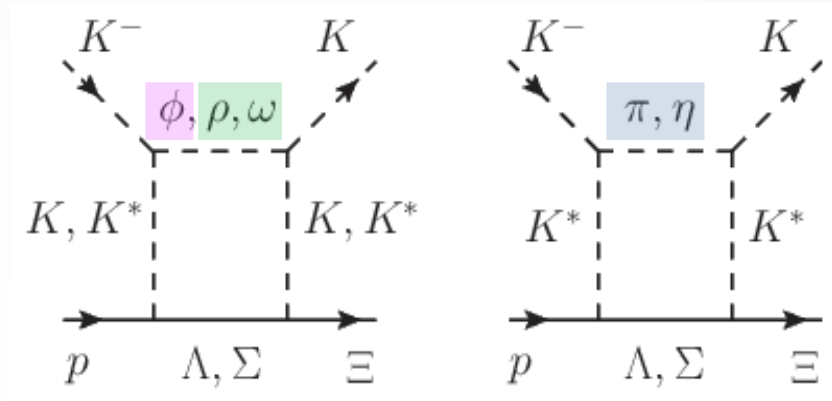
3. $K^- p \rightarrow K \Xi$ results

□ Rescattering amplitude

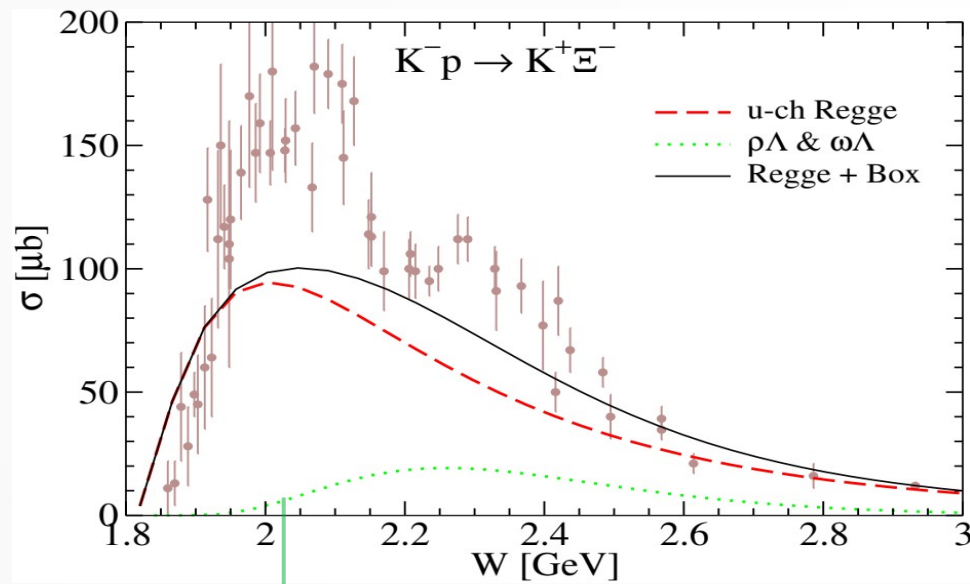
$$T_{V\Lambda} = \int \frac{d^3 \vec{p}}{(2\pi)^3} \frac{M_\Lambda}{E_\Lambda} \frac{1}{p_V^2 - M_V^2 + i\epsilon} T_{K^- p \rightarrow V\Lambda} T_{V\Lambda \rightarrow K\Xi}$$

$$T_{V\Lambda} = -i \frac{p_{c.m.}}{16\pi^2} \frac{M_\Lambda}{\sqrt{s}} \int d\Omega [T_{K^- p \rightarrow V\Lambda}(t_K) T_{V\Lambda \rightarrow K\Xi}(t_K)] + \mathcal{P}$$

$$V = (\phi, \rho, \omega)$$



□ We **fully** calculate the singular part.



($\rho\Lambda, \omega\Lambda$)

$$g_{K^*K\rho} = g_{K^*K\omega} = \frac{1}{\sqrt{2}} g_{K^*K\phi} = \frac{1}{2} g_{\omega\rho\pi}$$

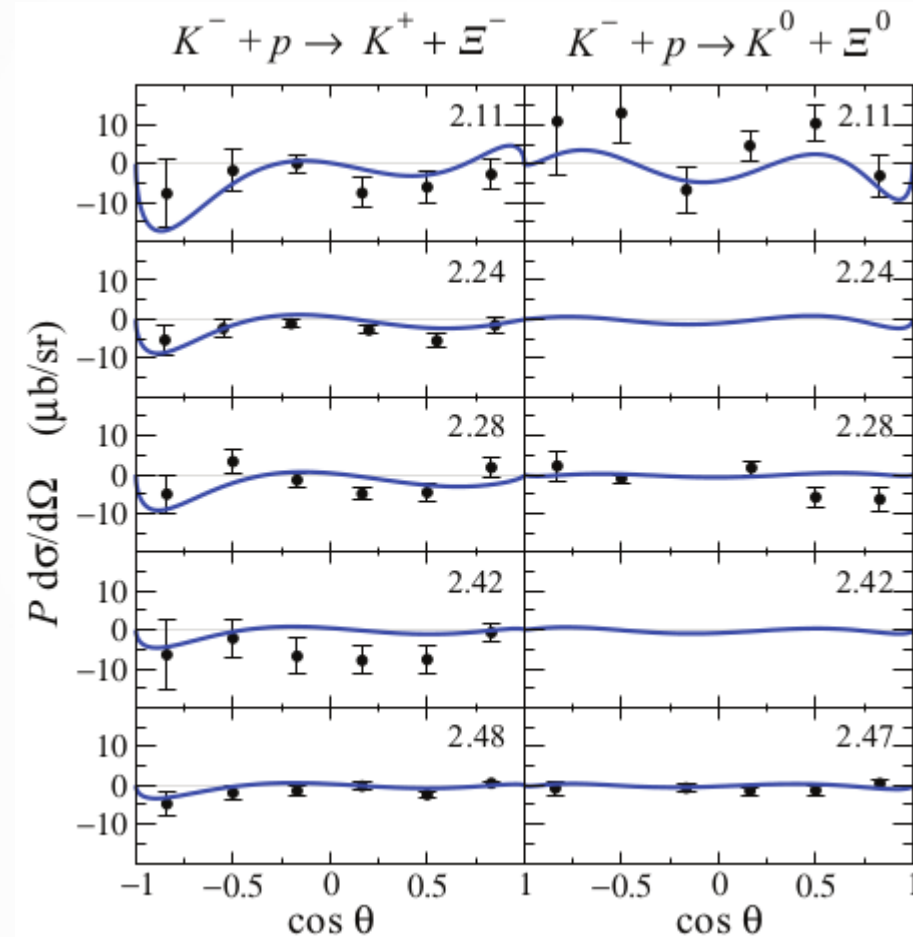
$$g_{KK\rho} = g_{KK\omega} = \frac{1}{2} g_{\pi\pi\rho}$$

> It is difficult to clarify the role of the box diagrams with only the TCS data.

3. $K^- p \rightarrow K \Xi$ results

- We can polarize “the incoming nucleon” or “the outgoing Ξ baryon”:
Target (T), Recoil (P), Target-recoil (K) asymmetries

Recoil asymmetries

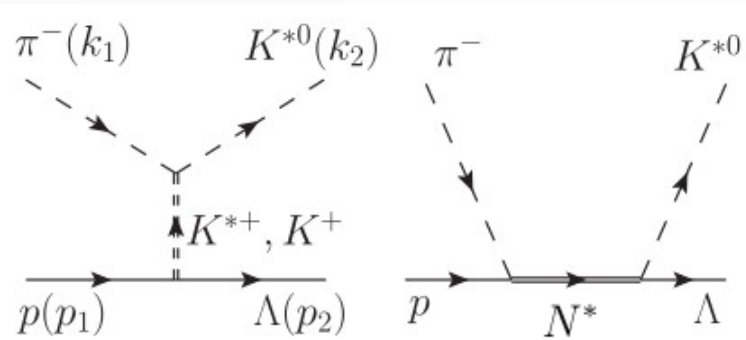


Theory: [Jackson et al. PRC.91.065208 \(2015\)](#)

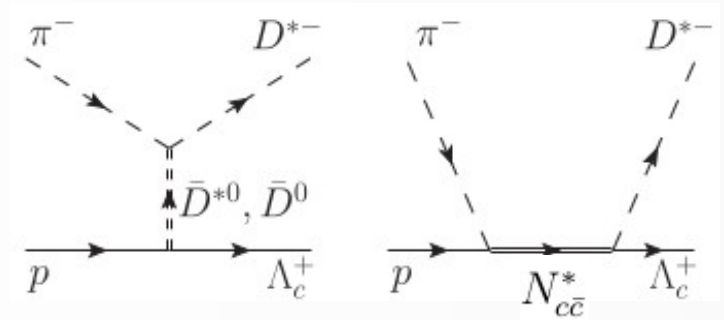
4. Application

(a) “open” strange (**charm**) production

$$\pi^- p \rightarrow K^{*0} \Lambda$$



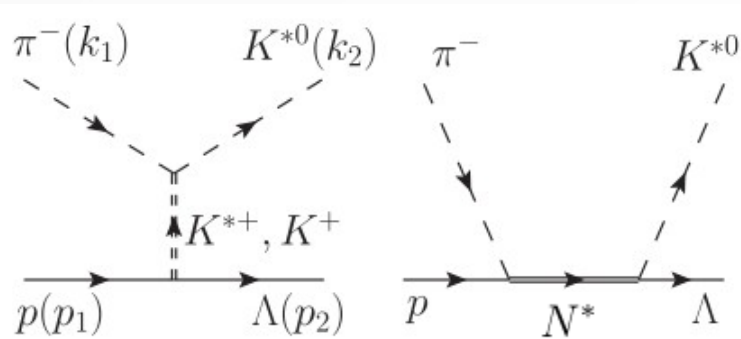
[Regge + Resonance] $\pi^- p \rightarrow D^{*-} \Lambda_c^+$



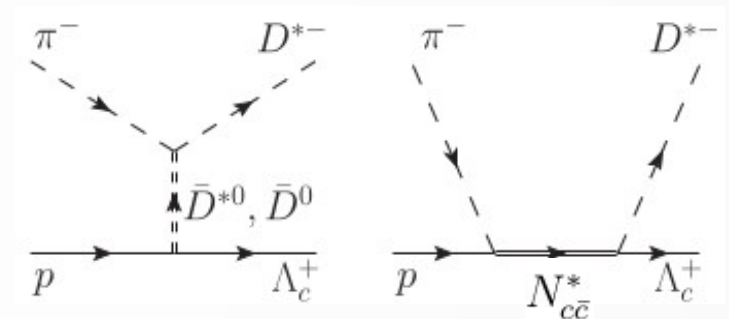
4. Application

(a) “open” strange (charm) production

$$\pi^- p \rightarrow K^{*0} \Lambda$$



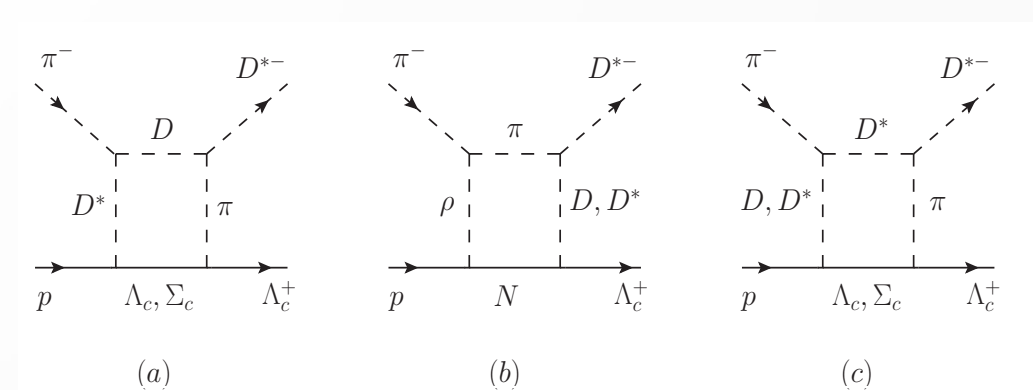
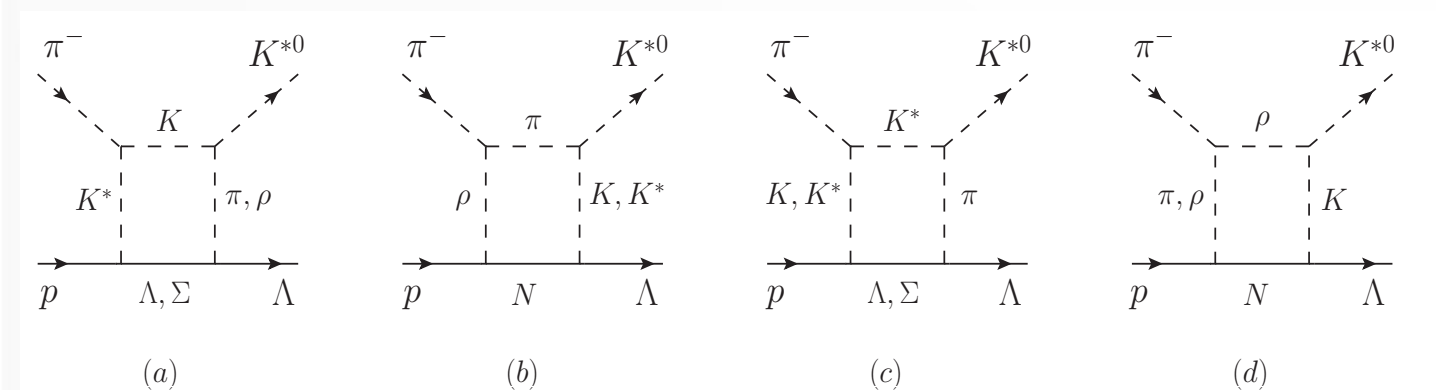
[Regge + Resonance] $\pi^- p \rightarrow D^{*-} \Lambda_c^+$



$$\pi^- p \rightarrow Mi Bi \rightarrow K^{*0} \Lambda$$

[Rescattering]

$$\pi^- p \rightarrow Mi Bi \rightarrow D^{*-} \Lambda_c^+$$



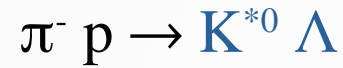
► Use the dominant decay process:

$$K^* \rightarrow K\pi, \rho \rightarrow \pi\pi$$

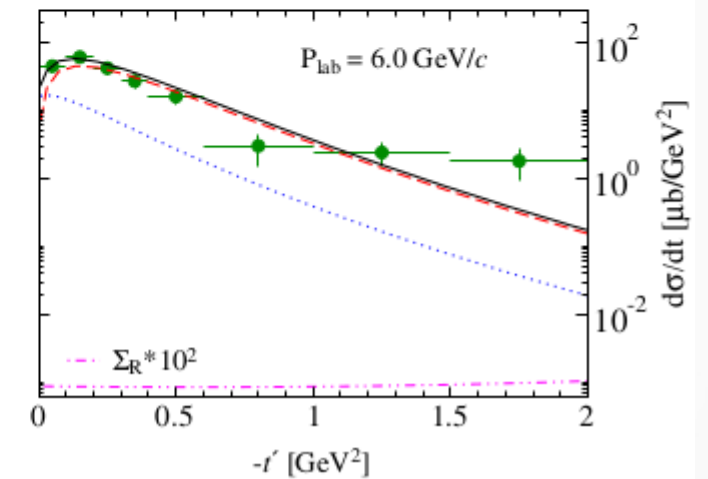
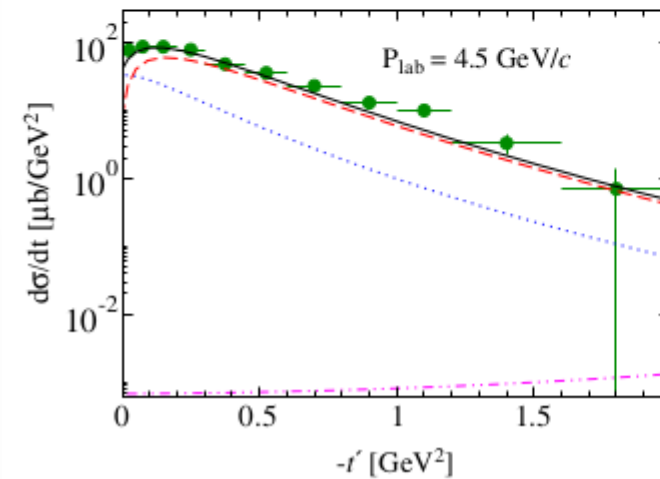
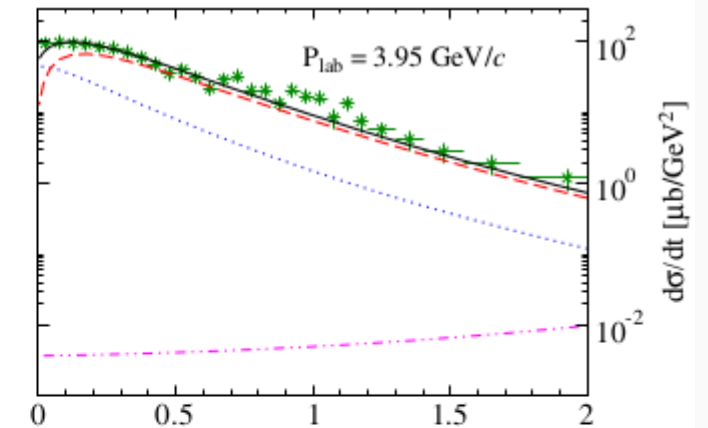
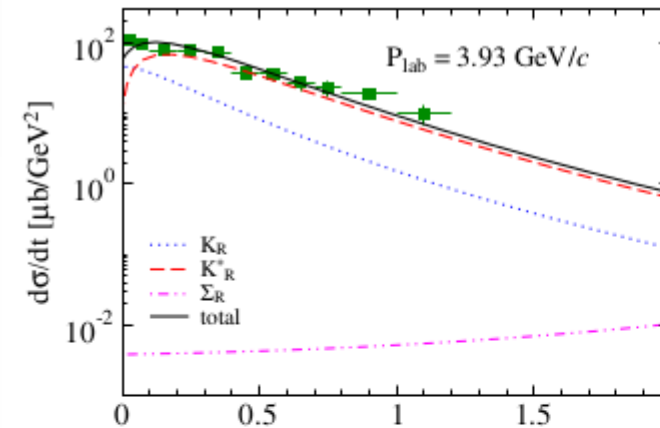
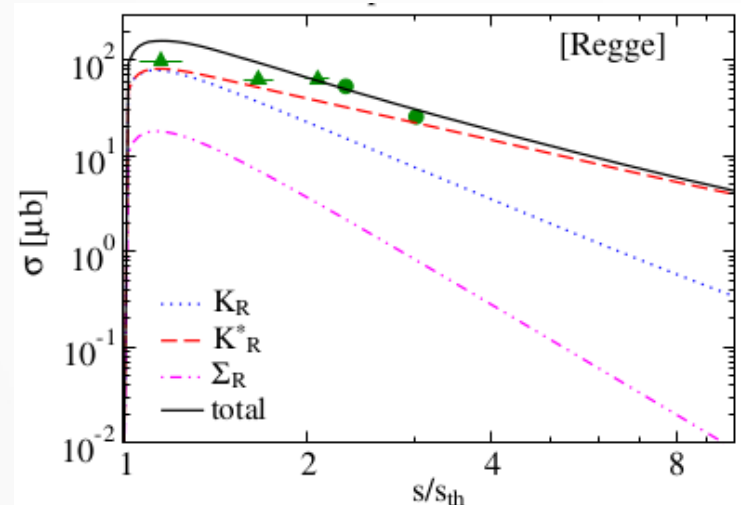
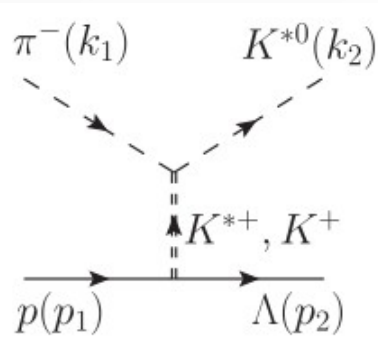
$$D^* \rightarrow D\pi, \rho \rightarrow \pi\pi$$

4. Application

(a) “open” strange (charm) production



S.H.Kim et al.
PRD.92.094021 (2015)



> K exchange governs $d\sigma/dt$ near $-t' \approx 0$, whereas K^* exchange becomes dominant as $-t'$ increases.

4. Application

(a) “open” strange (**charm**) production $[\pi^- p \rightarrow K^{*0} \Lambda (D^{*-} \Lambda_c^+)]$

How to describe the 3-body decay process

$$\pi^- + p \rightarrow V + Y \rightarrow (P + \pi) + Y$$

in the rest frame of the vector-meson?

□ Decay angular distributions

$$W(\Omega_f) = \sum_{m_i, m_f, \lambda_V, \lambda'_V} \mathcal{M}_{m_f, \lambda_V; m_i} \mathcal{M}_{m_f, \lambda'_V; m_i}^* \times Y_{1\lambda_V}(\Omega_f) Y_{1\lambda'_V}^*(\Omega_f),$$

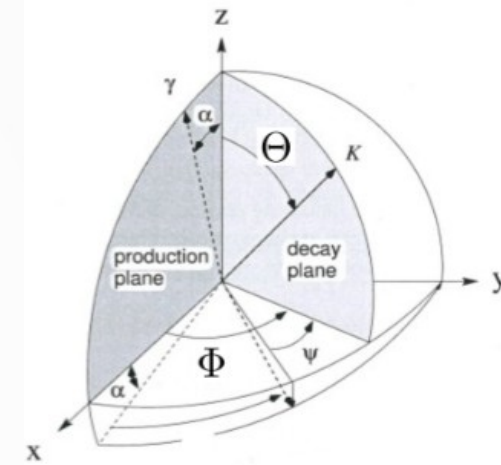
with $\mathcal{M}_{m_f, \lambda_V; m_i} = \frac{1}{\mathcal{N}} S_{m_f, \lambda_V; m_i}$

□ Normalization factor

$$\mathcal{N}^2 = \sum_{m_f, m_i, \lambda_V} |S_{m_f, \lambda_V; m_i}|^2$$

□ Differential cross section

$$\frac{d\sigma}{dt d\Omega_f} = \frac{d\sigma}{dt} W(\Omega_f)$$



Θ: polar angle
Φ: azimuthal angle

□ Spin factor

$$\left(\begin{aligned} S &= \epsilon_\mu^* \bar{u}_\Lambda S^\mu u_N \\ S'_K &= I_K i g_{\pi K K^*} \frac{g_{K N \Lambda}}{M_N + M_\Lambda} \gamma^\nu \gamma_5 k_1^\mu (k_2 - k_1)_\nu, \\ S^\mu_{K^*} &= I_{K^*} g_{\pi K^* K} g_{K^* N \Lambda} \epsilon^{\mu\nu\alpha\beta} \left[\gamma_\nu - \frac{i k_{K^* N \Lambda}}{M_N + M_\Lambda} \sigma_{\nu\lambda} (k_2 - k_1)^\lambda \right] k_{2\alpha} k_{1\beta} \end{aligned} \right)$$

4. Application

(a) “open” strange (charm) production $[\pi^- p \rightarrow K^{*0} \Lambda (D^{*-} \Lambda_c^+)]$

1. spin-density matrices ($\rho_{\lambda\lambda'}$)

(1) Unpolarized case

$$\rho_{\lambda\lambda'}^0 = \sum_{m_i = \pm \frac{1}{2}, m_f = \pm \frac{1}{2}} \mathcal{M}_{m_f, \lambda; m_i} \mathcal{M}_{m_f, \lambda'; m_i}^*$$

(2) Polarized Y hyperon

$$\rho_{\lambda\lambda'}^\pm = \sum_{m_i = \pm \frac{1}{2}} \mathcal{M}_{m_f, \lambda; m_i} \mathcal{M}_{m_f, \lambda'; m_i}^*$$

λ, λ' : helicity states of the vector meson

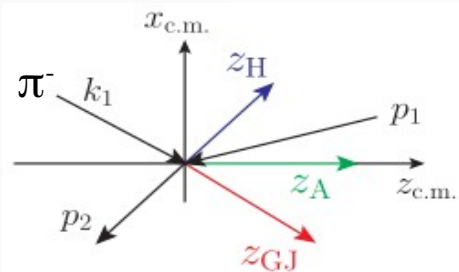
2. decay angular distributions (W)

(1) Unpolarized case

$$W^0(\Omega_f) = \frac{3}{4\pi} \left[\rho_{00}^0 \cos^2 \Theta + \rho_{11}^0 \sin^2 \Theta - \rho_{1-1}^0 \sin^2 \Theta \cos 2\Phi \right. \\ \left. - \sqrt{2} \operatorname{Re}(\rho_{10}^0) \sin 2\Theta \cos \Phi \right],$$

(2) Polarized Y hyperon

$$W^\pm(\Omega_f) = \frac{3}{4\pi} \left[\rho_{00}^\pm \cos^2 \Theta + \frac{1}{2} (\rho_{11}^\pm + \rho_{-1-1}^\pm) \sin^2 \Theta \right. \\ \left. - \rho_{1-1}^\pm \sin^2 \Theta \cos 2\Phi \right. \\ \left. - \frac{1}{\sqrt{2}} \operatorname{Re}(\rho_{10}^\pm - \rho_{-10}^\pm) \sin 2\Theta \cos \Phi \right],$$



□ Quantization axis in the rest frame of the V-meson

“s”-frame (helicity frame)

: anti-parallel to the outgoing Y

“t”-frame (Gottfried-Jackson frame): parallel to the incoming π

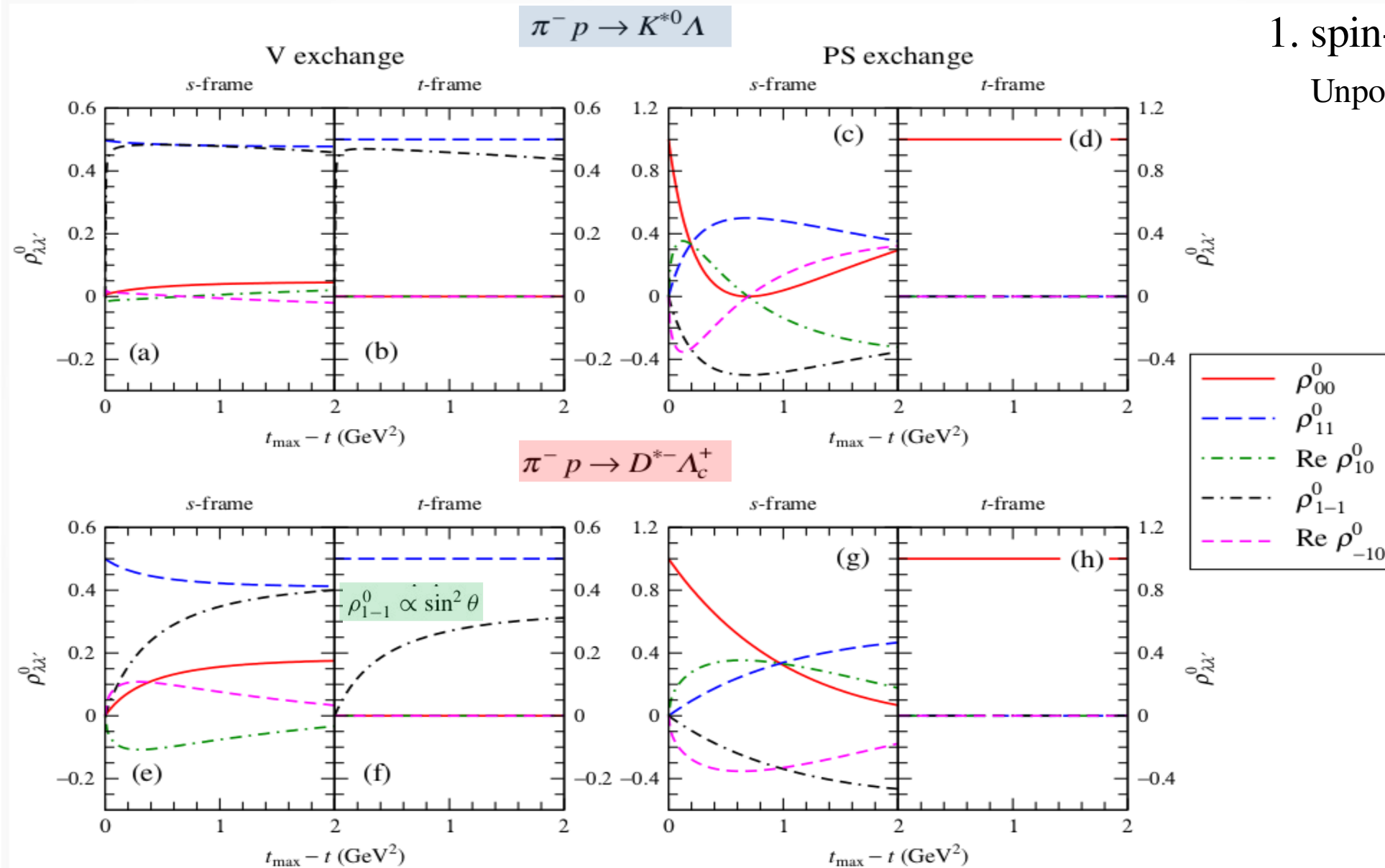
4. Application

1. spin-density matrices ($\rho_{\lambda\lambda'}$)

Unpolarized case

$p_\pi = 6$ and 15 GeV/c

S.H.Kim, Y,Oh, A.I.Titov,
PRC.95.055206 (2017)



enhancement of $\rho_{|\lambda|=1, |\lambda'|=1}^0$

$$\epsilon^{\mu\nu\alpha\beta} q_\mu p_{V\alpha} \epsilon_\beta^* \quad \epsilon^* \times \mathbf{p}_\pi \simeq i\lambda_V \epsilon^* |\mathbf{p}_\pi|$$

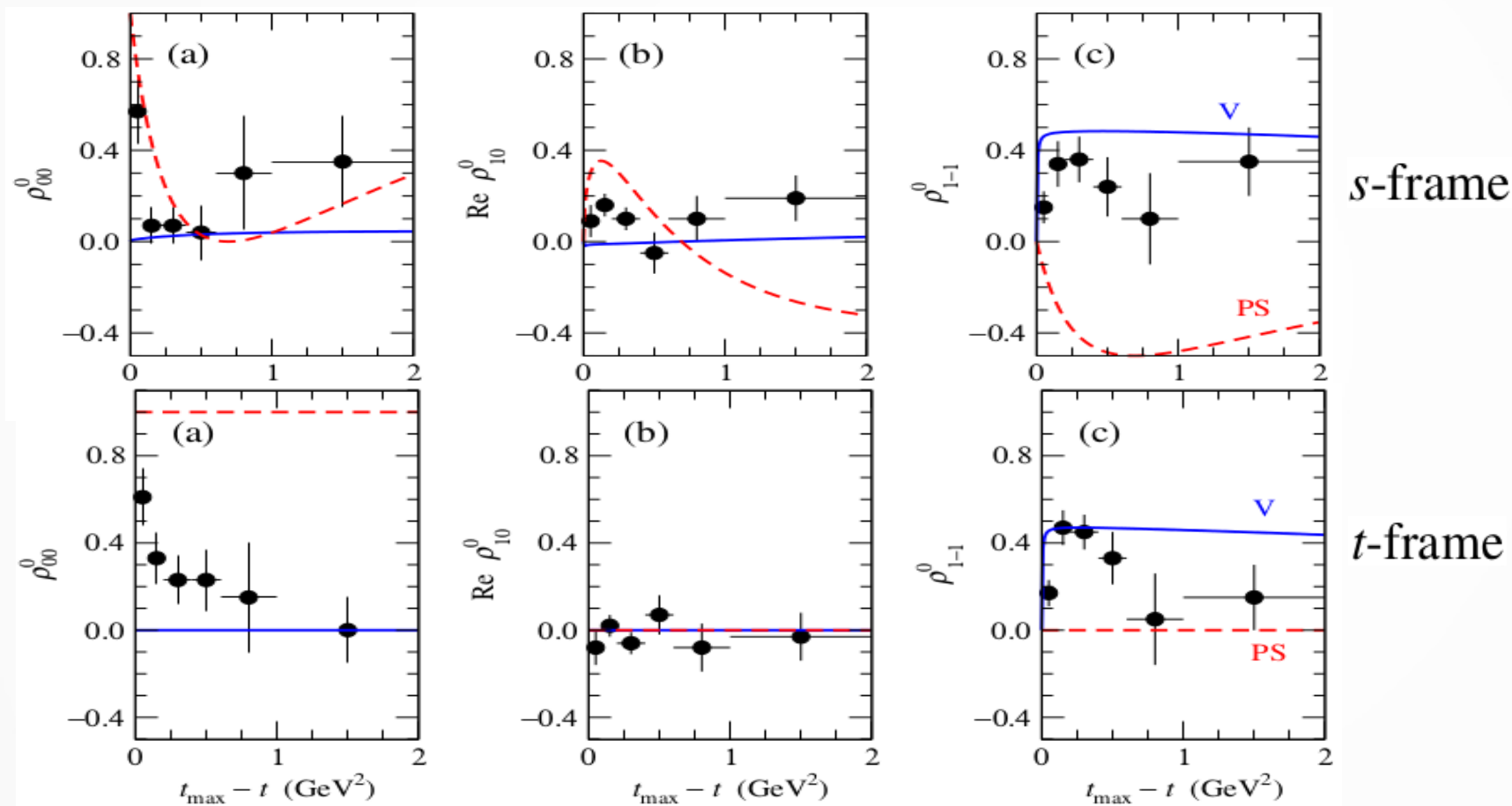
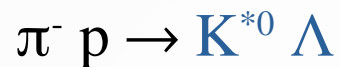
enhancement of ρ_{00}^0

$$\epsilon^* \cdot \mathbf{p}_\pi$$

4. Application

(a) “open” strange (charm) production

1. spin-density matrices ($\rho_{\lambda\lambda'}$) Unpolarized case



S.H.Kim, Y,Oh, A.I.Titov,
PRC.95.055206 (2017)

Exp.: Crennell et al,
PRD.6.1220 (1972)

enhancement of $\rho_{|\lambda|=1, |\lambda'|=1}^0$

$$\epsilon^{\mu\nu\alpha\beta} q_\mu p_{V\alpha} \epsilon_\beta^*$$

$$\epsilon^* \times \mathbf{p}_\pi \simeq i\lambda_V \epsilon^* |\mathbf{p}_\pi|$$

enhancement of

$$\epsilon^* \cdot \mathbf{p}_\pi$$

4. Application

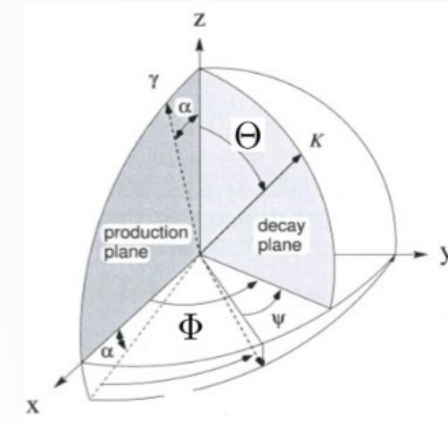
(a) “open” strange (charm) production

2. decay angular distributions (W)

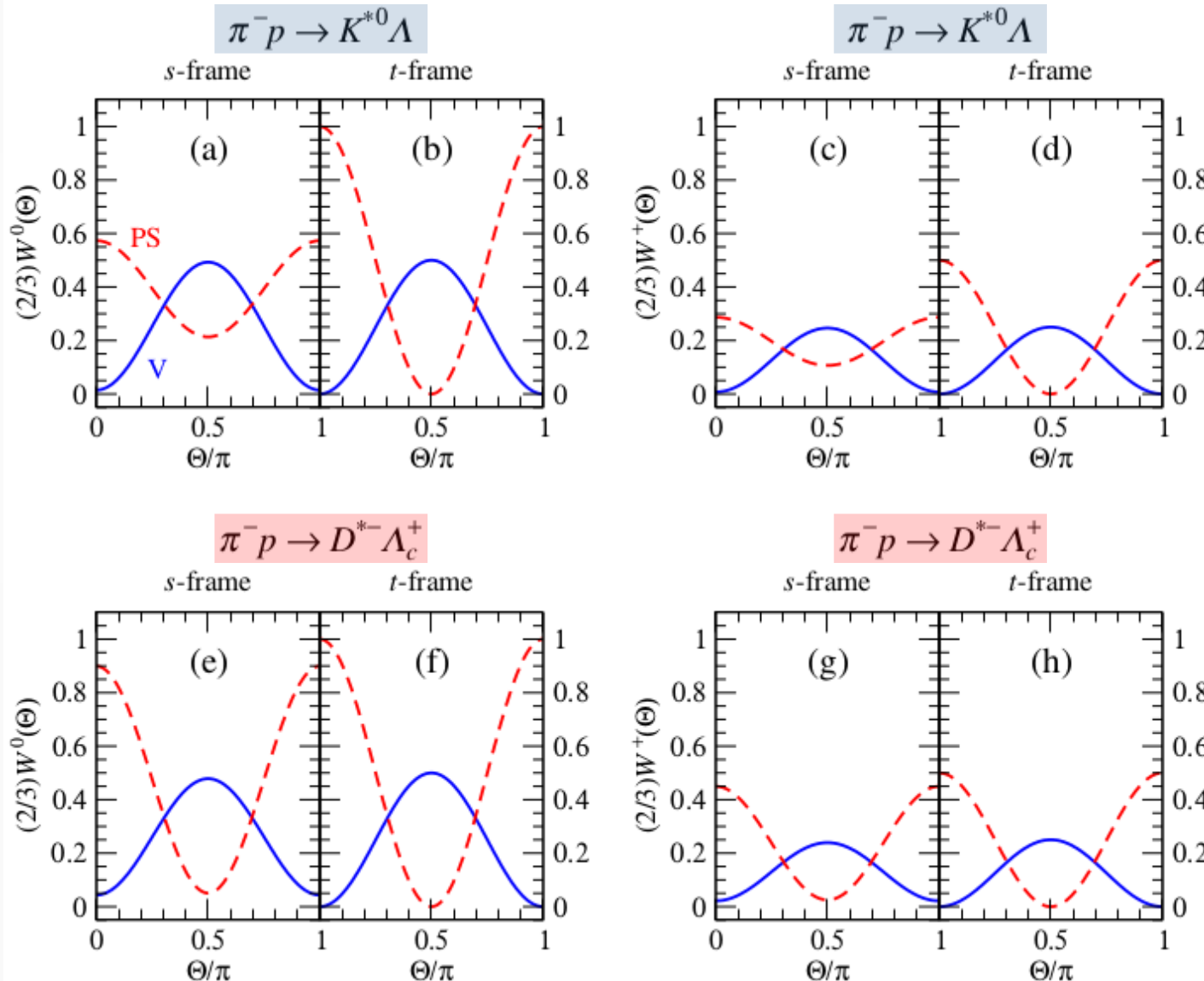
(1) Unpolarized case

(2) Polarized Y hyperon

S.H.Kim, Y,Oh, A.I.Titov,
PRC.95.055206 (2017)



Θ: polar angle
Φ: azimuthal angle



$$(1) \frac{2}{3} W^0(\Theta) = \rho_{00}^0 \cos^2 \Theta + \rho_{11}^0 \sin^2 \Theta,$$

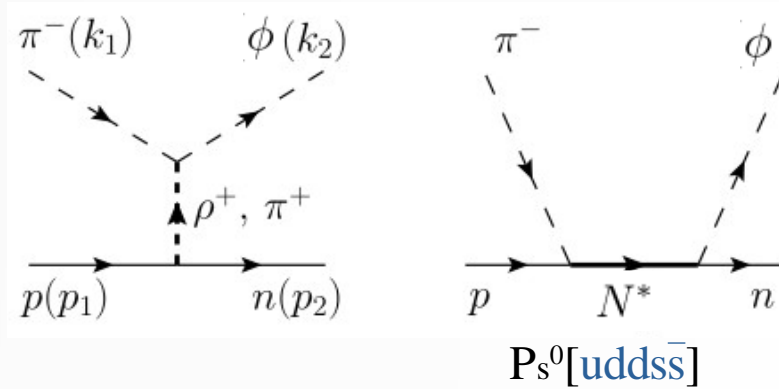
$$(2) \frac{2}{3} W^\pm(\Theta) = \rho_{00}^\pm \cos^2 \Theta + \frac{1}{2} (\rho_{11}^\pm + \rho_{-1-1}^\pm) \sin^2 \Theta$$

□ V- and PS-meson exchanges exhibit totally different shapes.

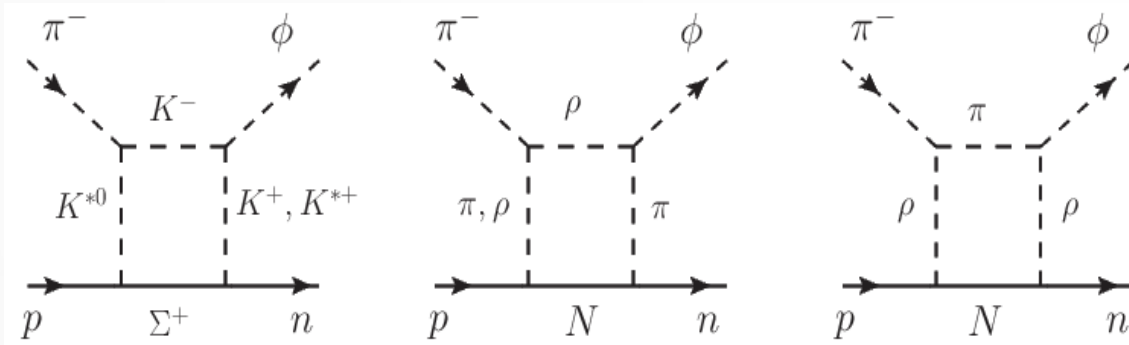
4. Application

(b) “hidden” strange (charm) production

$$\pi^- p \rightarrow \phi n \text{ [Regge + Resonance]}$$



$$\pi^- p \rightarrow M_i B_i \rightarrow \phi n \text{ [Rescattering]}$$

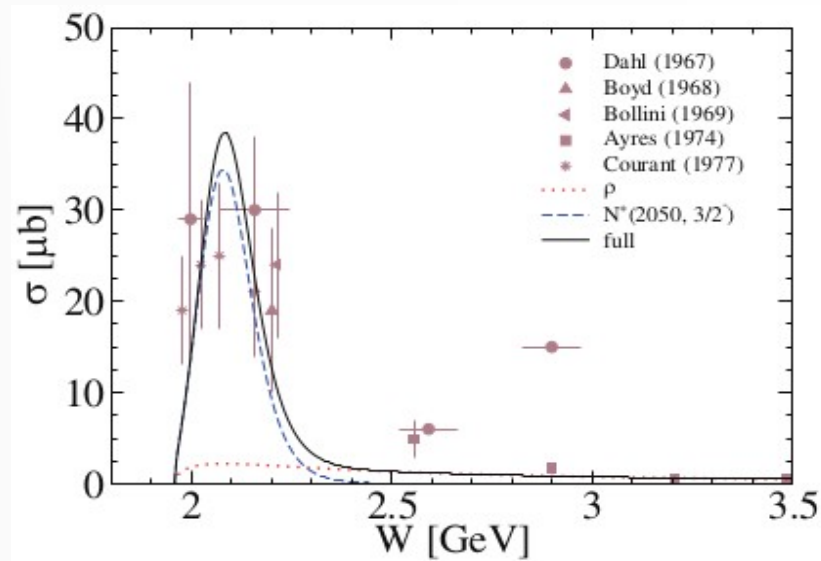
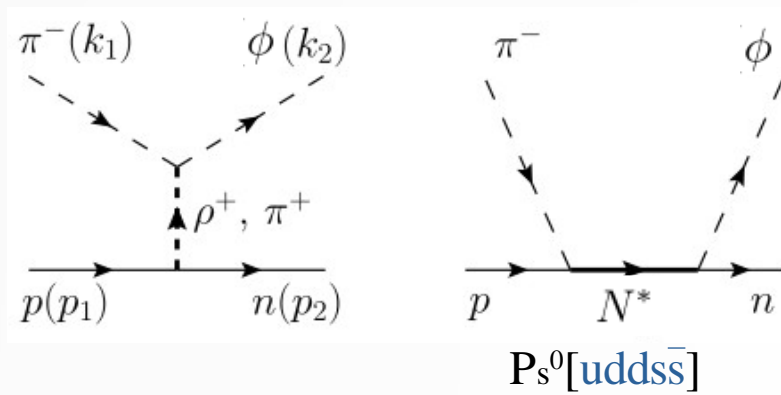


► Use the dominant decay process: $\phi \rightarrow K^+ K^-$, $\rho \pi$, $K^* \rightarrow K \pi$, $\rho \rightarrow \pi \pi$

4. Application

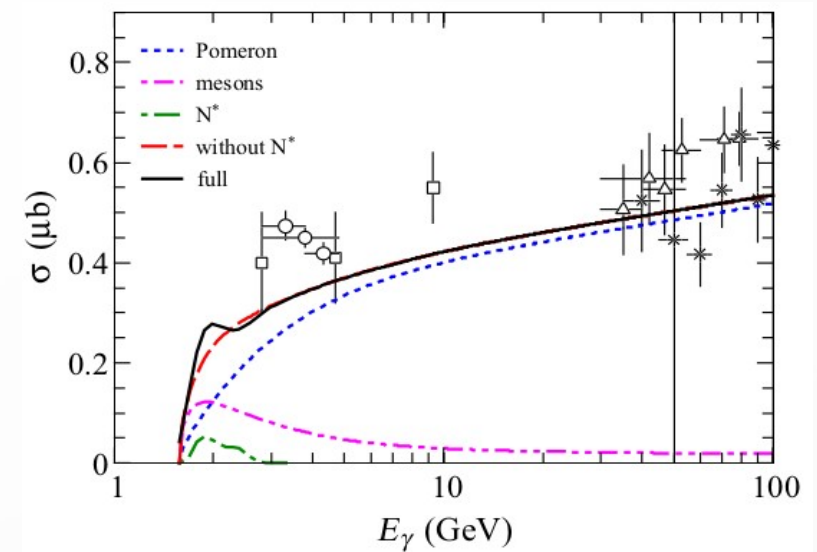
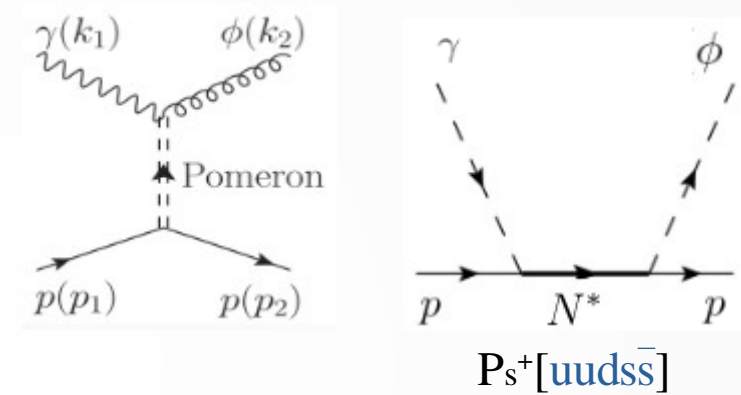
(b) “hidden” strange (charm) production

$\pi^- p \rightarrow \phi n$ [Regge + Resonance]



[T.Ishikawa et al. Proposal submitted using the J-PARC E16 spectrometer (2022)]

$\gamma p \rightarrow \phi p$ [Pomeron + Resonance]



[S.H.Kim, T.S.H.Lee, S.i.Nam, Y. Oh, PRC.104.045202 (2021)]

5. Summary & Future work

- ◇ Multistrangeness production, $K^- p \rightarrow K \Xi$, is investigated in a hybridized Regge model for two different isospin channels ($K^- p \rightarrow K^+ \Xi^-$ & $K^0 \Xi^0$).
- ◇ As for a background contribution, (Λ & Σ & Σ^*) hyperon Regge trajectories are considered in the u channel to describe the backward angles.
- ◇ We employ a “pseudovector” scheme for the KNY & $K\Xi Y$ vertices rather than a “pseudoscalar” scheme.
- ◇ For $K^- p \rightarrow K^0 \Xi^0$, only (Σ & Σ^*) Regge trajectories are possible and their relative contributions are well constrained.
- ◇ For $K^- p \rightarrow K^+ \Xi^-$, Λ Regge trajectory is more dominant than (Σ & Σ^*) ones.
- ◇ $\Lambda(1890, 3/2^+)$, $\Sigma(2030, 7/2^+)$, and $\Sigma(2250, 7/2^- ?)$ play a crucial role in explaining the bump structures.
- ◇ The box diagrams may play an important role.

5. Summary & Future work

◇ Production of multistrangeness ($S < -1$) baryons



> A distorted-wave impulse approximation within the multiple scattering formulation

> Ξ hypernuclei is important to study multistrangeness systems and strange neutron stars in astrophysics.

◇ Relevant experiments to date at [J-PARC](#):

[P05] Spectroscopic Study of Ξ -Hypernucleus, ${}^{12}_{\Xi}\text{Be}$, via the ${}^{12}\text{C}(K^-,K^+)$ Reaction

[P50] Charmed Baryon Spectroscopy via the (π^-, D^{*-}) reaction

[P85] Spectroscopy of Omega Baryons

[LoI] Study of Σ -N interaction using light Σ -nuclear system

[LoI] Ξ Baryon Spectroscopy High-momentum Secondary Beam

◇ Rescattering effects could be important for the meson induced production:



> The systematic analyses should be carried out.

5. Summary & Future work

- ◇ Production of multistrangeness ($S < -1$) baryons



> A distorted-wave impulse approximation within the multiple scattering formulation

> Ξ hypernuclei is important to study multistrangeness systems and strange neutron stars in astrophysics.

- ◇ Relevant experiments to date at [J-PARC](#):

[P05] Spectroscopic Study of Ξ -Hypernucleus, ${}^{12}_{\Xi}\text{Be}$, via the ${}^{12}\text{C}(K^-, K^+)$ Reaction

[P50] Charmed Baryon Spectroscopy via the (π^-, D^{*-}) reaction

[P85] Spectroscopy of Omega Baryons

[LoI] Study of Σ -N interaction using light Σ -nuclear system

[LoI] Ξ Baryon Spectroscopy High-momentum Secondary Beam

- ◇ Rescattering effects could be important for the meson induced production:



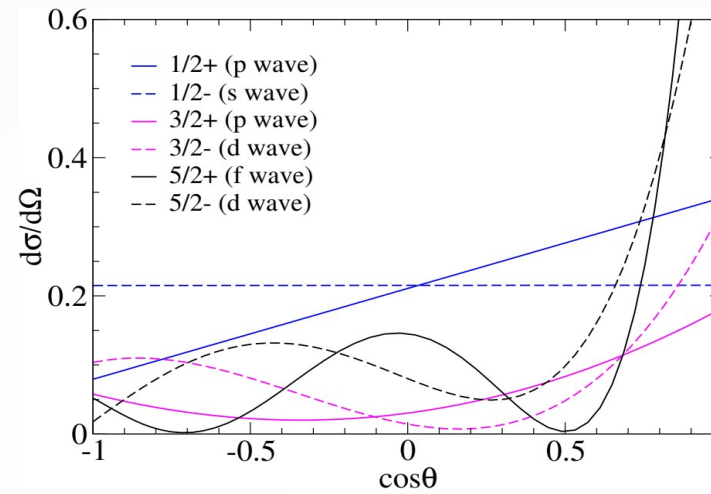
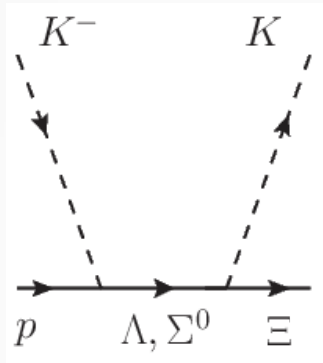
> The systematic analyses should be carried out.

Thank you very much for your attention

Back Up

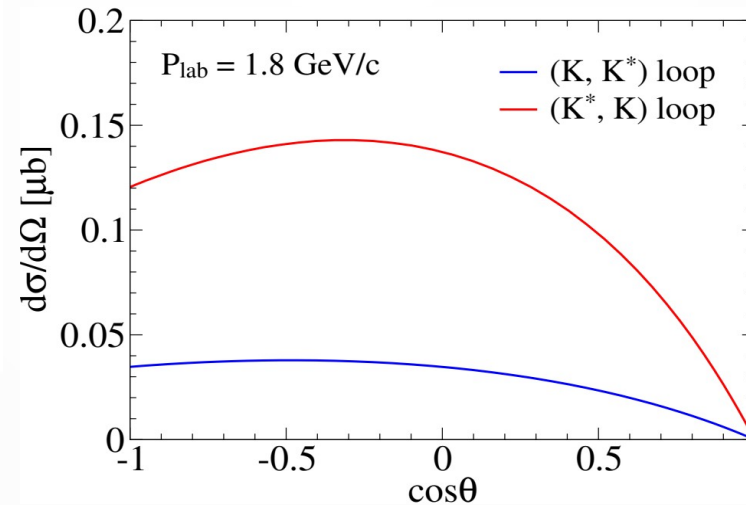
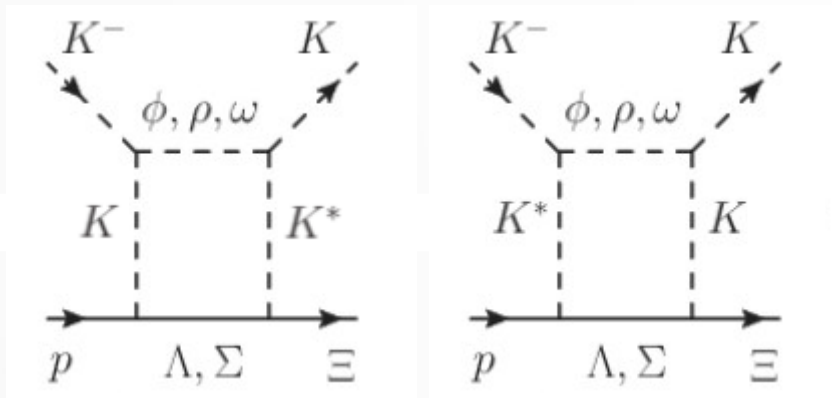
3. $K^- p \rightarrow K \Xi$ results

□ Resonant amplitude



> It becomes a forward peak as J increases.

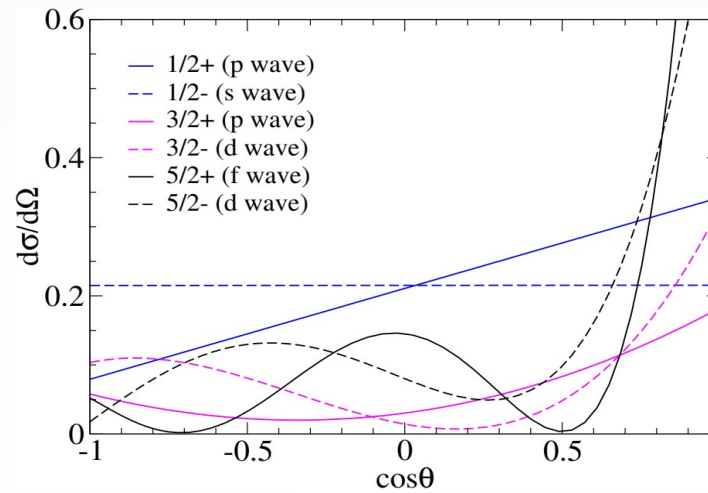
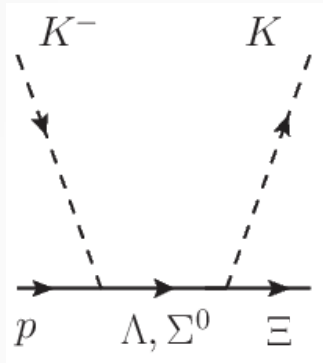
□ Rescattering amplitude



> It is the only channel which provides decreasing behavior at forward angles.

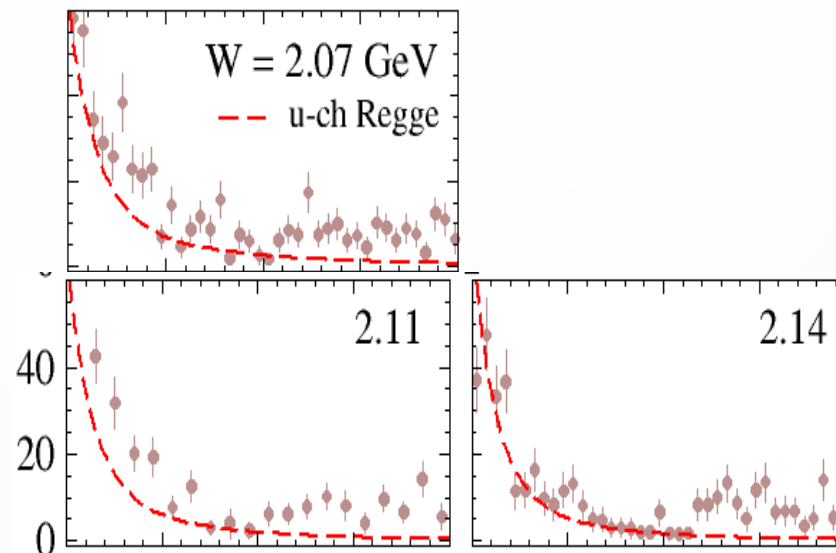
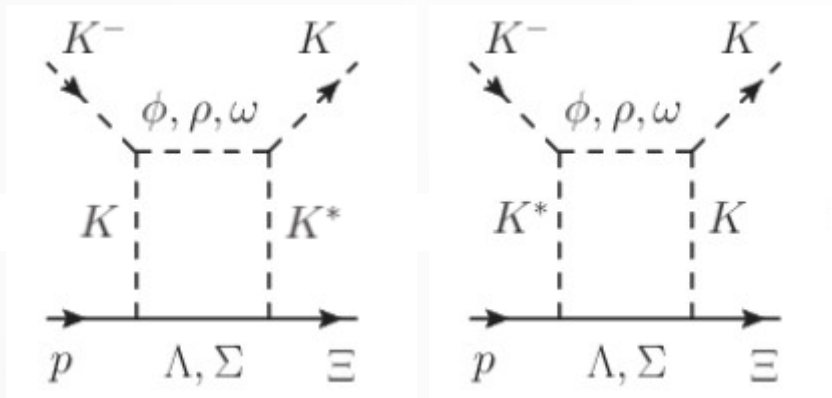
3. $K^- p \rightarrow K \Xi$ results

□ Resonant amplitude



> It becomes a forward peak as J increases.

□ Rescattering amplitude



> It is the only channel which provides decreasing behavior at forward angles.

> More accurate data are called for from the J-PARC.